THE DYNAMIC STUDY OF DRIVE-IN RACKS UNDER HOIZONTAL IMPACT LOAD

VINH HUA
KIM JR RASMUSSEN

RESEARCH REPORT R915
MARCH 2011

ISSN 1833-2781

SCHOOL OF CIVIL ENGINEERING

THE UNIVERSITY OF SYDNEY

THE UNIVERSITY OF SYDNEY

SCHOOL OF CIVIL ENGINEERING

THE DYNAMIC STUDY OF DRIVE-IN RACKS UNDER HORIZONTAL IMPACT LOAD

RESEARCH REPORT R915

VINH HUA

KIM JR RASMUSSEN

MARCH 2011

ISSN 1833-2781

Copyright Notice

School of Civil Engineering, Research Report R915
The Dynamic Study of Drive-in Racks Under Horizontal Impact Load
Vinh Hua & Kim Rasmussen
March 2011

ISSN 1833-2781

Published by:
School of Civil Engineering
The University of Sydney
Sydney NSW 2006
Australia

This report and other Research Reports published by the School of Civil Engineering are available at http://sydney.edu.au/civil

ABSTRACT

This report is concerned with the behaviour of drive-in steel storage racks under horizontal impact load in the down-aisle direction. Such impact loads due to forklifts striking an upright is a major cause of structural failure for drive-in rack systems.

The report investigates investigate the dynamic behaviour of a standard drive-in rack subjected to a down-aisle impact load. The effect of damping ratio, masses carried by the rack as well as the friction between the pallet and the rail track are investigated for impulse loading

KEYWORDS

Drive-in racks, steel storage racks, steel structures, dynamic, finite element analysis, design.

TABLE OF CONTENTS

1 INTRODUCTION

The static behaviour of a standard drive-in rack structure subjected to a horizontal impact load in the down-aisle direction has been studied and reported in [1]. The mechanical model developed in that report shows good agreement with the results of the FEA analysis.

The accidental impact force applied to the structure in reality is dynamic in nature and hence the dynamic properties of the drive-in rack such as natural frequency and damping may significantly affect the behaviour of the system. The purpose of this report is to investigate the dynamic behaviour of a standard drive-in rack subjected to a down-aisle impact load. The effect of damping ratio, masses carried by the rack as well as the friction between the pallet and the rail track are investigated for impulse loading.

2 METHODOLOGY

The study was carried out using the Strand7 finite element analysis model established in the research on static loading described in [1]. A nonlinear transient solver was used to investigate the dynamic behaviour of the system. A nominal impact force of 1000N was assumed to be applied within a time span of ΔT for ΔT = 0.086, 0.172, 0.258, 0.428, 0.856 and 5 seconds, and the rack response was obtained for a period of 10 second after the impact. Additional masses simulating the weight of a typical pallet were added to the model to determine the difference in the behaviour of loaded and unloaded racks under impact loading.

3 FEA MODELING

3.1 EMPTY RACK

As in [1], a standard 5 bays deep drive-in rack model was constructed for this study using beam-line elements based on centroidal line geometry. The 3D view of the FEA model is displayed in figure 1a while figure 1b shows the general arrangement of the drive-in rack system.

All structural steel components of the drive-in rack model are made from structural steel with Young's modulus E = 200 GPa, Poisson ratio μ = 0.3, density ρ = 7850 kg/m^3. For this study, elastic material has been assumed.

The properties of each type of element are given in Table 1 and its associated figures 1c to 1e.

For this study, the top plan portal beams were assumed to be pin-connected to the top of the uprights. The base of the uprights in the down-aisle direction were assumed to be semi-rigid with a rotational stiffness taken as 359 kNm/rad as described in [2]. The pallet runner beams were assumed to be pin-connected to the support cantilevers.

The frame was assumed to be simply supported at the base of the uprights in the cross-aisle direction.

A static load case with a down aisle force of 1000 N magnitude was applied to the model as shown in figure 2a. This static load case was then combined with the load factor versus time table in Strand7 to provide the instantaneous impulse force for the dynamic analysis. For different impulse periods ΔT, different load factor versus time tables were used. Figure 2b shows a typical load factor versus time table for the case ΔT = 0.086 second.

Due to a convergence problem arising from the use of tension-only beam elements (with zero compression limit) to model the 29CHS2.0 bracing members, the compression limit in these members had to be increased to about 400N. The design capacity of these 29CHS2.0 bracing members (effective length of 2m) is approximately 5 kN which is much higher than the above limit. The effect of the increased compression limit is to increase the stiffness of the top plan bracing, thus causing a slight reduction in the displacement at the front of the rack due to the impact load.

3.2 LOADED RACK

The rack described in section 3.1 was loaded with a standard load of 2000 kg/m per level. While there are multiple combinations for the arrangement of the pallets, the following six cases have been assumed for this study:

- Loaded Rack Case 1 - top pallet level loaded only
- Loaded Rack Case 2 - bottom level loaded only
- Loaded Rack Case 3 - both levels loaded
- Loaded Rack Case 4 - both levels loaded for the front bay only
- Loaded Rack Case 5 - both levels loaded for the middle bay only
- Loaded Rack Case 6 - both levels loaded for the back bay only.

Figure 3 illustrates the loading configuration of the above cases.

The masses due to the weight of the pallet were applied to the model as point masses approximately 1.5m above the rail beam at each level. The masses were linked to the rail beams by means of artificially inclined stiff beams as shown in figure 4. At the end of the inclined beam, a point contact element was used to connect the element to the rail beam. For this study, a friction coefficient of 0.1 was assigned to the point contact element. While this modelling is an approximate representation of the actual mass distribution, it is considered adequate for providing an understanding of the effect of mass on the dynamic behaviour of the rack.

4 DAMPING ASSUMPTION AND NATURAL FREQUENCIES

In Strand7, damping can be modelled through two viscous damping models: Rayleigh damping and modal damping. The modal damping model is only available in the linear transient solver with the use of the mode superposition method. The Rayleigh damping model is more versatile and can be used with the non-linear transient solver. In addition, due to the lack of accurate measurement of the critical damping ratio for drive-in rack systems, the Rayleigh damping model provides the more appropriate way to model the damping of the structure, and has been adopted in this study.

Limited studies have been carried out to investigate the damping of the drive-in rack systems. An early report [3] indicates that the first-mode damping values are much larger in the down-aisle direction (ranging from 3% to 9% of critical) than in the cross-aisle direction (ranging from 0.5% to 3% of critical). Further studies in [4] and [5] show substantial differences in the measured damping ratios, which vary from 0.5% to 4.5%.

Given the large range of experimental results, it has been decided to investigate several values of damping ratio, i.e. 1%, 3% and 5%. This should also indicate the sensitivity of the dynamic behaviour of the rack system to the damping ratio.

Rayleigh damping, also known as proportional damping, is one of the most common models of damping in finite element analysis. In this model, damping is assumed to be a linear combination of the stiffness and mass matrices of the following form

$$[C] = \alpha[M] + \beta[K]$$

where [C], [M] and [K] are the damping, mass and stiffness matrices respectively, and α and β are called the stiffness and mass proportional damping constants respectively. The damping matrix, defined as a linear combination of the mass and stiffness matrices, shares the common property of the two matrices that it also is an orthogonal matrix of the free vibration modes. Because of this, Rayleigh damping can be used to decouple modal responses in the mode superposition technique. The relationship between α and β and the damping ratio ζ at some specified frequency ω is given by

$$\zeta = \frac{1}{2}\left(\frac{\alpha}{\omega} + \beta\omega\right)$$

The constants α and β are often determined by using values of the damping ratio ζ_1 and ζ_2 at two chosen frequencies ω_1 and ω_2. Solving two simultaneous equations based on the above relationship yields

$$\alpha = \frac{2\omega_1\omega_2\left(\zeta_2\omega_1 - \zeta_1\omega_2\right)}{\omega_1^{\,2} - \omega_2^{\,2}}$$

$$\beta = \frac{2\left(\zeta_1\omega_1 - \zeta_2\omega_2\right)}{\omega_1^{\,2} - \omega_2^{\,2}}$$

Usually ω_1 and ω_2 are chosen such that they cover all the frequencies of interest in the design, with ω_1 as the lowest and ω_2 the highest in the frequency range.

Whilst Rayleigh damping tends to under-damp the structure over the frequency range between ω_1 and ω_2 and over-damp the frequencies outside this range, in most cases it provides an efficient and straightforward method of modelling damping of the system. When choosing the two frequencies at which the damping factors are to be specified, the frequencies should be as close as possible to the upper and lower limits of the frequency range of interest, to minimize any error in the Rayleigh method.

Reference [6] suggests that the damping ratios of the lower and upper range of frequency may be assumed to be equal, or $\zeta_1 = \zeta_2 = \zeta$. The first natural frequency of the empty drive-in rack model was determined from the Strand7 natural frequency analysis to be 1.186 Hz. Therefore, 0.05Hz and 2Hz have been adopted as the lower and upper frequencies for the Rayleigh damping model respectively. Graphs of the damping ratio versus frequency for ζ equal to 0.01, 0.03 and 0.05 are shown in figures 5a to 5c respectively.

The natural frequencies and periods (T) for the first mode of vibrations are tabulated in table 2 for the unloaded rack and each of the loaded rack cases with the mode shapes shown in figures 6a to 6g. For the loaded rack cases, it has been assumed that the pallet mass and its stiffness are an integral part of the system for the natural frequency analysis. It can be observed from the table that all the loaded rack case have higher period of oscillation than the empty rack case. As a result, it can be expected that longer impact load duration is required to excite the loaded racks.

For the empty rack case, further inspection of the second mode indicates that the period of oscillation of the impacted upright is 0.25 second. The second mode shape is given in figure 6h.

5 RESULTS OF FINITE ELEMENT DYNAMIC ANALYSIS

5.1 EMPTY RACK RESULTS

The deflection responses at the front face of the empty drive-in rack (refer to figure 7a) are given in figures 8a to 8f for various load duration cases with 1%, 3% and 5% damping. Similarly, the displacement gap response at the top pallet level (figure 7b) and the down aisle bending moment at the base of the outer upright (figure 7a) are plotted in figures 8g to 8l and 8m to 8r respectively.

Inspection of those figures indicates that while the displacement at the front face of the rack has one complete cycle equal to the first mode period of the rack, the period of oscillation of the gap displacement and bending moment at the base of upright is approximately one fourth of the first mode period.

The peak response of the front face deflection, the displacement gap at the top pallet level and the bending moment at the base for various cases are summarized in tables 3a to 3c respectively.

The above results indicate that the displacements and bending moments of the empty drive-in rack system are amplified considerably when taking into account dynamic effects, especially for longer load durations. It has been noticed that for load duration ΔT/T above 0.5 (or ΔT larger than 0.428 second), the peak response of the front face deflection remains unchanged. However, the peak response of the gap displacement and the bending moment at the base of the impacted upright are constant when the load duration ΔT is more than 0.086 second. The reason for this is that the period of oscillation of the upright in the second mode shown in figure 7 is about a quarter of the period of the first (sway) mode of the frame.

Furthermore, it can be observed that the maximum peak gap displacement for the 1000N dynamic load is 40.5mm (for 1% damping) which is nearly twice the static analysis value (22.5mm). It has also been noticed that the minimum pallet bearing width, which varies depending on the rack manufacturer requirement, is generally set at 20 to 25mm.

For the empty rack case, the peak bending moment at the base of the impacted front upright is 1937 Nm which is again significantly more than the linear static result (1202 Nm). While this number is small compared to the section capacity of the RF12519 upright (9130 Nm), a larger impact load in the order of 5000 N can lead to localized failure for the upright even with the rack in its empty state.

5.2 LOADED RACK RESULTS

The results for various loading scenarios are given in the following subsections.

5.2.1 Load Rack Case 1 – Top Level Loaded Only

The deflection responses at the front face of the loaded rack case 1 are given in figures 9a to 9f for the six load duration cases with 1%, 3% and 5% damping. Similarly, the displacement gap response at the top pallet level and the down aisle bending moment at the base of the impacted upright are plotted in figures 9g to 9l and 9m to 9r respectively.

The peak response of the front face deflection, the displacement gap at the top pallet level and the bending moment at the base for the loaded rack case 1 model are summarized in tables 4a to 4c respectively.

The above results indicate that longer load durations cause slightly larger peak displacements at the top of the rack and larger gap displacement at second pallet level. The peak values however are less than the static value for load durations less than 1 second, which is significantly lower than the natural period of oscillation of this rack case (3.98 second). For a load duration of 5 seconds, the peak value becomes significantly larger than the static results. This load duration of 5 second however is for the purpose of this study only as in practice the impact duration would be realistically less than 1 second. It has also been noticed that the peak displacements slightly increase as the damping ratio decreases.

It can be observed for the above case that the stiff pallets acted as some type of bracing at the loaded pallet level since the static friction force between the pallets and the rail support is greater than the applied horizontal load. As a result, the gap displacement at the second pallet level becomes rather small when compared to the empty rack case.

5.2.2 Load Rack Case 2 – Bottom Level Loaded Only

The deflection responses at the front face of the loaded rack case 2 are given in figures 10a to 10f for the six load duration cases with 1%, 3% and 5% damping. Similarly, the displacement gap response at the top pallet level and the down aisle bending moment at the base of the impacted upright are plotted in figures 10g to 10l and 10m to 10r respectively.

The peak response of the front face deflection, the displacement gap at the top pallet level and the bending moment at the base for the loaded rack case 2 model are summarized in tables 5a to 5c respectively.

For this loaded rack case (T = 1.66s), the results indicate that the peak displacement at the top of the rack and the peak bending moment at the base of the front upright are considerably larger than the static results for load durations larger than 0.428 second ($\Delta T/T$ larger than 0.26). For load durations larger than 1 second, the peak displacements remain essentially unchanged. Also, it has also been observed that the peak displacements and bending moments slightly increase as the damping ratio decreases.

It has also been noticed that the peak displacement gap response at the top pallet level remains constant for any load duration for a given coefficient of friction, and that the peak gap displacements are slightly larger than the static value.

As for loaded rack case 1, the stiff pallets in this case provide additional stiffness to the rack at the bottom pallet level. With this extra bracing system in place, the lateral force applied will be attracted to the stiffer bottom half of the rack rather than the top half. As a result, the peak displacement at the front face of the rack in this case is significantly smaller than that of the loaded rack case 1.

5.2.3 Loaded Rack Case 3 - both levels loaded

The deflection responses at the front face of the loaded rack case 3 are given in figures 11a to 11f for the six load duration cases with 1%, 3% and 5% damping. Similarly, the displacement gap response at the top pallet level and the down aisle bending moment at the base of the impacted upright are plotted in figures 11g to 11l and 11m to 11r respectively.

The peak response values of the front face deflection, the displacement gap at the top pallet level and the bending moment at the base for the loaded rack case 3 model are summarized in tables 6a to 6c respectively.

It can be observed that the behaviour of this fully loaded rack case (T = 3.38s) is similar to that of the loaded rack case 1 with the longer load duration resulting in larger peak displacement responses. The peak value however is less than the static value for the load durations less than 1 second. For the load duration of 5 seconds, the peak value becomes significantly larger than the static results.

5.2.4 Loaded Rack Case 4 - both levels loaded for the front bay only

The deflection responses at the front face of the loaded rack case 4 are displayed in figures 12a to 12f for the six load duration cases with 1%, 3% and 5% damping. Similarly, the displacement gap response at the top pallet level and the down aisle bending moment at the base of the impacted upright are plotted in figures 12g to 12l and 12m to 12r respectively.

The peak response of the front face deflection, the displacement gap at the top pallet level and the bending moment at the base for the loaded rack case 4 model are summarized in tables 7a to 7c respectively.

Observing the above results indicates that the behaviour of this loaded rack case (T = 2.13s) is similar to that of loaded rack case 2 with the exception of the peak gap displacement response. While for loaded rack case 2, the peak gap displacement tends to remain constant for all the load duration, for this case the peak gap displacement increases with longer load duration. Also, for load durations more than 0.5 second, the peak gap displacement is larger than that from static analysis. This behaviour also applies to the peak displacement at the front face and the bending moment at the base of the impacted upright.

Based on the results for the loaded rack cases 1 to 4, it can be concluded that the influence of the dynamic factors is decreased when the system is loaded with sufficient friction between the pallets and the supporting rail beams. Under these circumstances, the added mass as well as the enhancement in the down-aisle stiffness of the system result in significant reduction of the rack response when the rack is loaded in the bay where impact occurs (loaded rack case 1 to 4). As expected, loading the rack at the lower pallet level (loaded rack case 2) has a more significant effect in reducing the peak response than loading at the upper level (loaded rack case 1).

However, when the magnitude of the dynamic impact load is significantly larger than the static friction force between the pallet and the rail beams, the extra masses from the pallets are no longer part of the lateral load resistance system. As a result, the behaviour of the rack in that instance is similar to that of the empty one.

5.2.5 Loaded Rack Case 5 - both levels loaded for the middle bay only

The deflection responses at the front face of the loaded rack case 5 are given in figures 13a to 13f for the six load duration cases with 1%, 3% and 5% damping. Similarly, the displacement gap response at the top pallet level and the down aisle bending moment at the base of the impacted upright are plotted in figures 13g to 13l and 13m to 13r respectively.

The peak response of the front face deflection, the displacement gap at the top pallet level and the bending moment at the base for the loaded rack case 5 model are summarized in tables 8a to 8c respectively.

The results for this case (T = 2.13s) show that the behaviour is similar to that for the empty rack case where all the peak top displacement at the front upright, gap displacement and the bending moment at the base of the impacted upright increase with longer load durations. Also, for load durations larger than 0.5 second, the peak responses are significantly higher than the static analysis value.

Observing the response graphs indicates similarities with those of the empty rack case, especially for the gap displacement and the bending moment response.

5.2.6 Loaded Rack Case 6 - both levels loaded for the back bay only

The deflection responses at the front face of the loaded rack case 6 are given in figures 14a to 14f for the six load duration cases with 1%, 3% and 5% damping. Similarly, the displacement gap response at the top pallet level and the down aisle bending moment at the base of the impacted upright are plotted in figures 14g to 14l and 14m to 14r respectively.

Also, the peak response of the front face deflection, the displacement gap at the top pallet level and the bending moment at the base for the loaded rack case 6 model are summarized in tables 9a to 9c respectively.

Inspecting the above result show that this loaded rack case (T = 2.15s) is similar to the previous loaded rack case 5 for which the responses at the impacted bay are close to those of the empty rack case. Hence it can be concluded that the pallets loaded at bays away from the impacted bay have little effect on the behaviour of the impacted upright.

6 A SINGLE DEGREE OF FREEDOM (SDOF) SYSTEM FOR THE EMPTY RACK CASE

A simple SDOF system for the empty rack case can be developed based on the results of the mechanical model in reference [1]. The dynamic equation for this SDOF can be solved explicitly using the central difference method. The results can be used to validate the FE analysis results.

Based on the mechanical model in reference [1], the equivalent stiffness of the SDOF system can be determined as

$K = F_p / \Delta_T = 485 / 0.01127 = 43041$ N/m

where F_P is the force transferred to the top plan bracing and Δ_T is the displacement at the top front face of the rack.

The effective mass is taken as the mass of the components at the top level and is estimated to be 750kg.

Hence, the natural period of this SDOF system is

$$T = 2\pi\sqrt{\frac{M}{K}} = 2\pi\sqrt{\frac{750}{43401}} = 0.829s$$

This value is reasonably close to the natural period calculated by the FE model which is 0.843 second.

The general dynamic equation of a SDOF system is given in the form

$$\ddot{X} + 2\zeta\omega_n\dot{X} + \omega_n^2 X = \frac{P(t)}{M} \qquad (1)$$

The central difference method assumes a linear variation of X, using the known values X_{-1} and X_0 to determine the value X_1 as shown in figure 15. The following relations can be derived

Velocity $\dot{X}_0 = \frac{X_1 - X_{-1}}{2\Delta t}$ (1a)

Velocity $\dot{X}_{-1/2} = \frac{X_0 - X_{-1}}{\Delta t}$ (1b)

Velocity $\dot{X}_{1/2} = \frac{X_1 - X_0}{\Delta t}$ (1c)

Acceleration $\ddot{X}_0 = \frac{\dot{X}_{1/2} - \dot{X}_{-1/2}}{\Delta t} = \frac{X_1 - 2X_0 + X_{-1}}{\Delta t^2}$ (2)

At time t = 0, the dynamic equation can be written as

$$M\ddot{X}_0 + C\dot{X}_0 + KX_0 = P_0 \quad (3)$$

Where P_0 is the applied external force at time t = 0.

$$C = 2\zeta\omega_n M = \zeta(2\pi f)^2 M$$

Replacing (1) and (2) into (3), we obtain

$$M\frac{X_1 - 2X_0 + X_{-1}}{\Delta t^2} + C\frac{X_1 - X_{-1}}{\Delta t} + KX_0 = P_0 \quad (4)$$

Equation (4) can be rearranged as

$$\left\{\frac{1}{\Delta t^2}M + \frac{1}{2\Delta t}C\right\}X_1 = P_0 - \left\{K - \frac{2}{\Delta t^2}M\right\}X_0 - \left\{\frac{1}{\Delta t^2}M - \frac{1}{2\Delta t}C\right\}X_{-1} \quad (5)$$

Displacement X_1 can then be determined from equation (5).

A simple spreadsheet can be set up to calculate the displacement response for a time period of 2 seconds and time step Δt = 0.02 second. The results from this calculation as compared to the finite element analysis results are given in figures 16a to 16c for the case of 3% damping and load durations ΔT = 0.086, 0.428 and 0.856 second respectively. The figures indicate reasonable agreement between the FEA results and the simple SDOF analysis with differences in the peak displacement of 50%, 39% and 39% for load durations ΔT = 0.086, 0.428 and 0.856 second respectively.

7 CONCLUSIONS

A dynamic study has been carried out for a typical drive-in rack for various loading configurations with impact load durations from 0.086 second up to 5 seconds and damping ratios of the system of 1%, 3% and 5%. The results of those investigations are presented in Section 5 of this report. Based on the FE results, it was concluded that:

- For the empty rack case, all peak displacement and bending moment responses measured at the impacted upright are significantly larger than those obtained from static analysis.
- In general, the peak responses are higher when the load duration is longer but there is a limit at which the peak response is unchanged. As would be expected, that limit in load duration is dependent on the natural period of the drive-in rack system.
- For the case where the pallets are loaded in the impacted bay, when the magnitude of the impact load is less than the static friction between the pallets and the rail beams, the pallets enhance the overall lateral stiffness of the system in which they act as extra bracing at those pallet levels. As a result, for these cases, the peak responses of the system are generally less than the static analysis results.
- It can be argued that when the magnitude of the impact load is larger than the static friction force, the pallets no longer contribute to the lateral stiffness and hence the behaviour of the rack will become similar to that of an empty one. This is the situation that can lead to catastrophic failure as the peak gap displacement in this case will be enhanced by the dynamic factors and depending on the magnitude of the impact load, this may cause the pallets to fall off their supports. For this study, with an impact load of only 1000N, the peak displacement gap for the empty rack (22.5 mm) is very close to the nominal bearing width of rack manufacturers (between 20 and 25mm).
- Similarly, the peak bending moment at the base of the impacted upright in some cases can be significantly greater than the static analysis value. The magnitude of the increment in bending moment is dependent on the magnitude and duration of the impact load and to some extent, the dynamic characteristic of the system. However, in terms of member capacity, the upright is less likely to fail in bending alone, as in an empty bay, and is more likely to fail in a combination of axial load and bending moment when that bay is loaded. It is only when the pallets are not part of the system, due to negligible friction at the rail beam interface, that the increase in peak bending moment is likely to cause damage of the impacted upright.
- While the static friction coefficient between the pallets and the rail beams is a very important factor in determining the behaviour of the loaded rack system, it is however not well documented and further study is required to determine this parameter more accurately.
- For all load durations, the level of damping has minor influence on the response of the system with the higher damping ratios resulting in smaller system response as expected.
- A simple single degree of freedom (SDOF) system was established as a means of benchmarking the analytical results. The results of the SDOF model show reasonable agreement with the finite element analysis results.
- More studies are required to accurately assess the static friction coefficient between the pallets and the rail beam interface. From those results, one can determine approximately the level of impact force that is likely to cause damage to the system.
- The behaviour of drive-in racks can be greatly enhanced by increasing the friction between the pallets and the rail beam interface such that the pallets can be considered to be an integral part of the system when subjected to impact load.

8 REFERENCES

1. Vinh, H. and Rasmussen, K. *The Behaviour of drive-in racks under horizontal impact load*. , Research Report R871, 2006. University of Sydney.
2. Moll, Ing. R., *Floor Connection Tests*. 2002, Institut für Schweiβtechnik und Ingenieurbüro Dr. Möll GmbH.
3. Chen, C.K., Scholl, R.E. and Blume, J.A. *Seismic study of industrial steel storage racks*. 1980. San Francisco, California.
4. Williams, A., *High rise steel storage racks subject to earthquake loads*. 2004, BE(Hons) Thesis, University of Sydney.
5. Bermandi Kalantari, *High rise steel storage racks subject to earthquake*. 2005, BE(Hons) Thesis, University of Sydney.
6. Chopra, A.K., *Dynamic of structures - Theory and applications to earthquake engineering*, 1995, Prentice Hall p. 419.

APPENDIX A: NOTATION

C	damping coefficient in dynamic equation
ΔT	impact duration
Δt	time step for dynamic analysis
E	elastic modulus
f	first mode frequency
K	equivalent stiffness of a single degree of freedom system
M	equivalent mass of a single degree of freedom system
μ	Poisson ratio
ρ	density
$P(t)$	Force applied at time t
T	period of first mode of vibration of the structure
X	displacement of a single degree of freedom system
X_{-1}	displacement of a single degree of freedom system at time $T = -\Delta t$
X_0	displacement of a single degree of freedom system at time $T = 0$
X_1	displacement of a single degree of freedom system at time $T = \Delta t$
$\dot{X}$	velocity of a single degree of freedom system
$\ddot{X}$	acceleration of a single degree of freedom system
ω_n	circular frequency = $2\pi f$
ζ	damping ratio

TABLES

Element Name	Description	Modelling Type
Upright	Standard Siemens Upright RF12519 (figure 1b)	Beam
Portal Beam	Standard Siemens Sigma Beam 15019 (figure 1c)	Beam
Plan Bracing	26.9 CHS 2.0	Cut off bar – tension only (compression allowed to 400N)
Spine Bracing	26.9 CHS 2.0	Cut off bar – tension only (compression allowed to 400N)
Cross-aisle Single Frame Bracing	Standard Siemens bracing	Beam Cross Sectional Area = 10.2 mm^2
Cross-aisle Double Frame Bracing	Standard Siemens bracing	Beam Cross Sectional Area = 5.7 mm^2
Pallet Runner	Standard Siemens Rail Beam RB10019 (figure 1d)	Beam
Pallet Runner Support Cantilever	50x25 Channel	Beam

Table 1. Properties of beam elements

Case	First mode of vibration	
	Natural Frequency (Hz)	**Period (second)**
Empty Rack	1.16	0.86
Loaded Rack Case 1	0.25	3.98
Loaded Rack Case 2	0.60	1.66
Loaded Rack Case 3	0.30	3.38
Loaded Rack Case 4	0.47	2.13
Loaded Rack Case 5	0.47	2.13
Loaded Rack Case 6	0.46	2.15

Table 2. Summary of natural frequency and period (T) for the first mode of vibration of the frame

Load Duration (second)	Damping Ratio			Static Result
	5%	3%	1%	
0.086	10.4	10.9	11.6	14.6
0.172	17.7	17.7	19.1	
0.258	25.3	26.0	26.9	
0.428	31.3	32.0	33.2	
0.856	31.3	31.9	33.2	
5.000	31.3	31.9	33.2	

Table 3a. Summary of peak displacement (mm) at top front face of empty rack

Load Duration (second)	Damping Ratio			Static Result
	5%	3%	1%	
0.086	28.7	30.3	31.9	22.5
0.172	36.5	38.4	40.4	
0.258	36.5	38.4	40.4	
0.428	36.5	38.4	40.4	
0.856	36.5	38.4	40.4	
5.000	36.5	38.4	40.4	

Table 3b. Summary of peak gap (mm) at top pallet level of empty rack

Load Duration (second)	Damping Ratio			Static Result
	5%	3%	1%	
0.086	1303	1377	1482	1202
0.172	1701	1794	1924	
0.258	1701	1794	1924	
0.428	1701	1794	1924	
0.856	1701	1794	1924	
5.000	1701	1794	1924	

Table 3c. Summary of peak bending moment (Nm) at the base of outer upright empty rack

Load Duration (second)	Damping Ratio			Static Result
	5%	3%	1%	
0.086	74.0	74.4	75.0	106.0
0.172	76.8	77.4	78.4	
0.258	79.3	80.0	80.9	
0.428	85.2	86.4	88.0	
0.856	98.2	99.9	102.0	
5.000	130.0	134.0	138.0	

Table 4a. Summary of peak displacement (mm) at top front face of loaded rack case 1

Load Duration (second)	Damping Ratio			Static Result
	5%	3%	1%	
0.086	0.30	0.30	0.30	0.39
0.172	0.31	0.31	0.31	
0.258	0.32	0.32	0.32	
0.428	0.34	0.35	0.36	
0.856	0.40	0.41	0.42	
5.000	0.56	0.59	0.62	

Table 4b. Summary of peak gap (mm) at top pallet level of loaded rack case 1

Load Duration (second)	Damping Ratio			Static Result
	5%	3%	1%	
0.086	954	941	972	1389
0.172	960	990	1047	
0.258	960	990	1047	
0.428	963	990	1047	
0.856	1092	1096	1110	
5.000	1714	1767	1831	

Table 4c. Summary of peak bending moment (Nm) at the base of outer upright loaded rack case 1

Load Duration (second)	**Damping Ratio**			Static Result
	5%	**3%**	**1%**	
0.086	20.5	20.7	21.1	33.8
0.172	24.0	24.4	24.9	
0.258	27.0	27.6	28.3	
0.428	32.0	32.6	33.5	
0.856	45.5	46.4	47.3	
5.000	45.5	46.4	47.3	

Table 5a. Summary of peak displacement (mm) at top front face of loaded rack case 2

Load Duration (second)	**Damping Ratio**			Static Result
	5%	**3%**	**1%**	
0.086	12.0	12.3	12.7	10.1
0.172	12.0	12.3	12.7	
0.258	12.0	12.3	12.7	
0.428	12.0	12.3	12.7	
0.856	12.0	12.3	12.7	
5.000	12.0	12.3	12.7	

Table 5b. Summary of peak gap (mm) at top pallet level of loaded rack case 2

Load Duration (second)	**Damping Ratio**			Static Result
	5%	**3%**	**1%**	
0.086	140	146	176	255
0.172	217	229	264	
0.258	283	293	305	
0.428	422	441	475	
0.856	651	674	697	
5.000	457	481	524	

Table 5c. Summary of peak bending moment (Nm) at the base of outer upright loaded rack case 2

Load Duration (second)	**Damping Ratio**			Static Result
	5%	**3%**	**1%**	
0.086	137.0	137.0	137.0	177.0
0.172	140.0	140.0	141.0	
0.258	143.0	144.0	144.0	
0.428	150.0	151.0	151.0	
0.856	165.0	166.0	166.0	
5.000	216.0	217.0	219.0	

Table 6a. Summary of peak displacement (mm) at top front face of loaded rack case 3

Load Duration (second)	**Damping Ratio**			Static Result
	5%	**3%**	**1%**	
0.086	0.43	0.43	0.43	0.85
0.172	0.47	0.47	0.47	
0.258	0.51	0.51	0.51	
0.428	0.60	0.60	0.61	
0.856	0.82	0.83	0.84	
5.000	1.74	1.77	1.81	

Table 6b. Summary of peak gap (mm) at top pallet level of loaded rack case 3

Load Duration (second)	**Damping Ratio**			Static Result
	5%	**3%**	**1%**	
0.086	1888	1891	1895	2487
0.172	1942	1948	1956	
0.258	1995	2002	2012	
0.428	2105	2114	2123	
0.856	2328	2335	2342	
5.000	3098	3116	3137	

Table 6c. Summary of peak bending moment (Nm) at the base of outer upright loaded rack case 3

Load Duration (second)	**Damping Ratio**			Static Result
	5%	**3%**	**1%**	
0.086	18.6	18.8	19.0	33.3
0.172	23.3	23.6	24.1	
0.258	27.7	28.1	28.7	
0.428	36.2	36.2	36.2	
0.856	49.5	49.9	50.2	
5.000	52.8	53.3	54.1	

Table 7a. Summary of peak displacement (mm) at top front face of loaded rack case 4

Load Duration (second)	**Damping Ratio**			Static Result
	5%	**3%**	**1%**	
0.086	6.2	6.2	6.3	7.7
0.172	6.5	6.6	6.6	
0.258	6.8	6.9	7.0	
0.428	7.5	7.6	7.7	
0.856	8.7	8.8	9.0	
5.000	10.4	10.5	10.7	

Table 7b. Summary of peak gap (mm) at top pallet level of loaded rack case 4

Load Duration (second)	**Damping Ratio**			Static Result
	5%	**3%**	**1%**	
0.086	202	206	216	677
0.172	305	316	339	
0.258	400	421	449	
0.428	582	614	658	
0.856	1009	1022	1017	
5.000	1151	1164	1180	

Table 7c. Summary of peak bending moment (Nm) at the base of outer upright loaded rack case 4

Load Duration (second)	**Damping Ratio**			Static Result
	5%	**3%**	**1%**	
0.086	25.3	25.8	26.5	35.0
0.172	29.9	30.4	30.9	
0.258	30.9	31.0	31.1	
0.428	31.6	31.8	32.5	
0.856	37.8	37.5	37.9	
5.000	48.2	49.4	51.7	

Table 8a. Summary of peak displacement (mm) at top front face of loaded rack case 5

Load Duration (second)	**Damping Ratio**			Static Result
	5%	**3%**	**1%**	
0.086	28.7	30.3	32.0	22.5
0.172	36.6	38.5	40.4	
0.258	36.6	38.5	40.4	
0.428	36.6	38.5	40.4	
0.856	36.6	38.5	40.4	
5.000	36.6	38.5	40.4	

Table 8b. Summary of peak gap (mm) at top pallet level of loaded rack case 5

Load Duration (second)	**Damping Ratio**			Static Result
	5%	**3%**	**1%**	
0.086	1435	1509	1614	1351
0.172	1833	1926	2056	
0.258	1833	1926	2056	
0.428	1833	1926	2056	
0.856	1833	1926	2056	
5.000	1833	1926	2056	

Table 8c. Summary of peak bending moment (Nm) at the base of outer upright loaded rack case 5

Load Duration (second)	Damping Ratio			Static Result
	5%	3%	1%	
0.086	20.3	20.9	21.5	29.4
0.172	25.0	25.5	26.0	
0.258	26.2	26.2	26.1	
0.428	27.4	28.0	28.9	
0.856	34.7	34.9	35.0	
5.000	40.2	40.6	42.8	

Table 9a. Summary of peak displacement (mm) at top front face of loaded rack case 6

Load Duration (second)	Damping Ratio			Static Result
	5%	3%	1%	
0.086	28.8	30.4	32.1	22.6
0.172	36.7	38.6	40.5	
0.258	36.7	38.6	40.5	
0.428	36.7	38.6	40.5	
0.856	36.7	38.6	40.5	
5.000	36.7	38.6	40.5	

Table 9b. Summary of peak gap (mm) at top pallet level of loaded rack case 6

Load Duration (second)	Damping Ratio			Static Result
	5%	3%	1%	
0.086	1395	1470	1575	1308
0.172	1794	1887	2017	
0.258	1794	1887	2017	
0.428	1794	1887	2017	
0.856	1794	1887	2017	
5.000	1794	1887	2017	

Table 9c. Summary of peak bending moment (Nm) at the base of outer upright loaded rack case 6

FIGURES

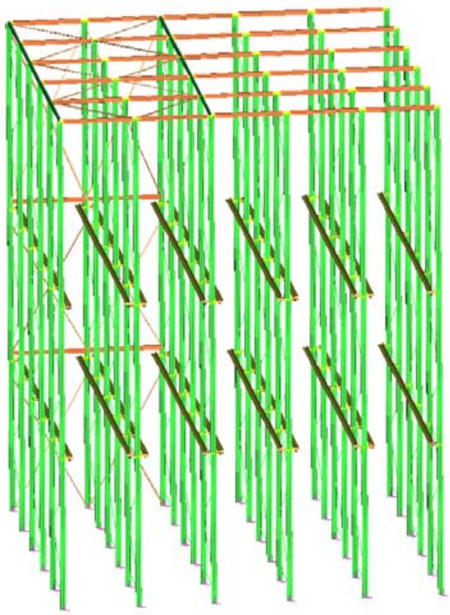

Figure 1a. 3D view of the standard 5 bays Siemens drive-in rack model

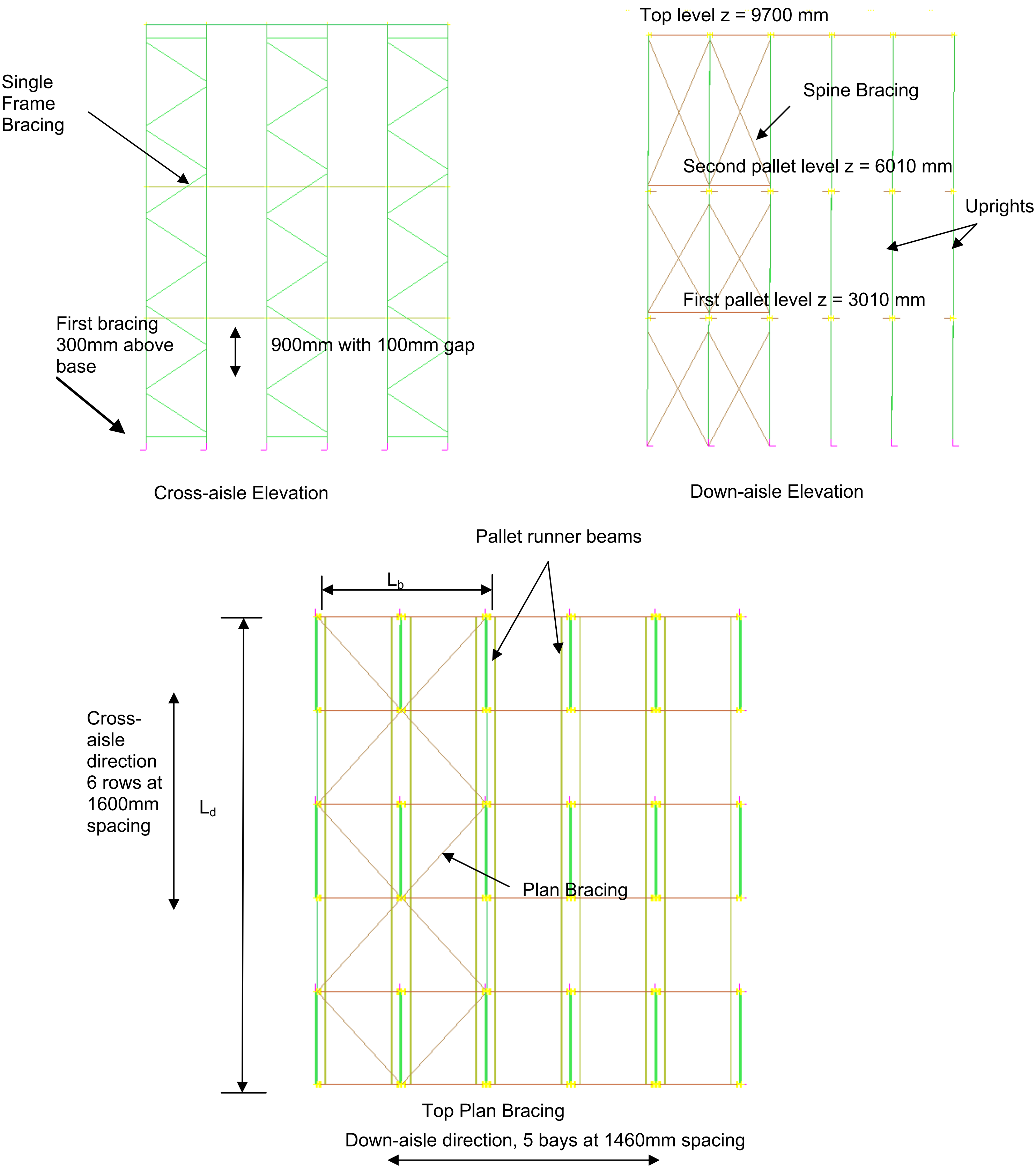

Figure 1b. Drive-in Rack Arrangement

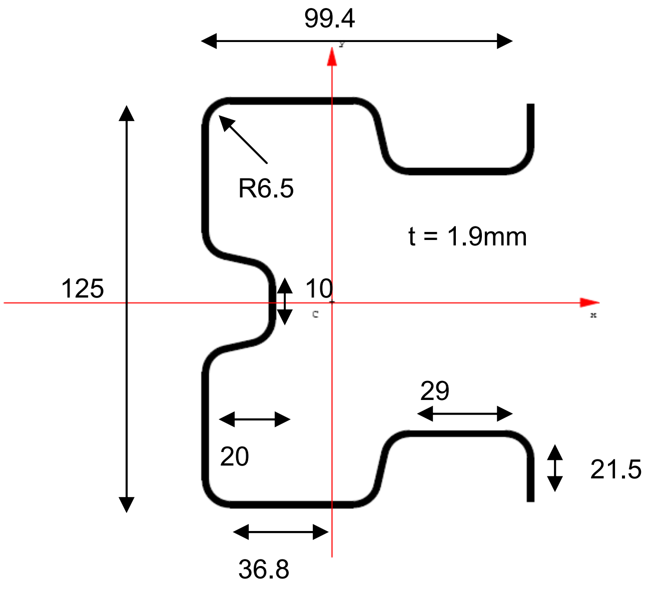

Section Class: New Colby Upright – URF
Section Designation: RF12519/G450
Material: G450

Full Section (Accurate)

A	=	7.562 E-04 m2
Ixx	=	1.599 E-06 m4
Iyy	=	8.779 E-07 m4
Ixy	=	0.000 E+00 m4
Theta	=	0.000 deg
J	=	9.100 E-10 m4
xc	=	3.791 E-02 m
yc	=	0.000 E+00 m

Figure 1c. Standard Siemens Upright RF12519

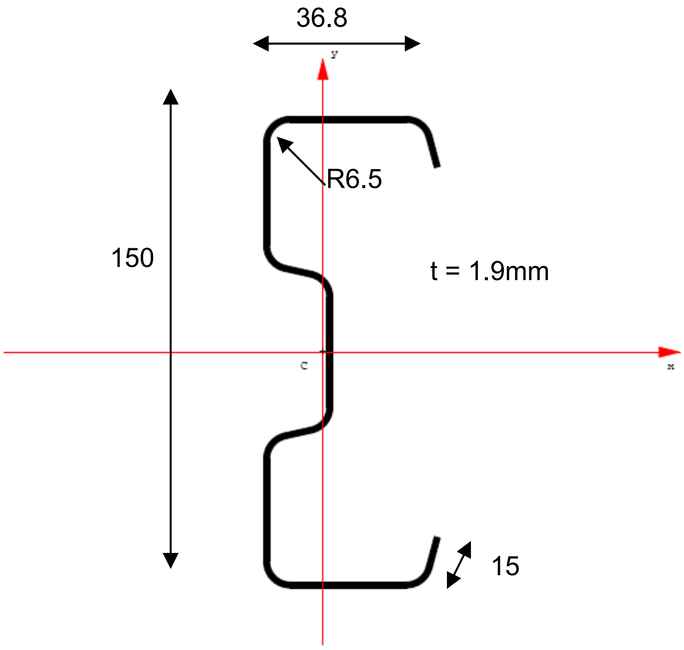

Section Class: Lipped Sigma Section
Section Designation: SB15019/G450
Material: G450

Full Section (Accurate)

A	=	5.591 E-04 m2
Ixx	=	1.746 E-06 m4
Iyy	=	1.683 E-07 m4
Ixy	=	0.000 E+00 m4
Theta	=	0.000 deg
J	=	6.728 E-10 m4
xc	=	1.780 E-02 m
yc	=	0.000 E+00 m

Figure 1d. Standard Siemens Sigma Beam SB15019

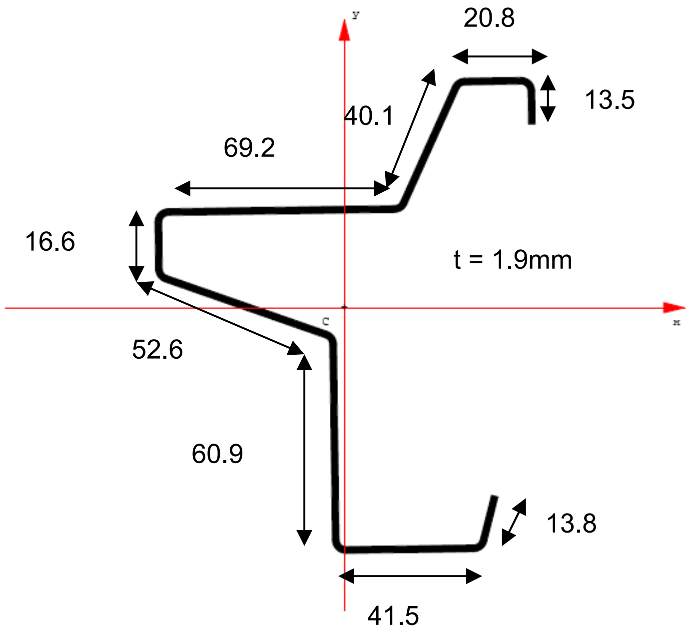

Section Class: New Colby Drive-in Rail
Section Designation: DR10019/G450
Material: G450

Full Section (Accurate)

A	=	6.233 E-04 m2
Ixx	=	1.233 E-06 m4
Iyy	=	5.680 E-07 m4
Ixy	=	0.000 E+00 m4
Theta	=	-0.762 deg
J	=	7.500 E-10 m4
xc	=	-4.262 E-02 m
yc	=	5.489 E-02 m

Figure 1e. Standard Siemens Pallet Runner

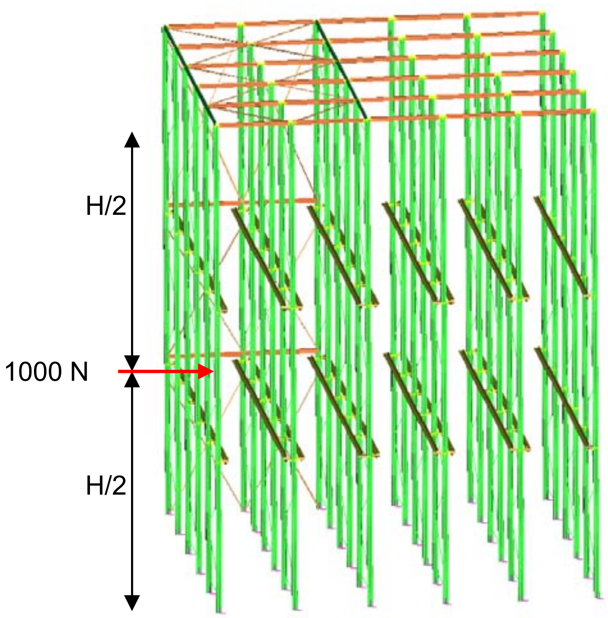

Figure 2a. Static Load 1000N applied at mid height of front row upright

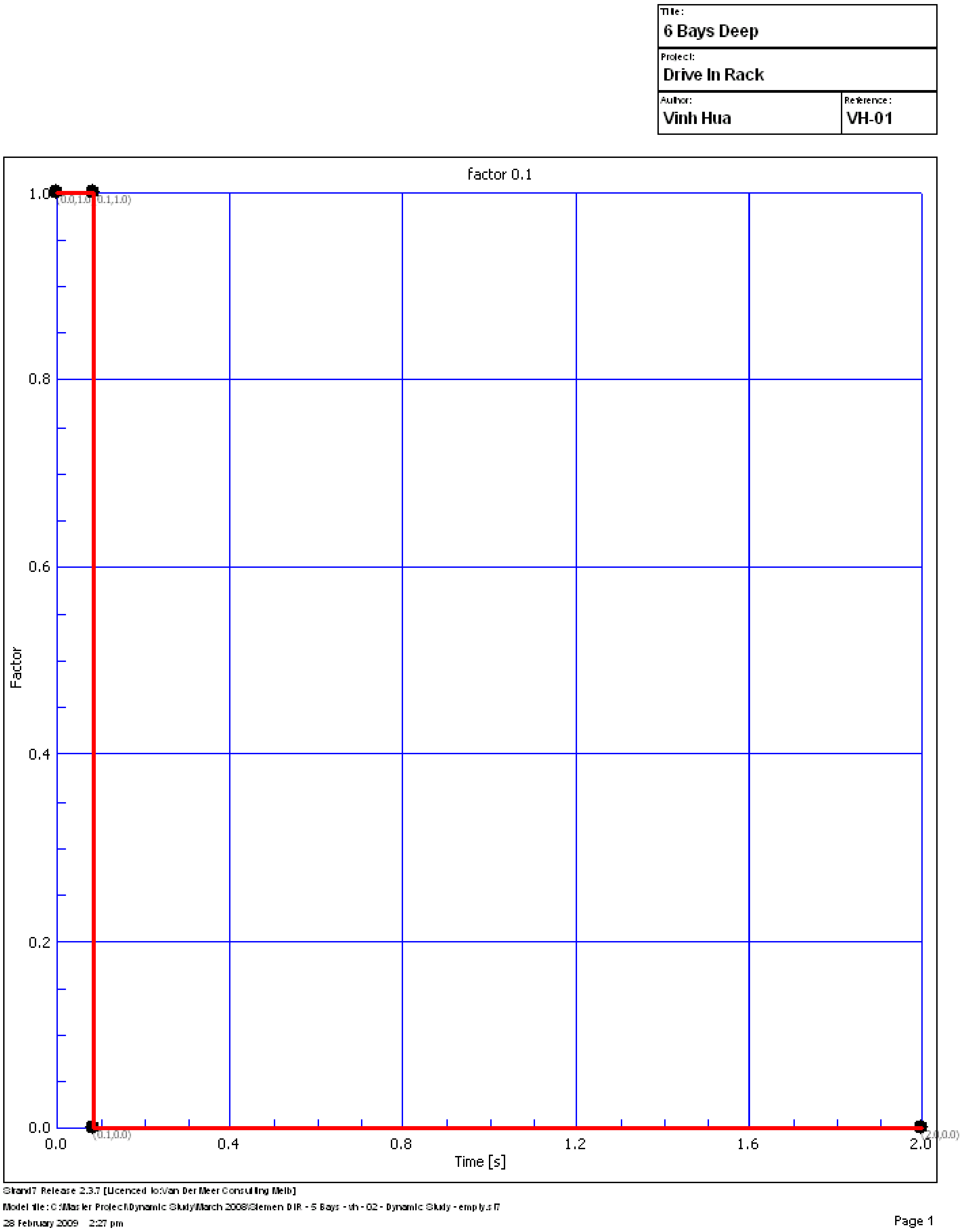

Figure 2b. Factor versus time table for the application of impulse load – ΔT = 0.086s

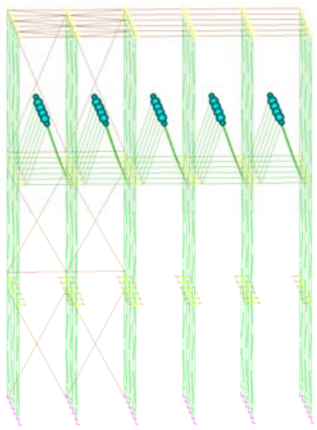

Loaded Rack Case 1
Top pallet level loaded only

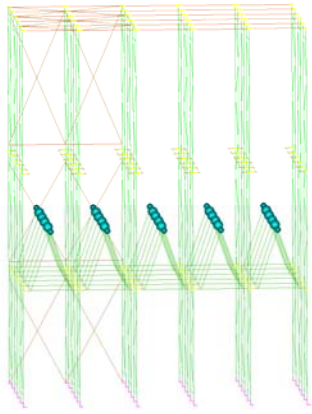

Loaded Rack Case 2
Bottom pallet level loaded only

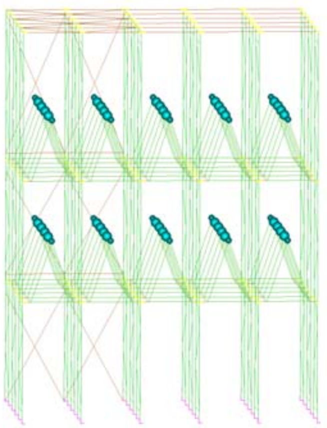

Loaded Rack Case 3
Both pallet levels loaded

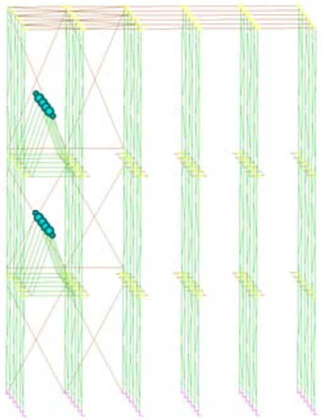

Loaded Rack Case 4
Both levels loaded for the front bay only

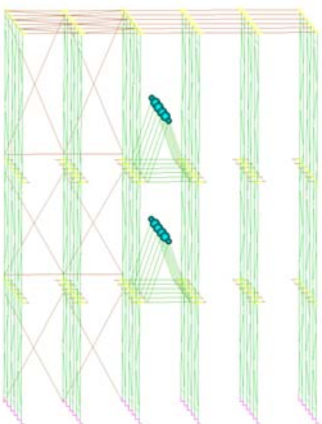

Loaded Rack Case 5
Both levels loaded for the middle bay only

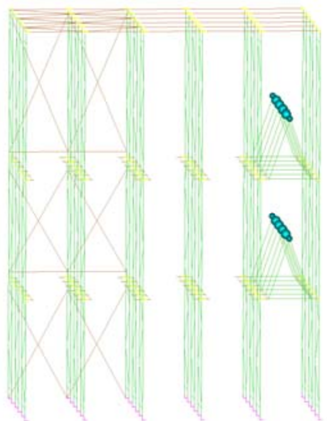

Loaded Rack Case 6
Both levels loaded for the back bay only

Figure 3. Loaded Rack Cases

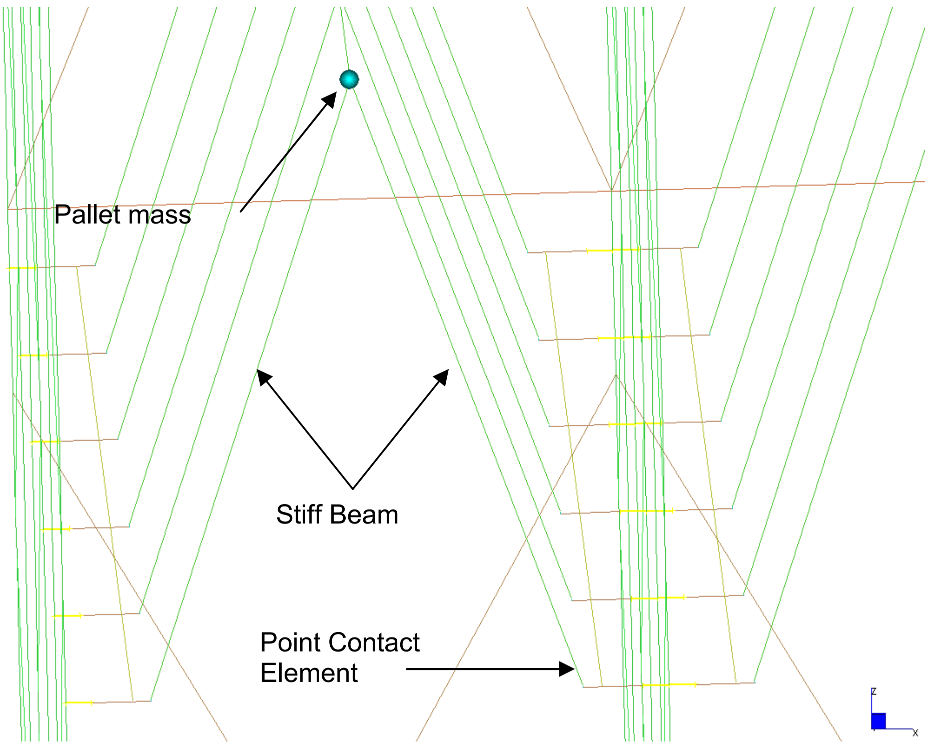

Figure 4. Modelling pallet mass for loaded rack cases

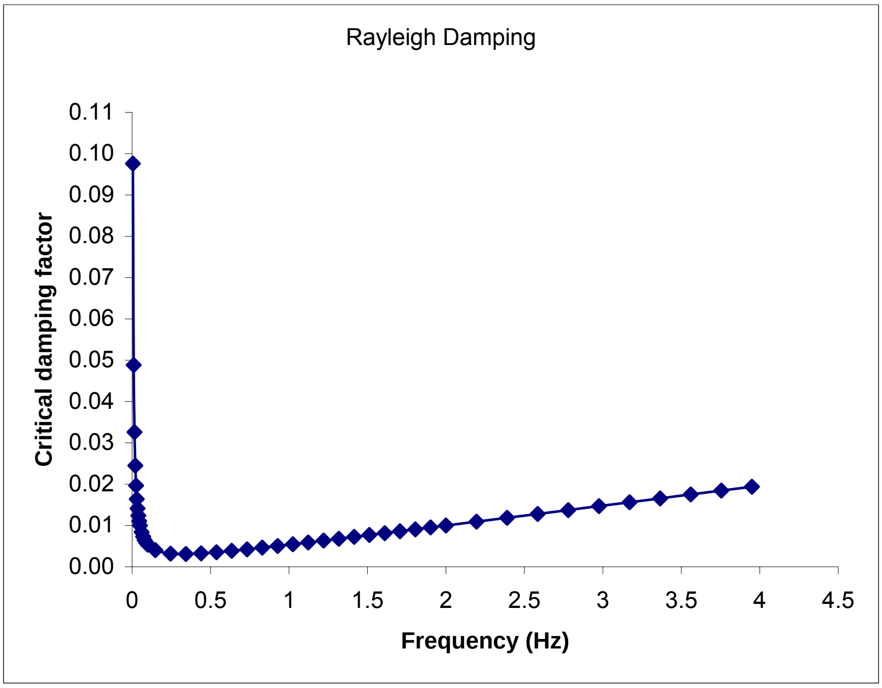

Figure 5a. Damping Ratio vs Frequency (1% critical damping ratio)

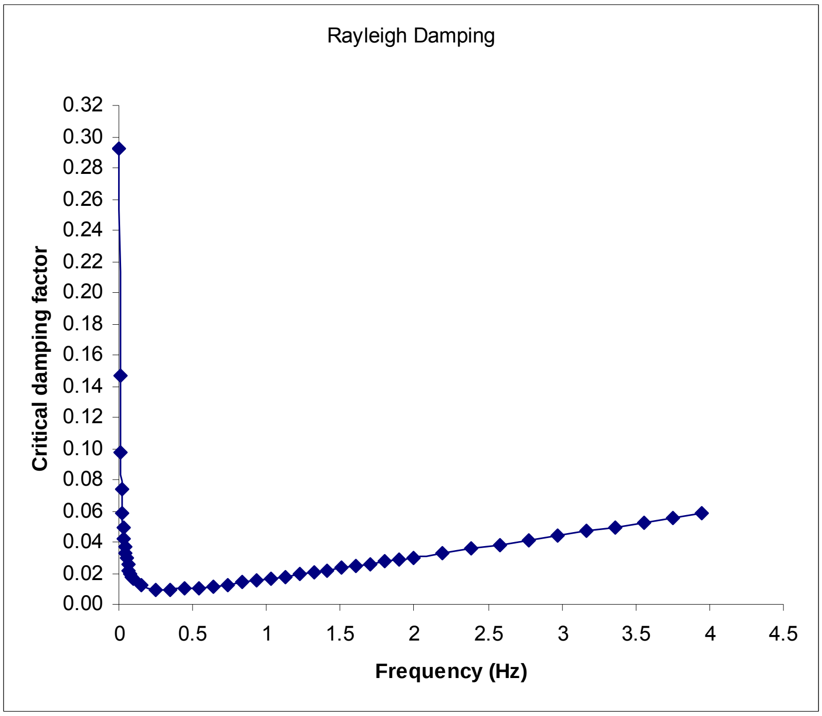

Figure 5b. Damping Ratio vs Frequency (3% critical damping ratio)

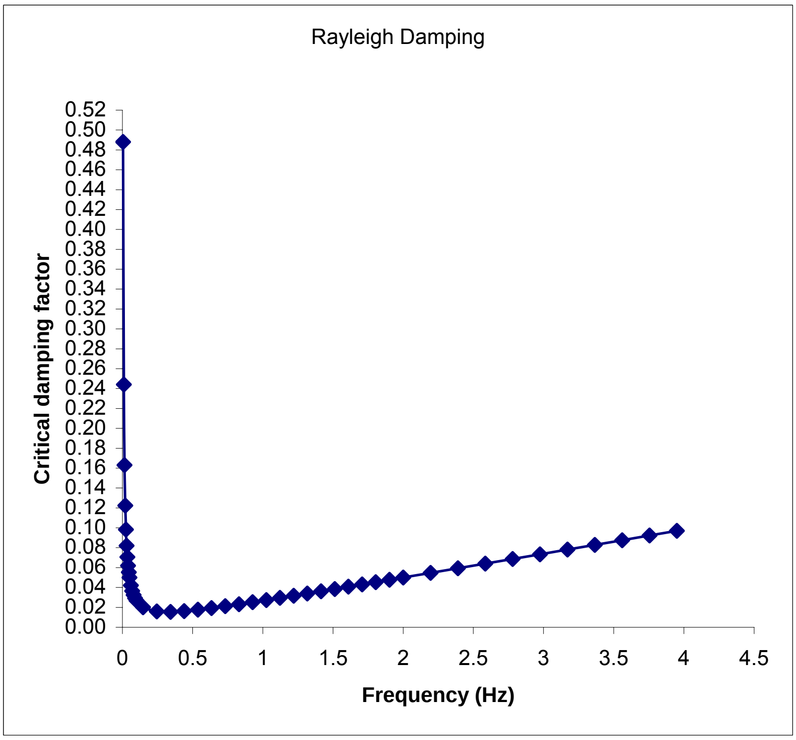

Figure 5c. Damping Ratio vs Frequency (5% critical damping ratio)

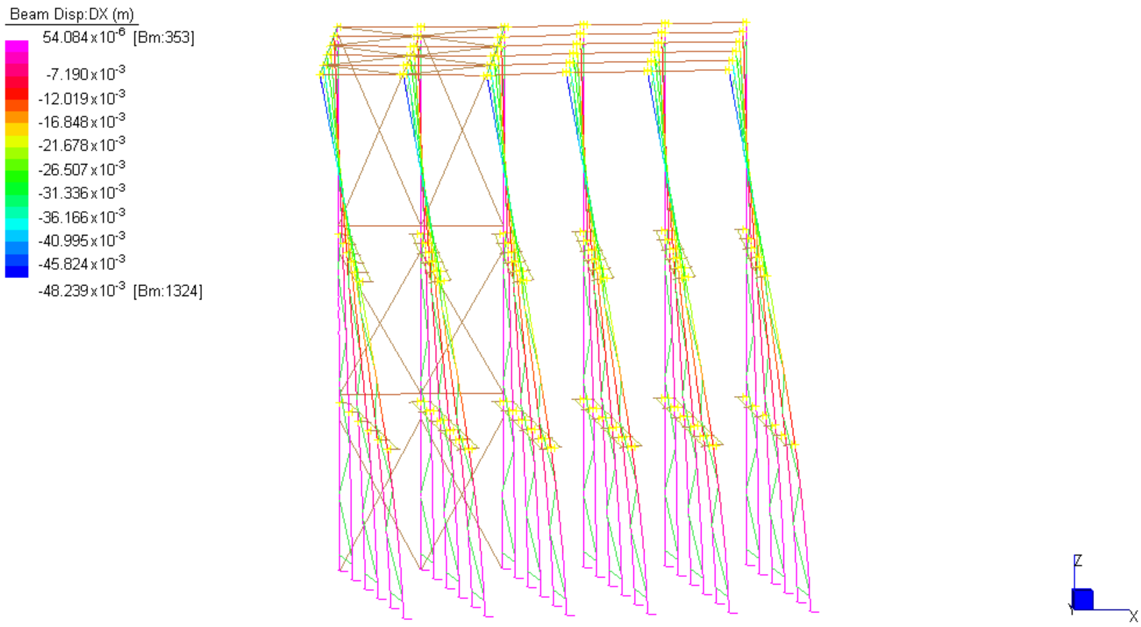

Figure 6a. Mode shape - first mode of vibration of the frame – empty rack

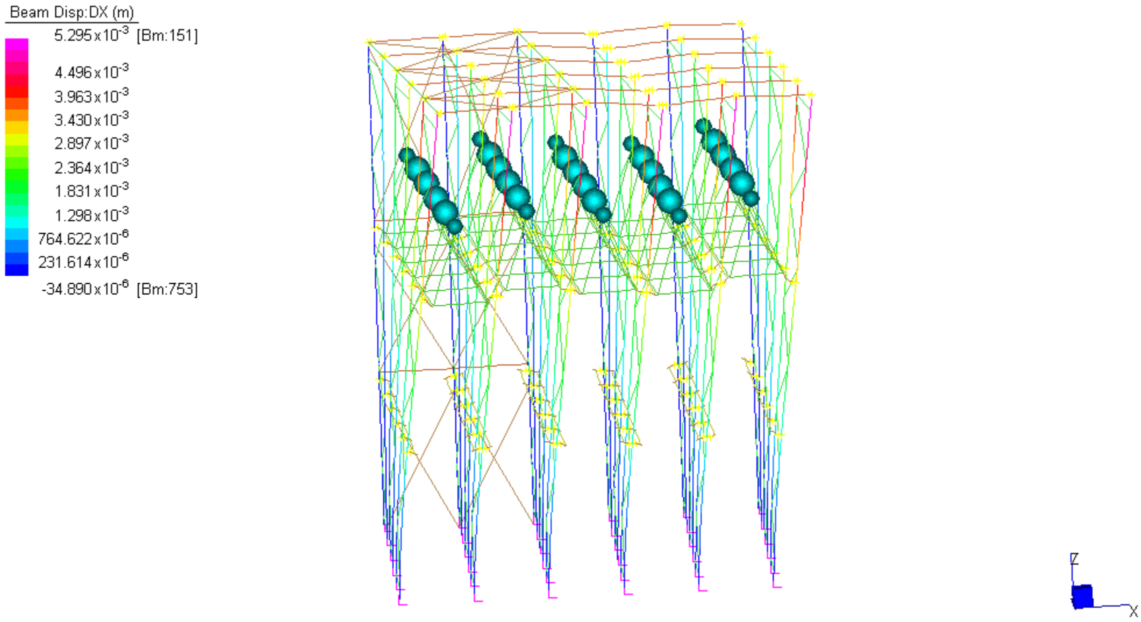

Figure 6b. Mode shape - first mode of vibration of the frame – loaded rack case 1

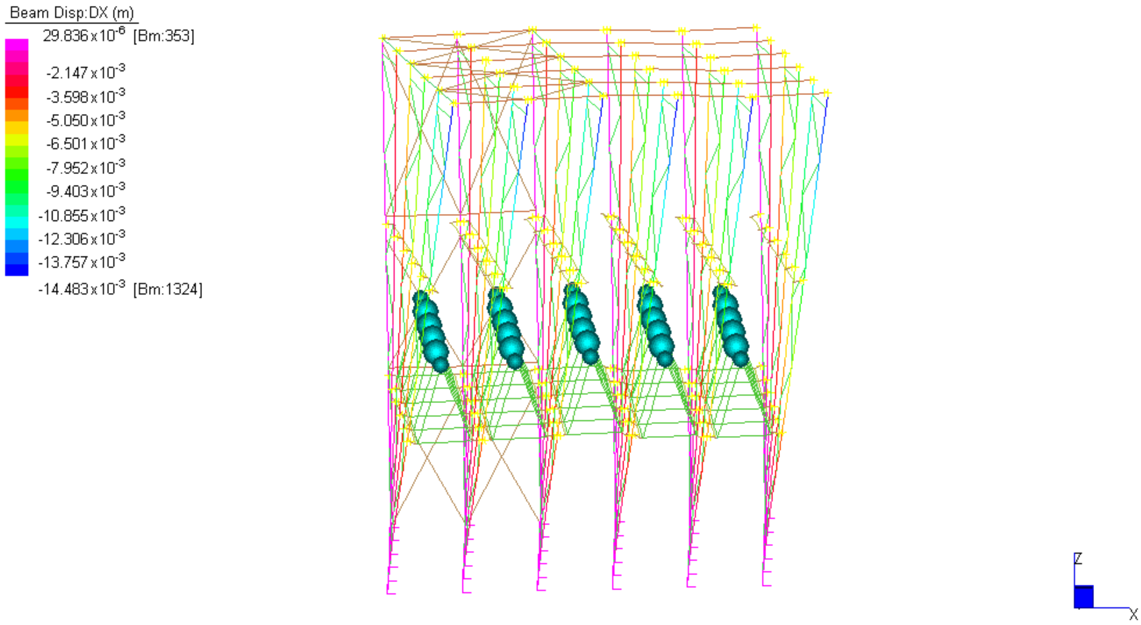

Figure 6c. Mode shape - first mode of vibration of the frame – loaded rack case 2

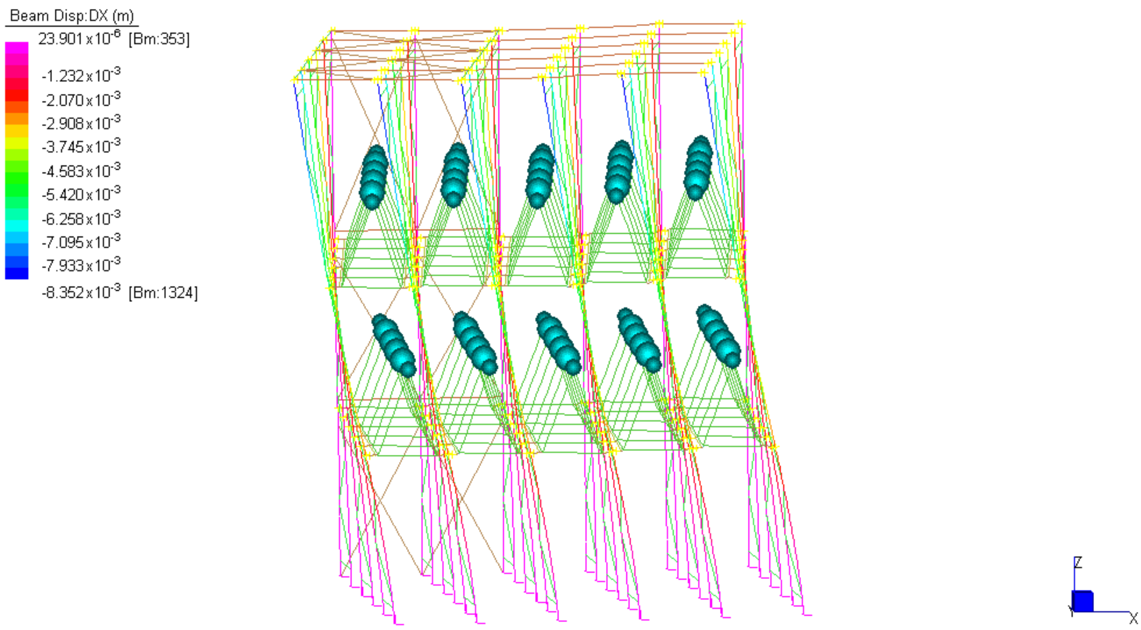

Figure 6d. Mode shape - first mode of vibration of the frame – loaded rack case 3

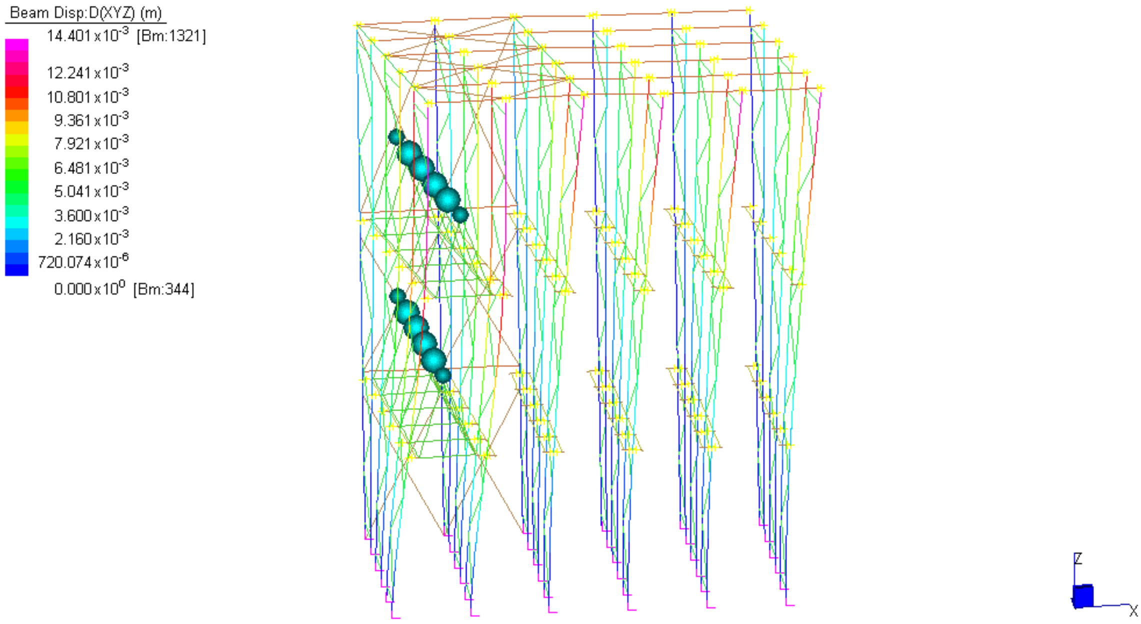

Figure 6e. Mode shape - first mode of vibration of the frame – loaded rack case 4

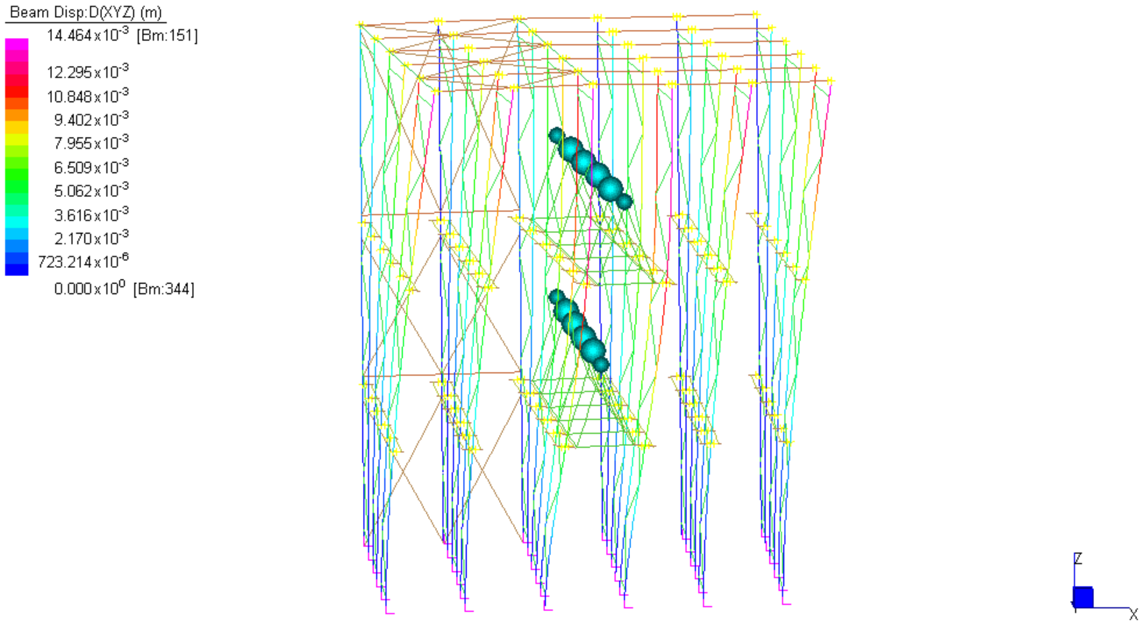

Figure 6f. Mode shape - first mode of vibration of the frame – loaded rack case 5

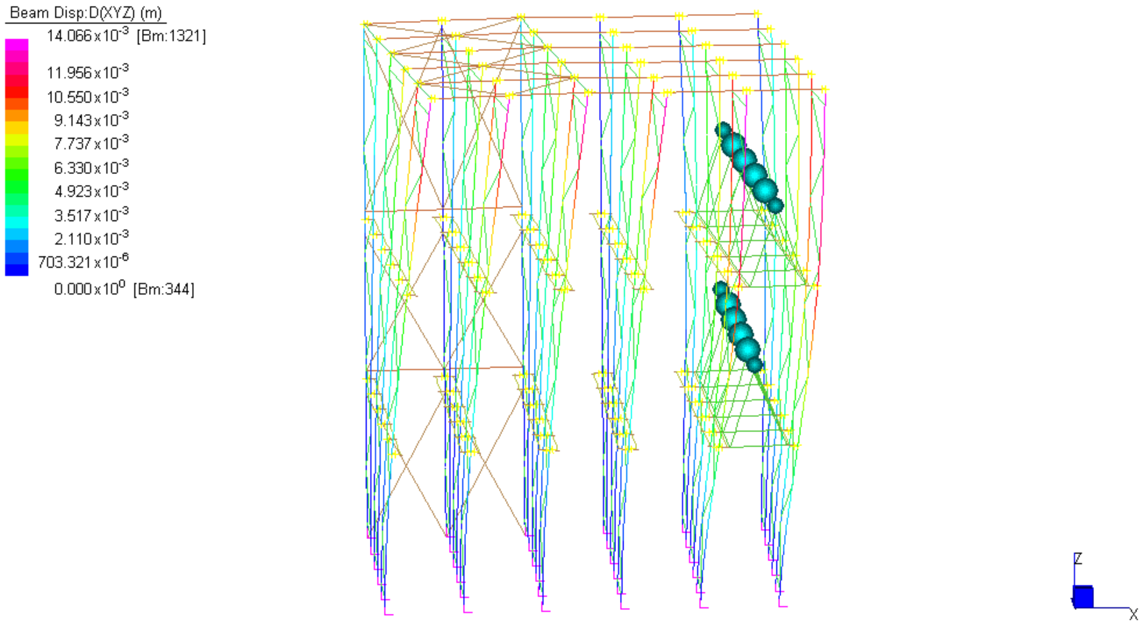

Figure 6g. Mode shape - first mode of vibration of the frame – loaded rack case 6

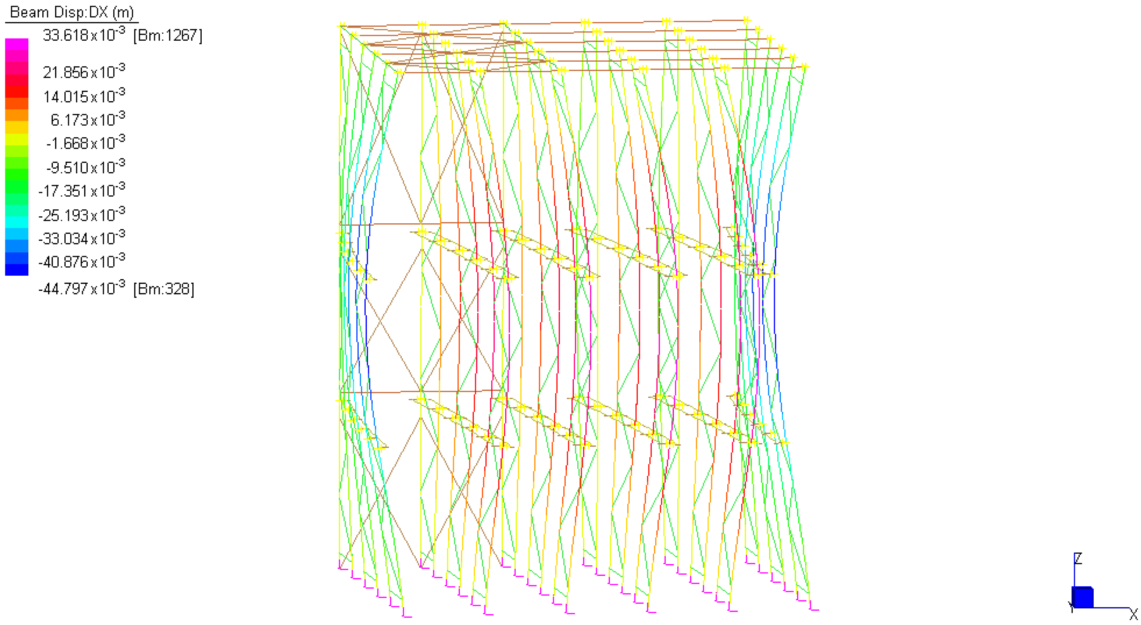

Figure 6h. Mode shape – second mode of vibration of the impacted upright – empty rack

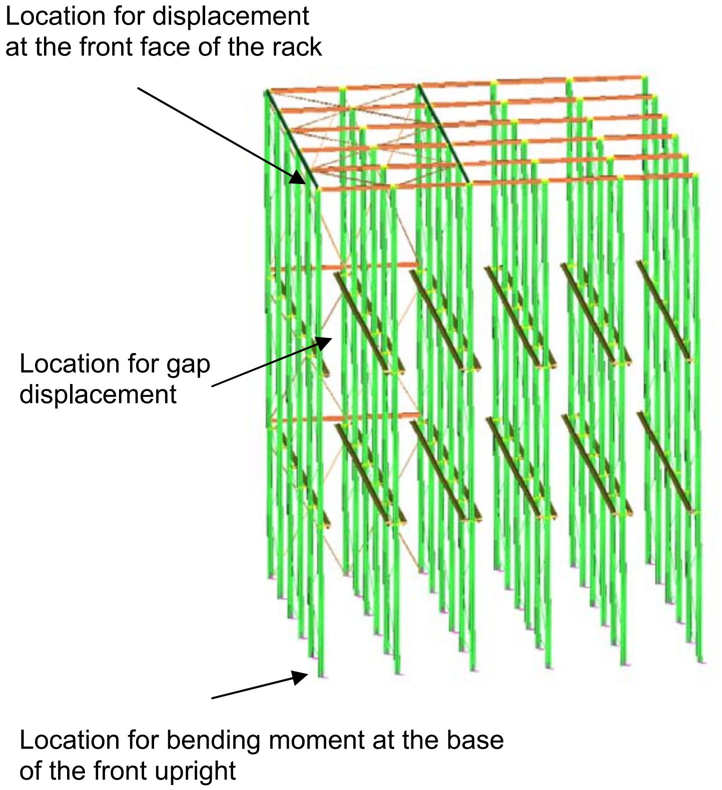

Figure 7a. Location of displacement and bending moment recorded points

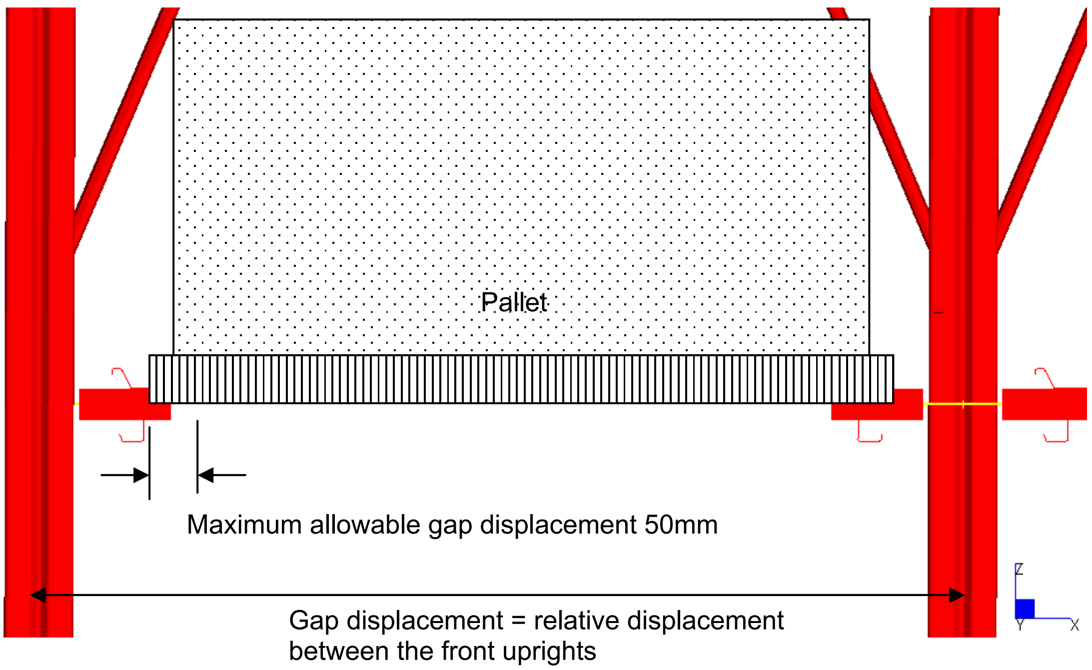

Figure 7b. Gap displacement between uprights

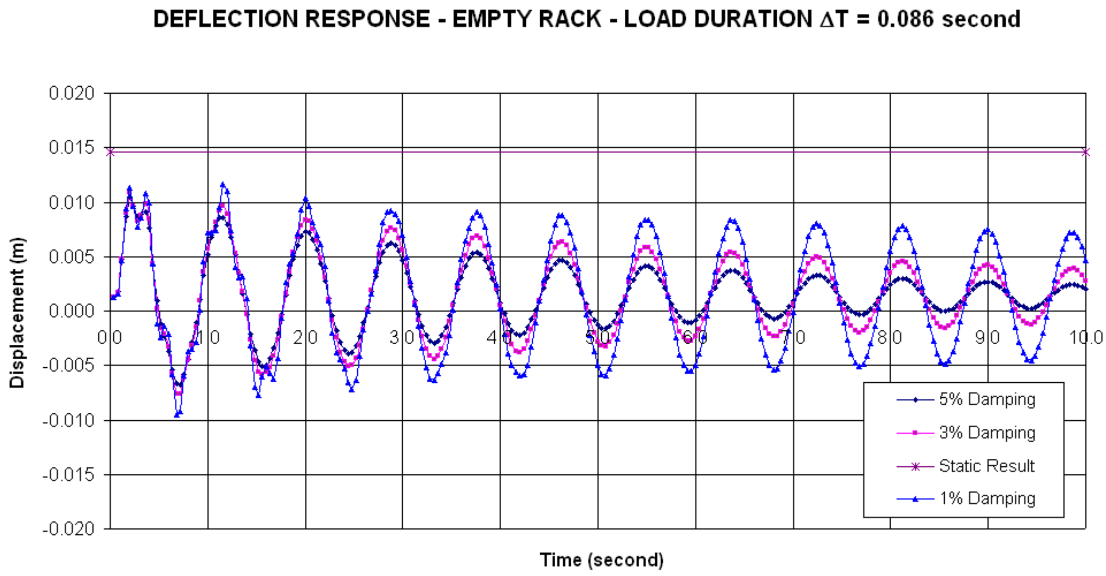

Figure 8a. Deflection Response at the front face of the rack – Empty Rack – Load Duration ΔT = 0.086 second

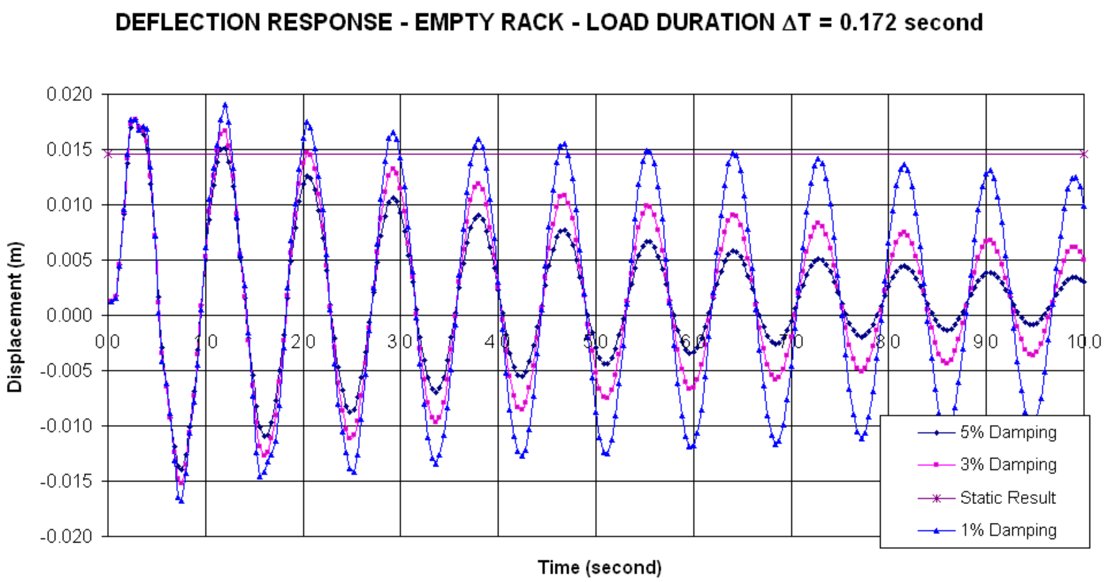

Figure 8b. Deflection Response at the front face of the rack – Empty Rack – Load Duration ΔT = 0.172 second

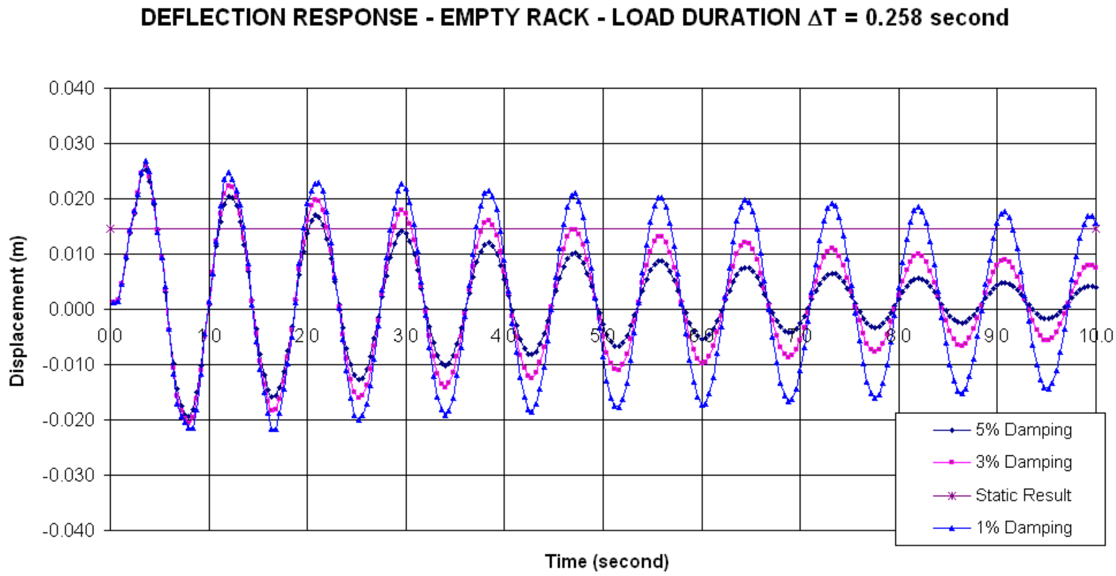

Figure 8c. Deflection Response at the front face of the rack – Empty Rack – Load Duration ΔT = 0.258 second

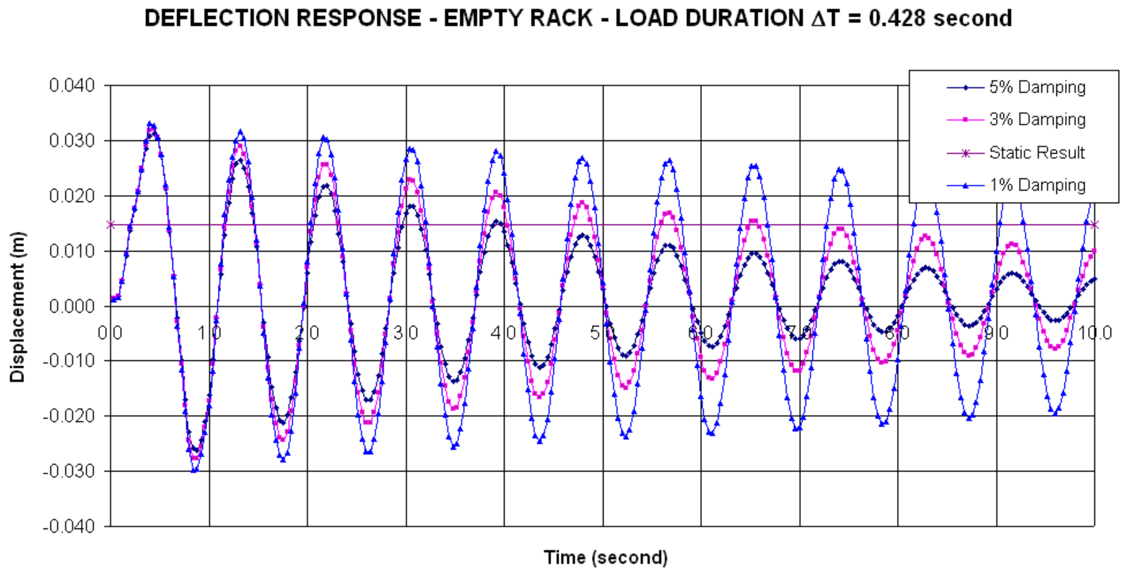

Figure 8d. Deflection Response at the front face of the rack – Empty Rack – Load Duration ΔT = 0.428 second

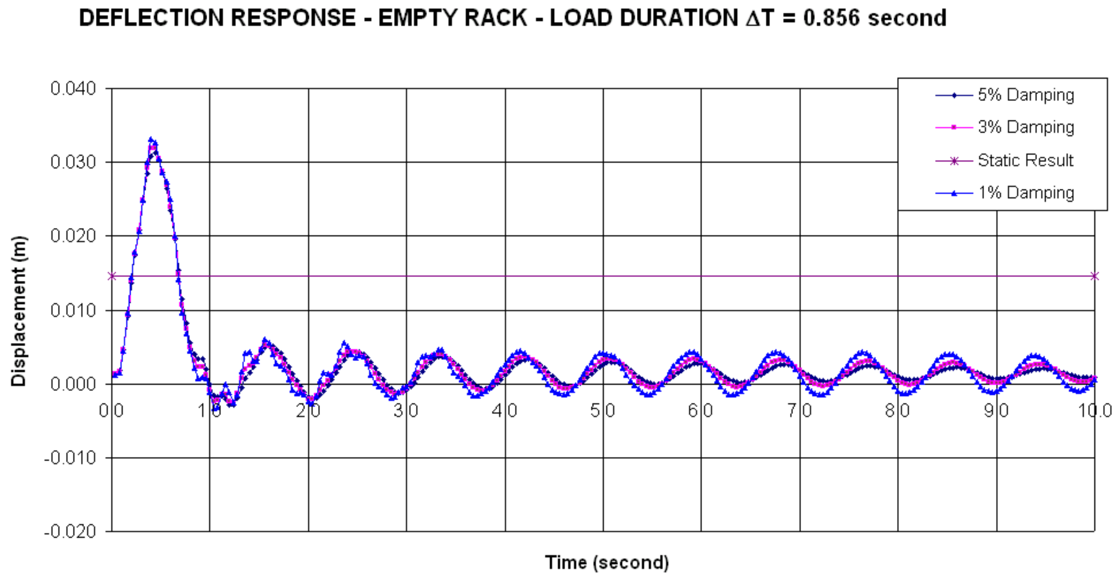

Figure 8e. Deflection Response at the front face of the rack – Empty Rack – Load Duration ΔT = 0.856 second

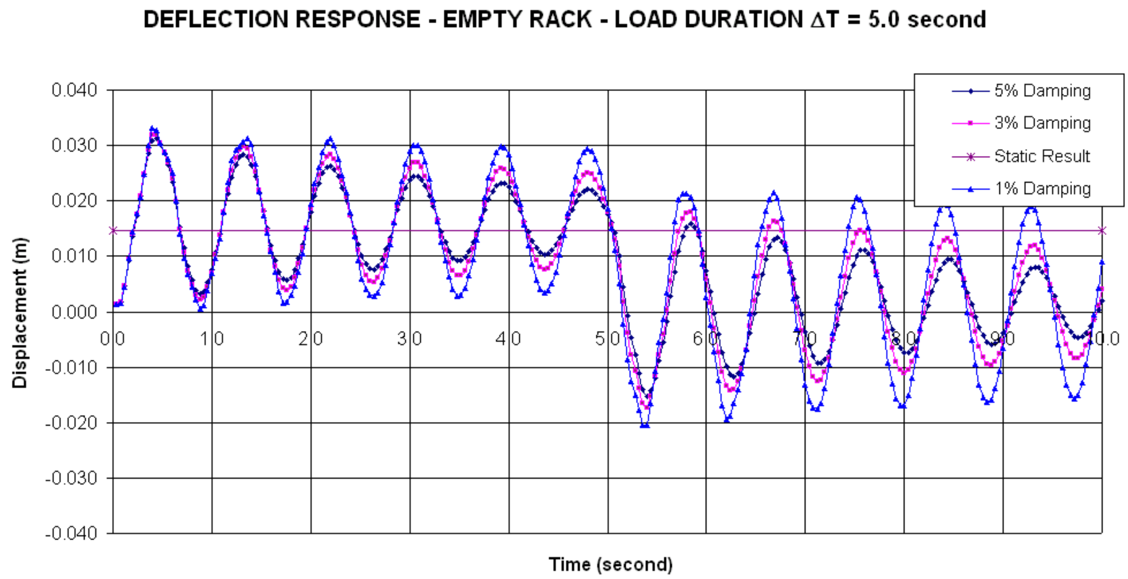

Figure 8f. Deflection Response at the front face of the rack – Empty Rack – Load Duration ΔT = 5.0 second

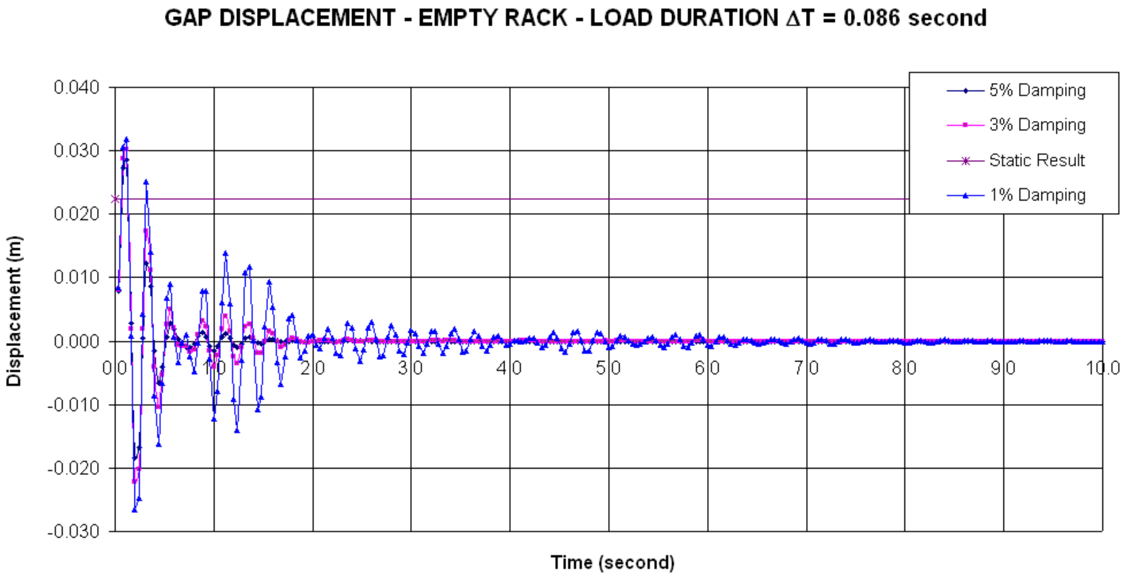

Figure 8g. Displacement Gap Response at the front face of top pallet level – Empty Rack – Load Duration ΔT = 0.086 second

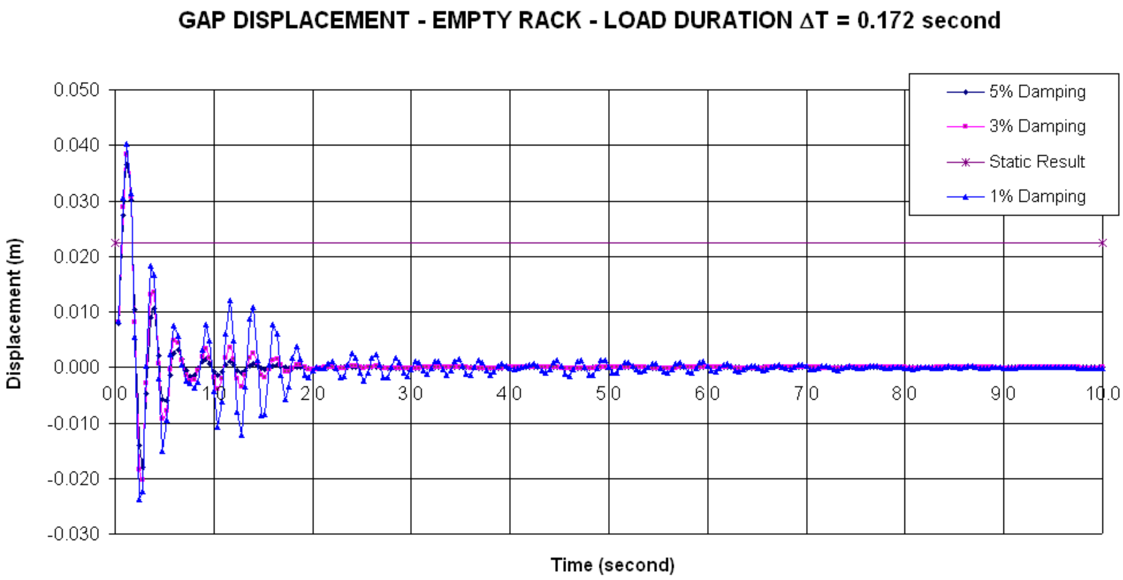

Figure 8h. Displacement Gap Response at the front face of top pallet level – Empty Rack – Load Duration ΔT = 0.172 second

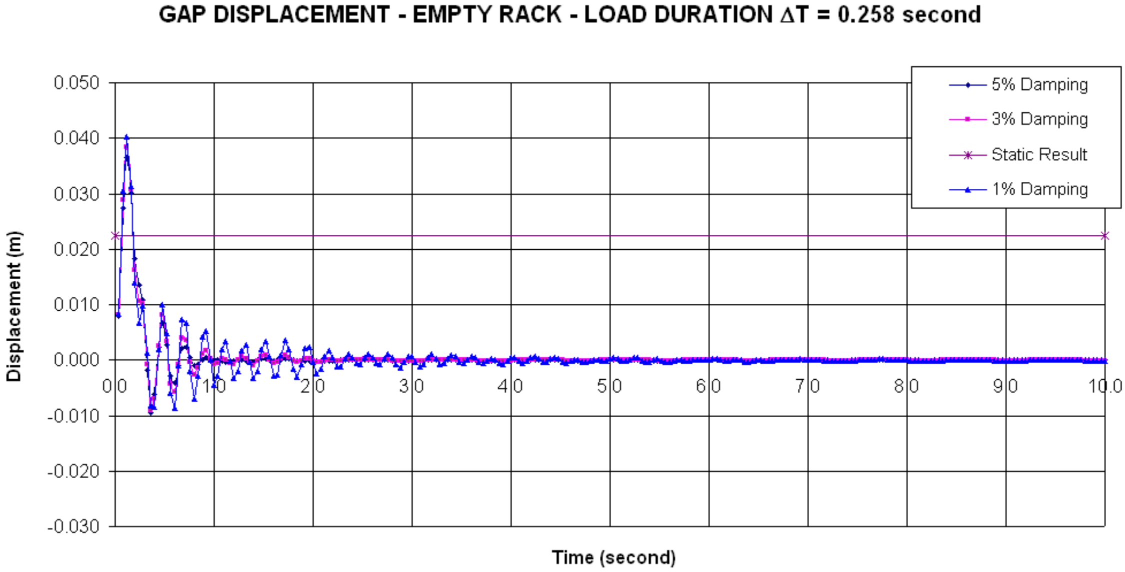

Figure 8i. Displacement Gap Response at the front face of top pallet level – Empty Rack – Load Duration ΔT = 0.258 second

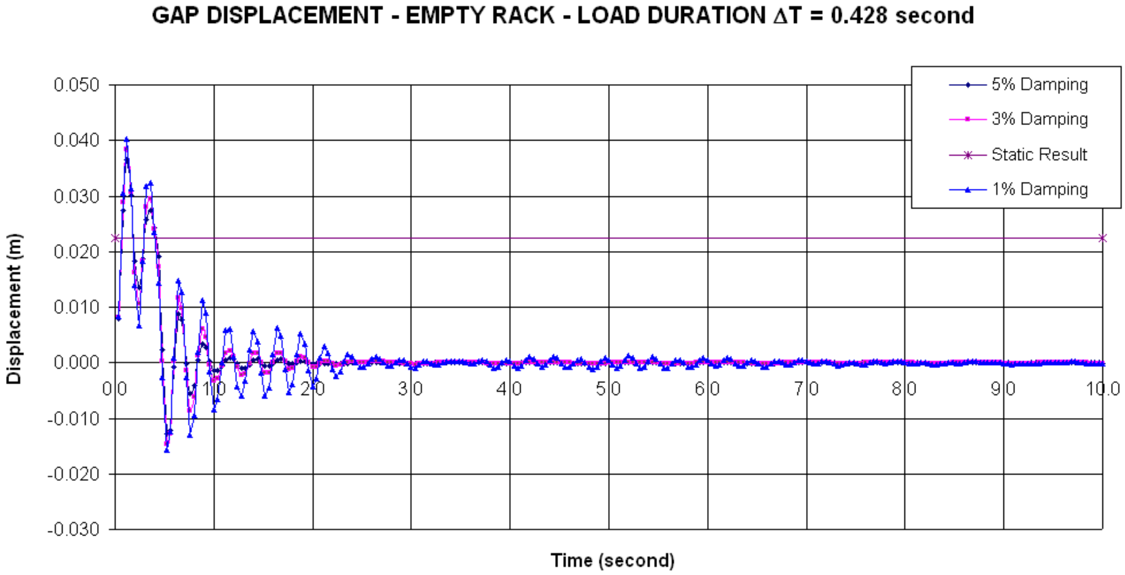

Figure 8j. Displacement Gap Response at the front face of top pallet level – Empty Rack – Load Duration ΔT = 0.428 second

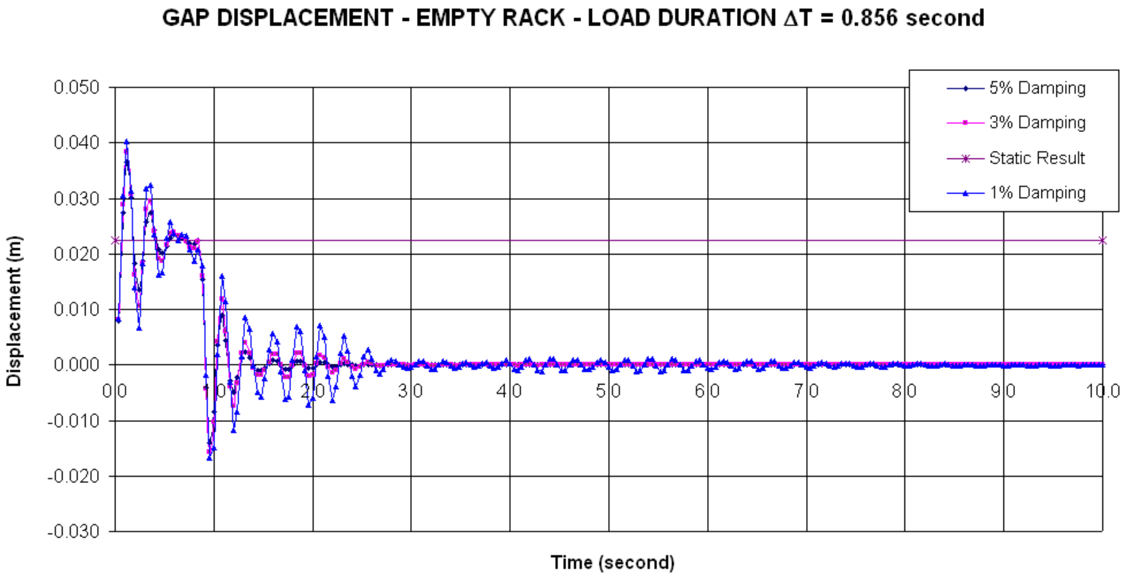

Figure 8k. Displacement Gap Response at the front face of top pallet level – Empty Rack – Load Duration ΔT = 0.856 second

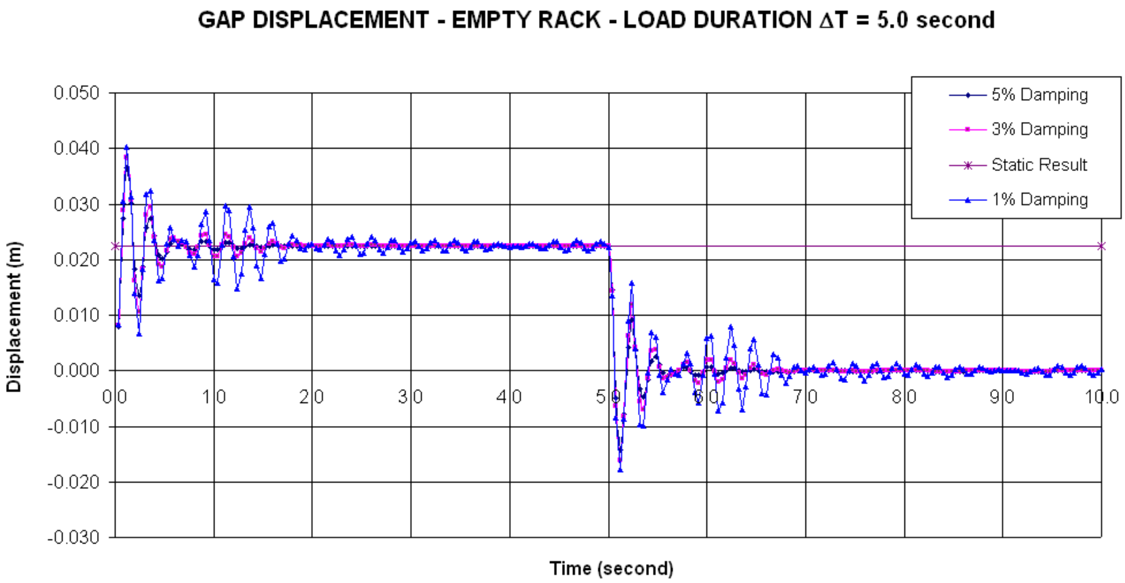

Figure 8l. Displacement Gap Response at the front face of top pallet level – Empty Rack – Load Duration ΔT = 5.0 second

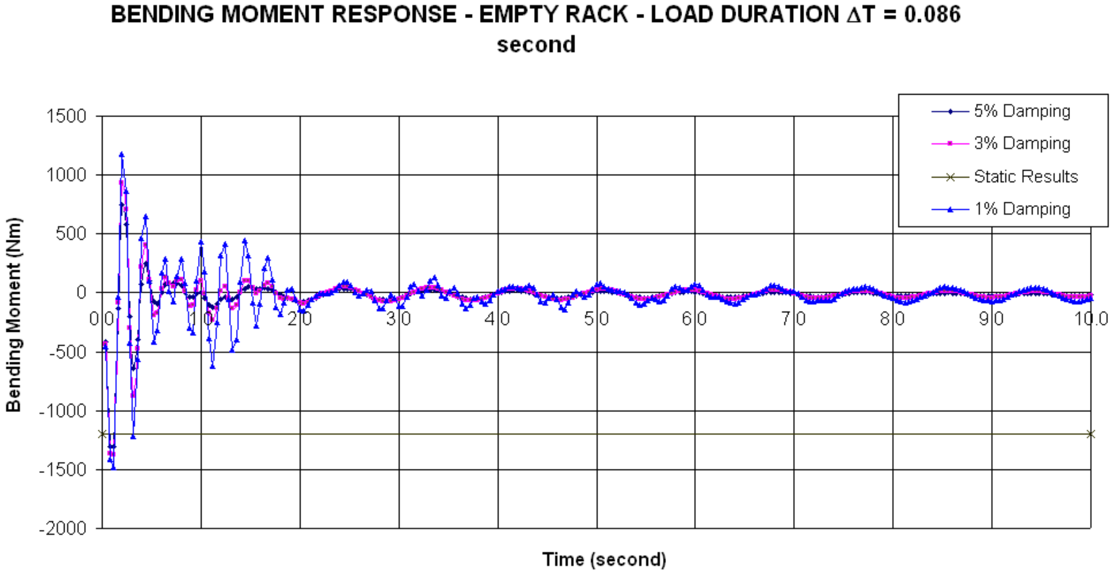

Figure 8m. Bending Moment Response at the base of impacted upright – Empty Rack – Load Duration ΔT = 0.086 second

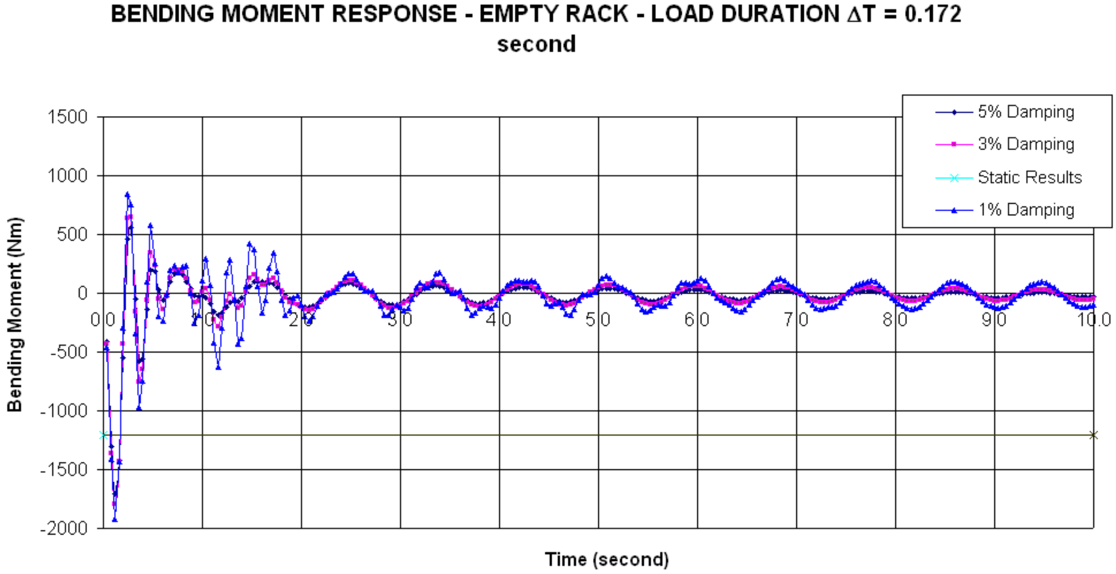

Figure 8n. Bending Moment Response at the base of impacted upright – Empty Rack – Load Duration ΔT = 0.172 second

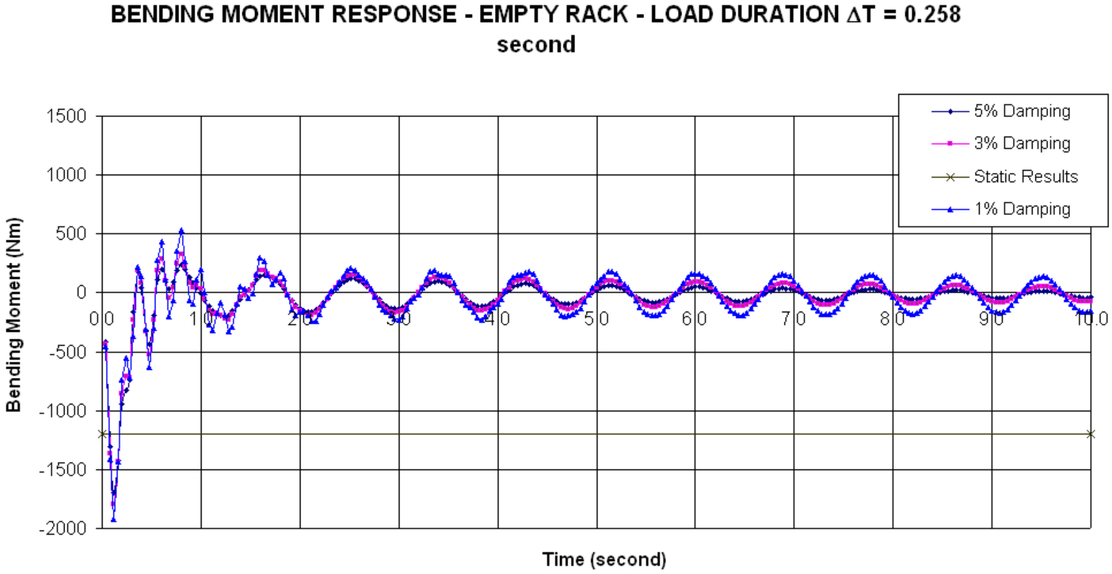

Figure 8o. Bending Moment Response at the base of impacted upright – Empty Rack – Load Duration ΔT = 0.258 second

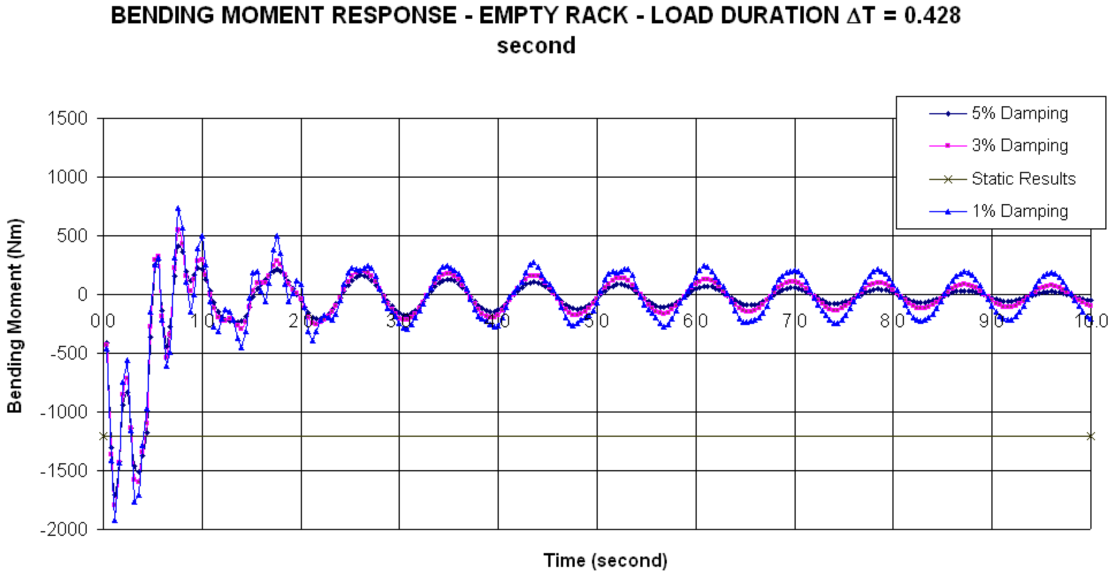

Figure 8p. Bending Moment Response at the base of impacted upright – Empty Rack – Load Duration ΔT = 0.428 second

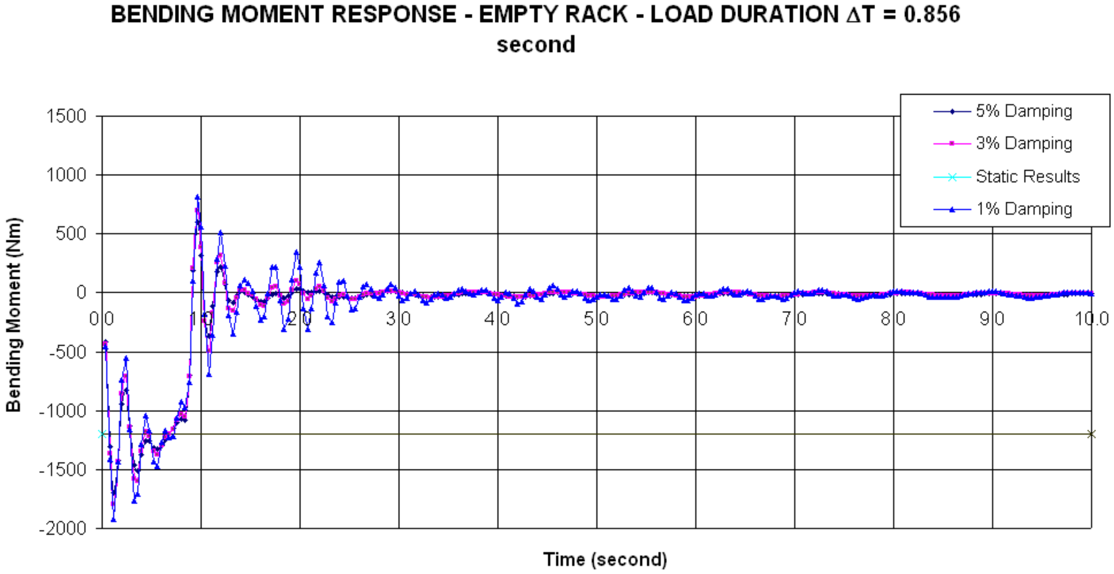

Figure 8q. Bending Moment Response at the base of impacted upright – Empty Rack – Load Duration ΔT = 0.856 second

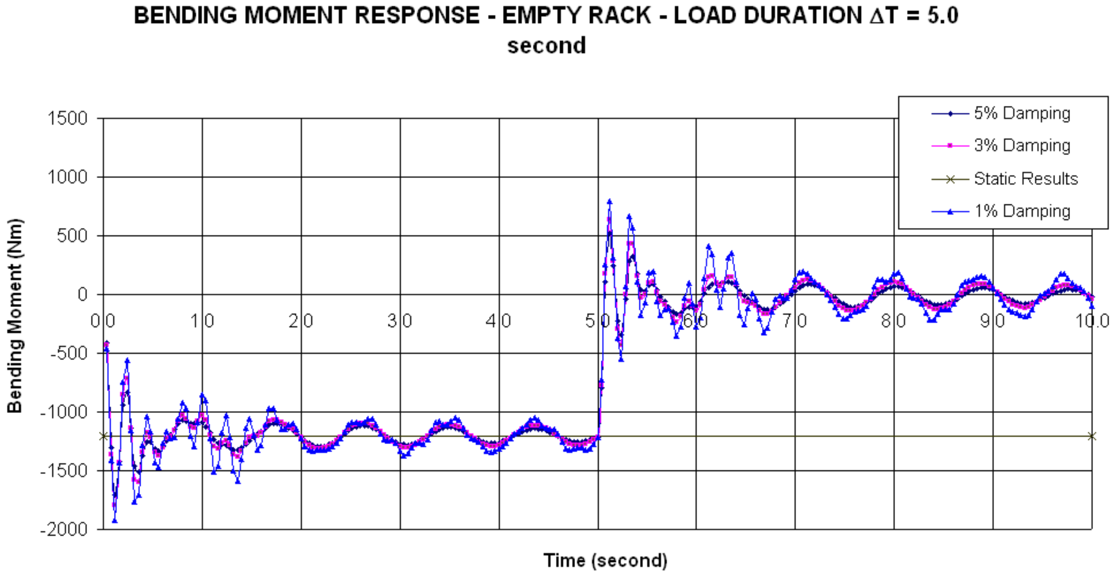

Figure 8r. Bending Moment Response at the base of impacted upright – Empty Rack – Load Duration ΔT = 5.0 second

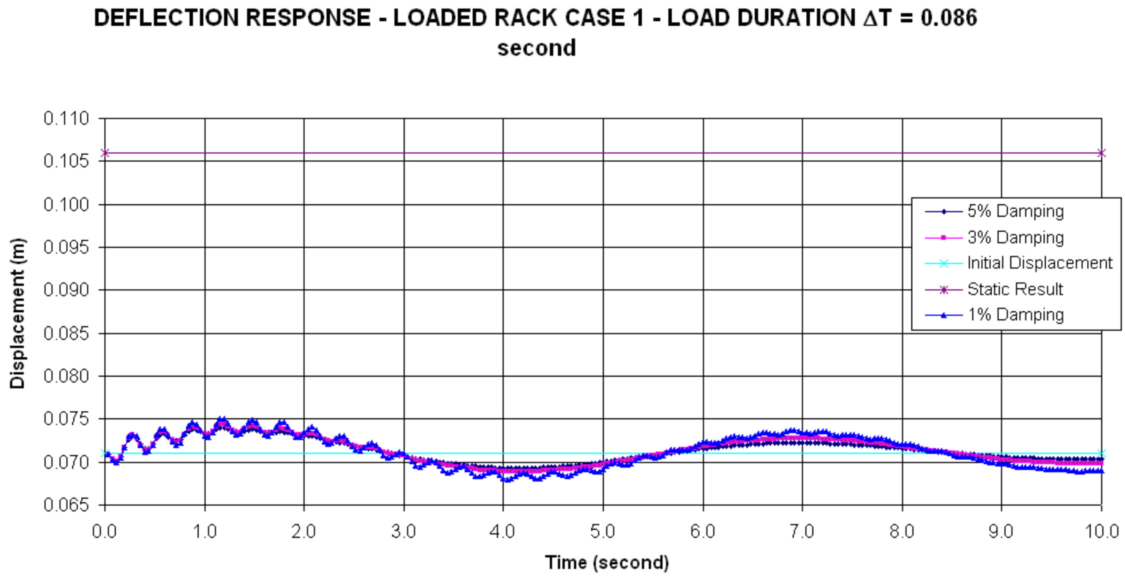

Figure 9a. Deflection Response at the front face of the rack – Loaded Rack Case 1 – Load Duration ΔT = 0.086 second

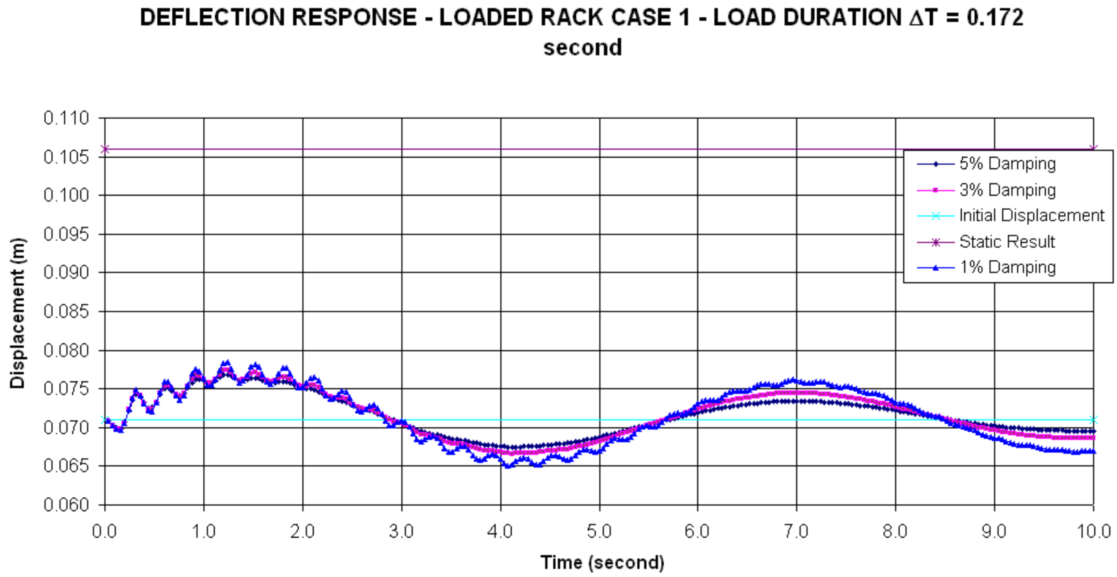

Figure 9b. Deflection Response at the front face of the rack – Loaded Rack Case 1 – Load Duration ΔT = 0.172 second

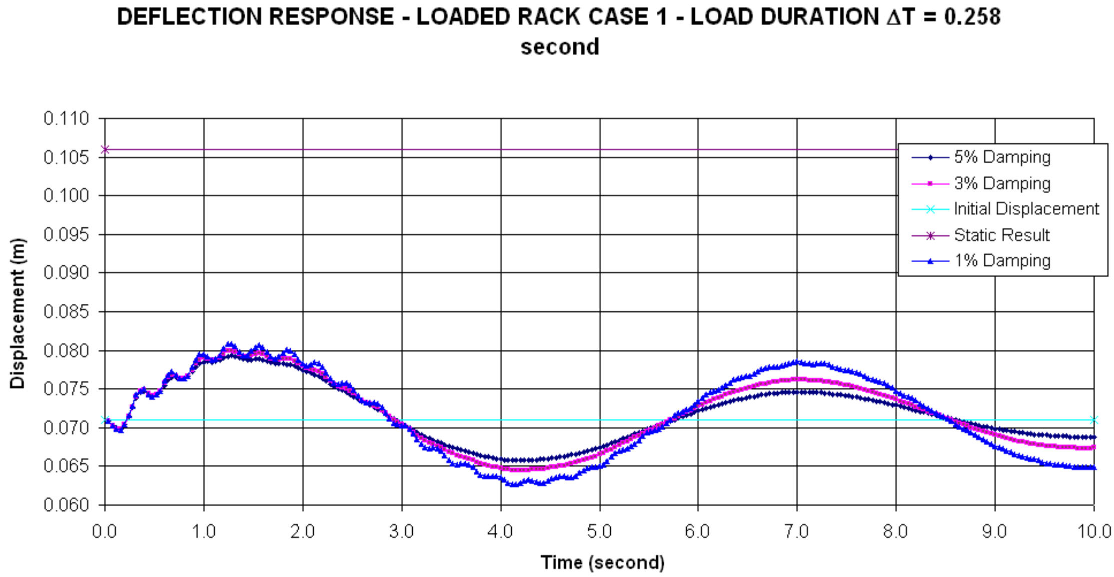

Figure 9c. Deflection Response at the front face of the rack – Loaded Rack Case 1 – Load Duration ΔT = 0.258 second

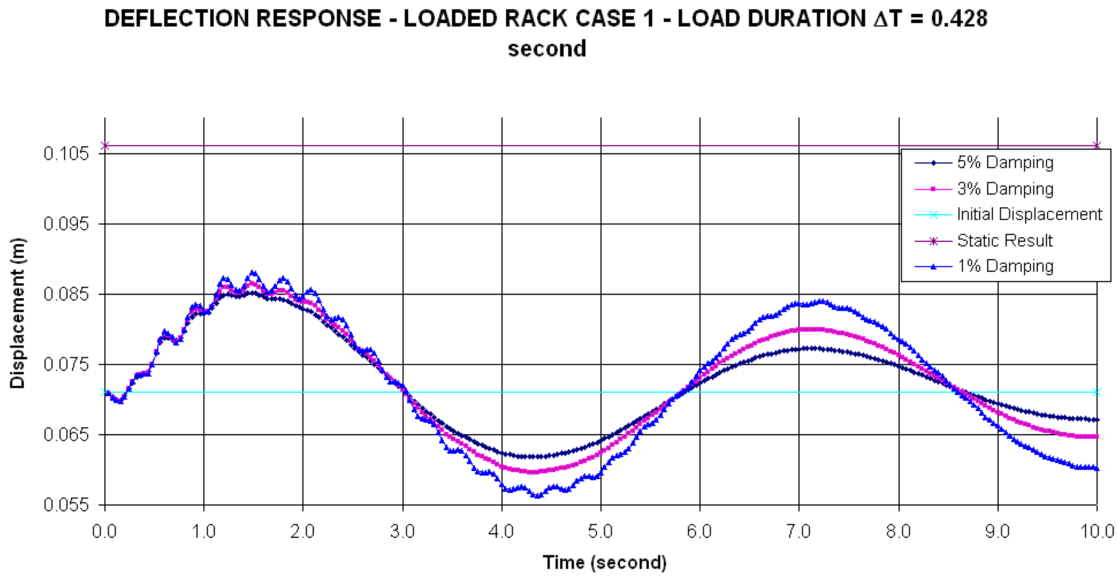

Figure 9d. Deflection Response at the front face of the rack – Loaded Rack Case 1 – Load Duration ΔT = 0.428 second

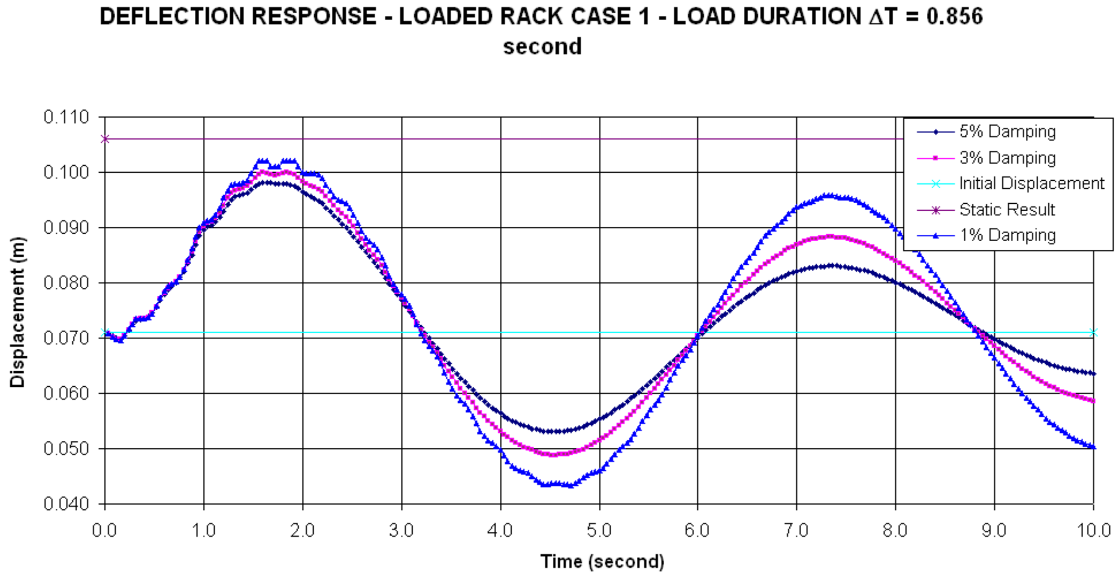

Figure 9e. Deflection Response at the front face of the rack – Loaded Rack Case 1 – Load Duration ΔT = 0.856 second

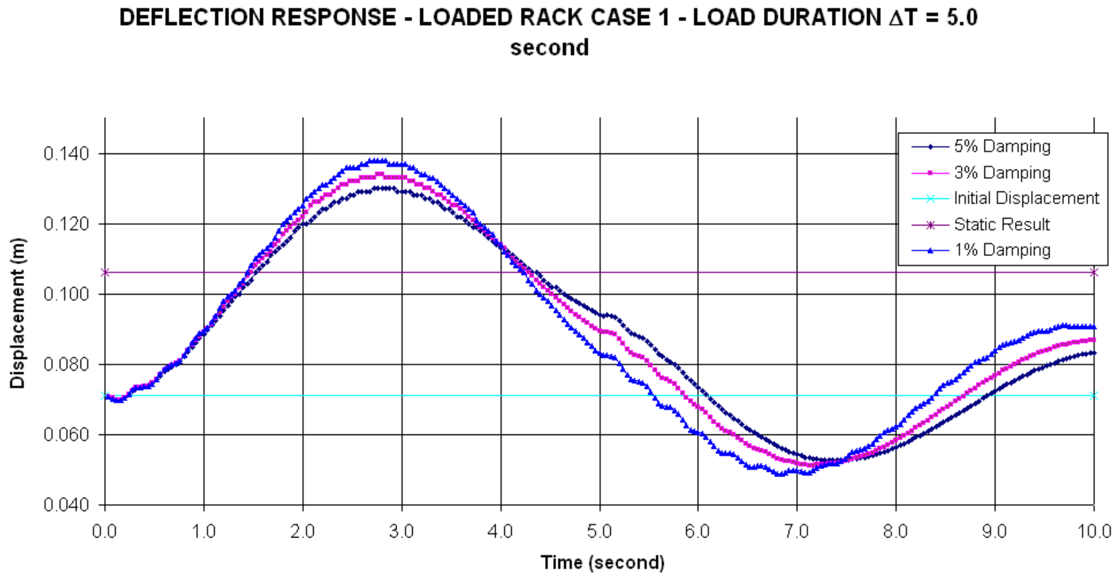

Figure 9f. Deflection Response at the front face of the rack – Loaded Rack Case 1 – Load Duration ΔT = 5.0 second

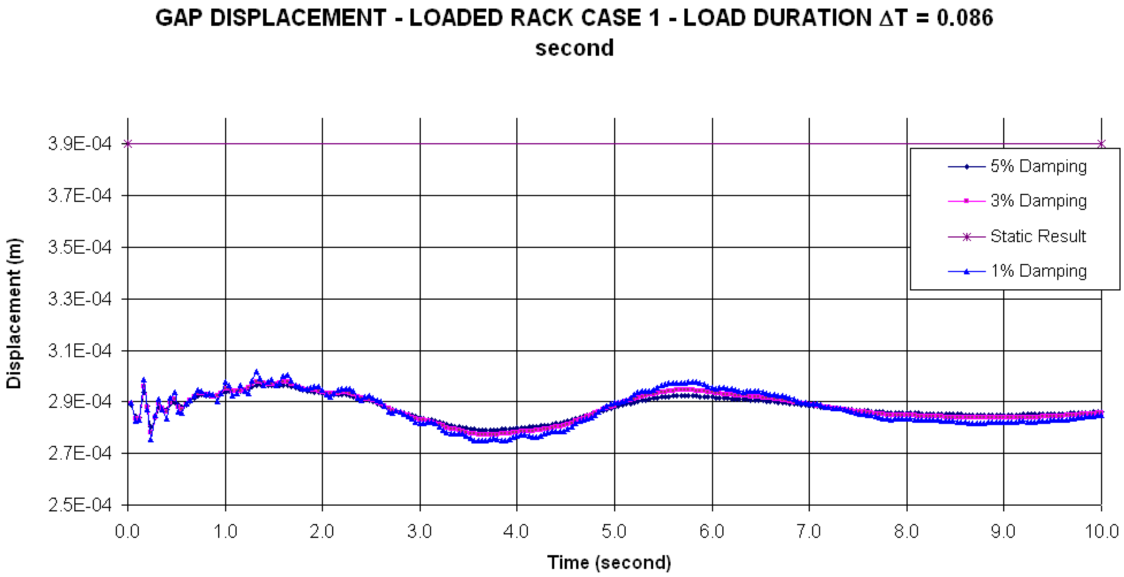

Figure 9g. Displacement Gap Response at the front face of top pallet level – Loaded Rack Case 1 – Load Duration ΔT = 0.086 second

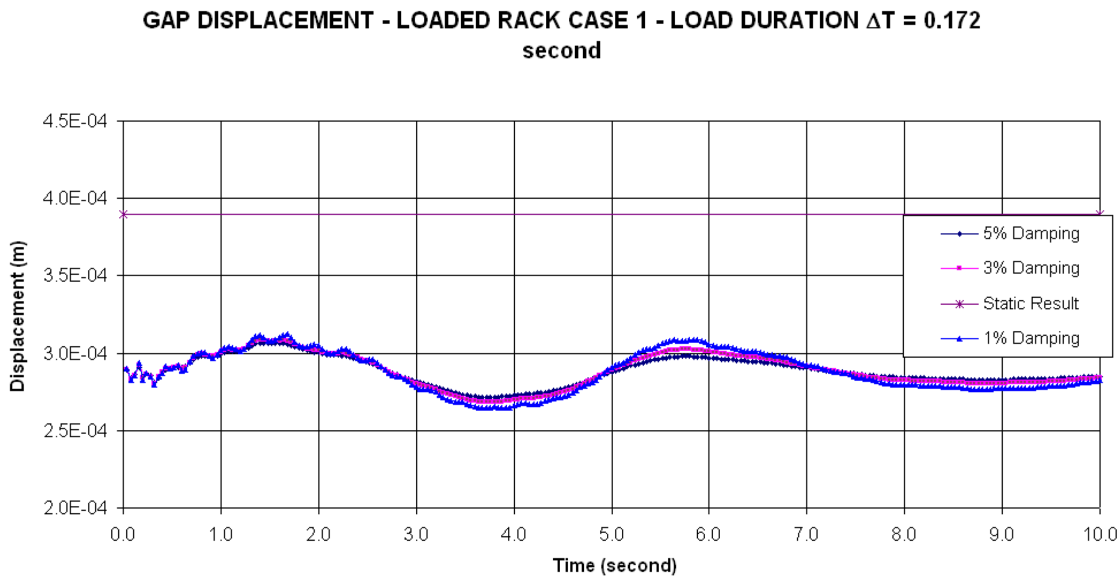

Figure 9h. Displacement Gap Response at the front face of top pallet level – Loaded Rack Case 1 – Load Duration ΔT = 0.172 second

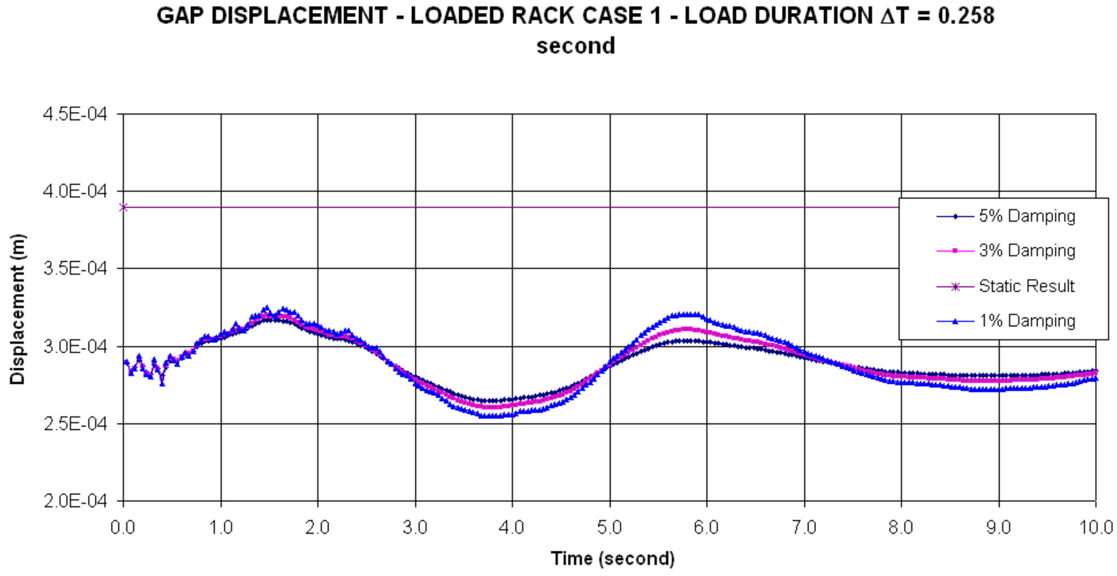

Figure 9i. Displacement Gap Response at the front face of top pallet level – Loaded Rack Case 1 – Load Duration ΔT = 0.258 second

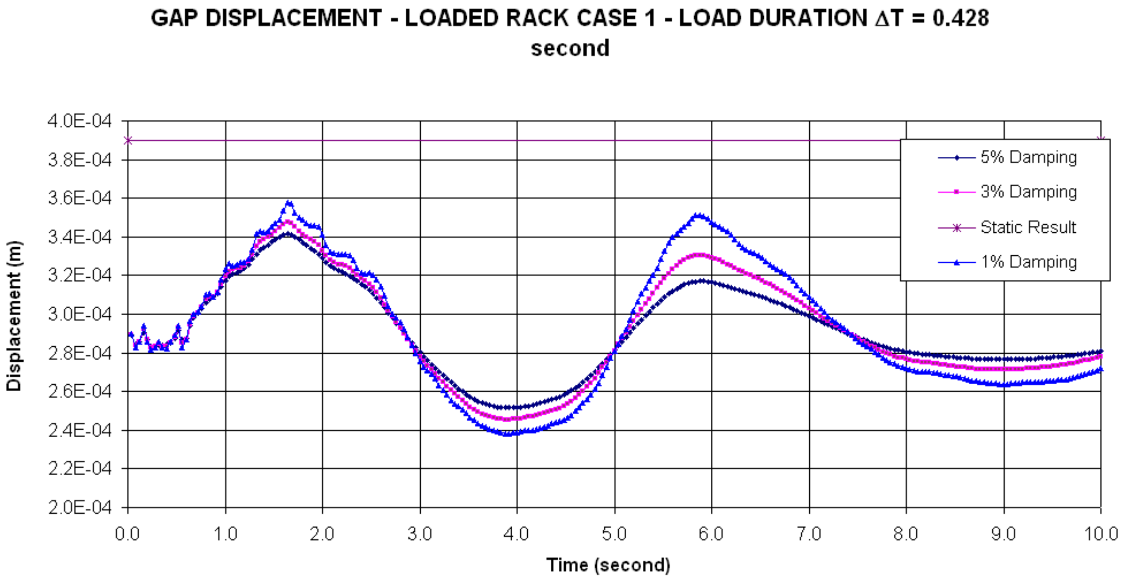

Figure 9j. Displacement Gap Response at the front face of top pallet level – Loaded Rack Case 1 – Load Duration ΔT = 0.428 second

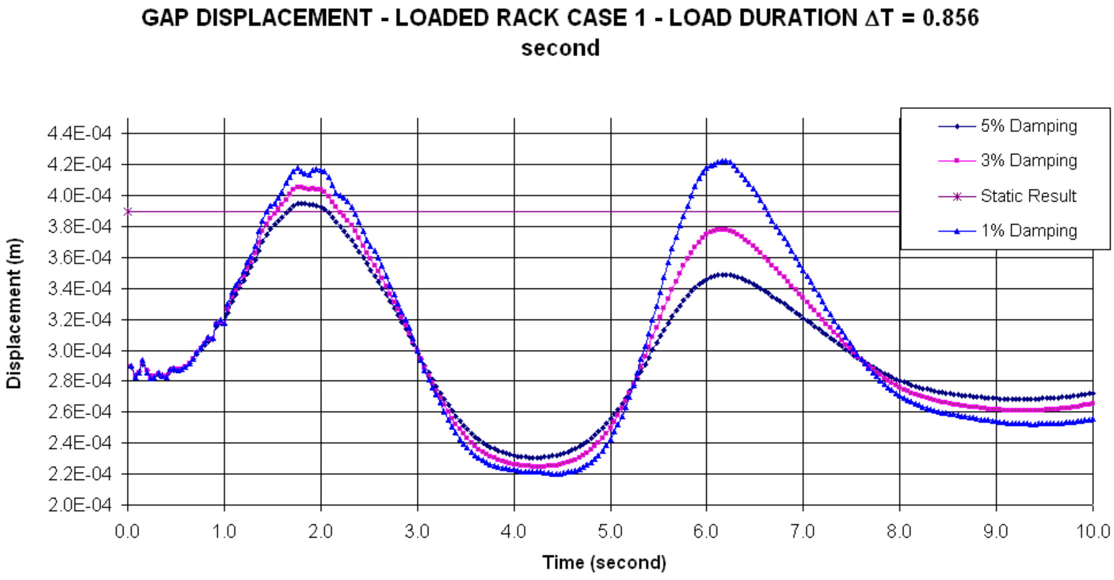

Figure 9k. Displacement Gap Response at the front face of top pallet level – Loaded Rack Case 1 – Load Duration ΔT = 0.856 second

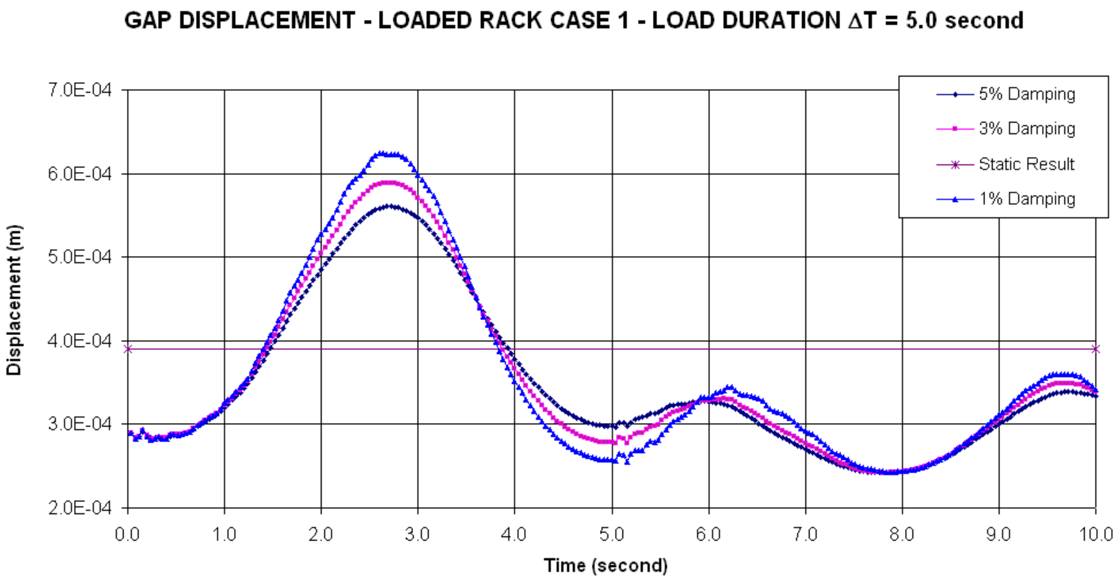

Figure 9l. Displacement Gap Response at the front face of top pallet level – Loaded Rack Case 1 – Load Duration ΔT = 5.0 second

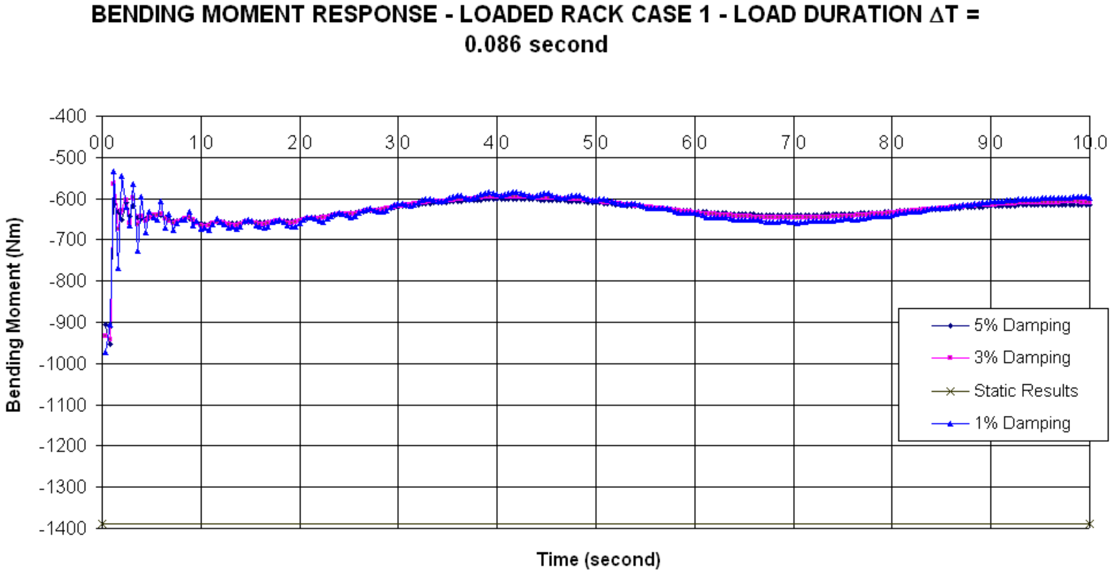

Figure 9m. Bending Moment Response at the base of impacted upright – Loaded Rack Case 1 – Load Duration ΔT = 0.086 second

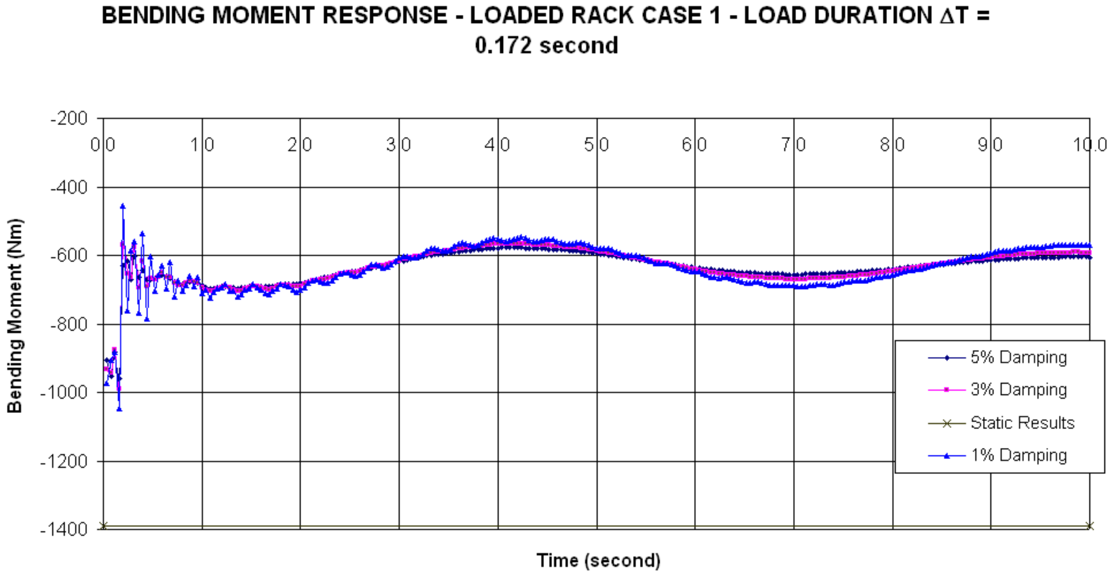

Figure 9n. Bending Moment Response at the base of impacted upright – Loaded Rack Case 1 – Load Duration ΔT = 0.172 second

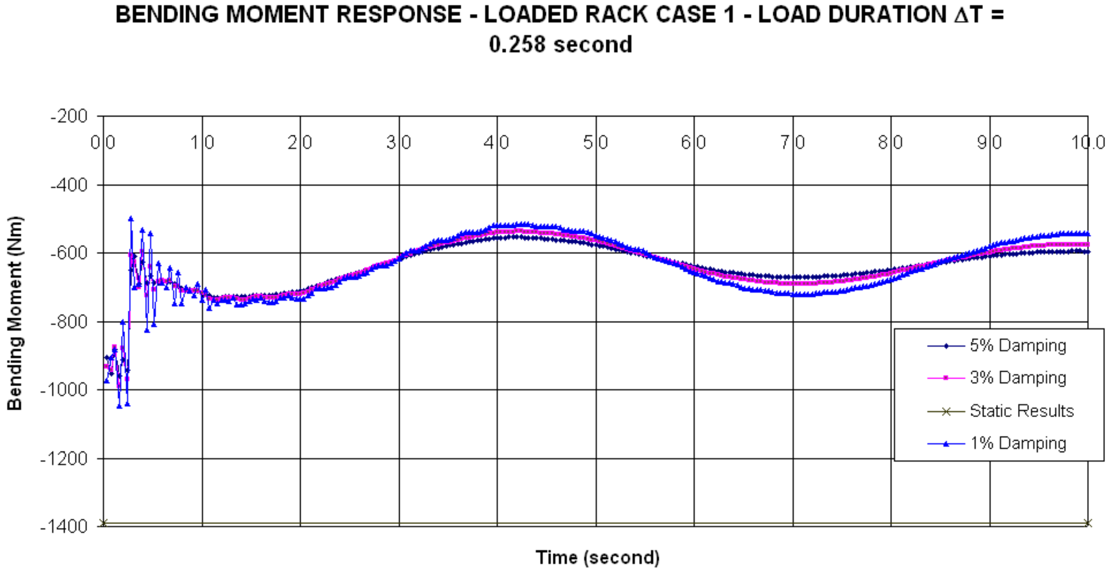

Figure 9o. Bending Moment Response at the base of impacted upright – Loaded Rack Case 1 – Load Duration ΔT = 0.258 second

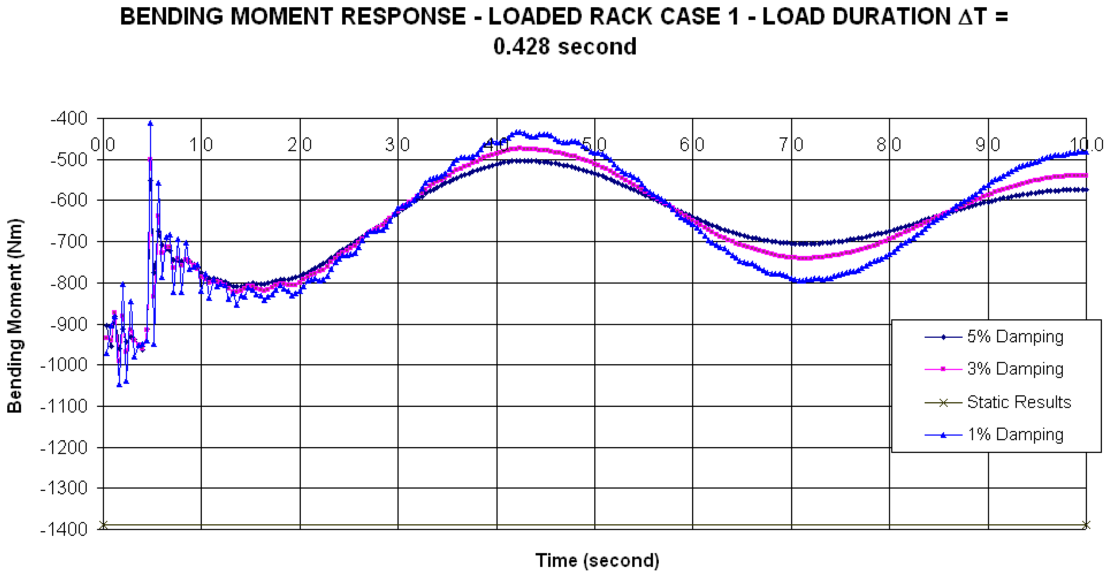

Figure 9p. Bending Moment Response at the base of impacted upright – Loaded Rack Case 1 – Load Duration ΔT = 0.428 second

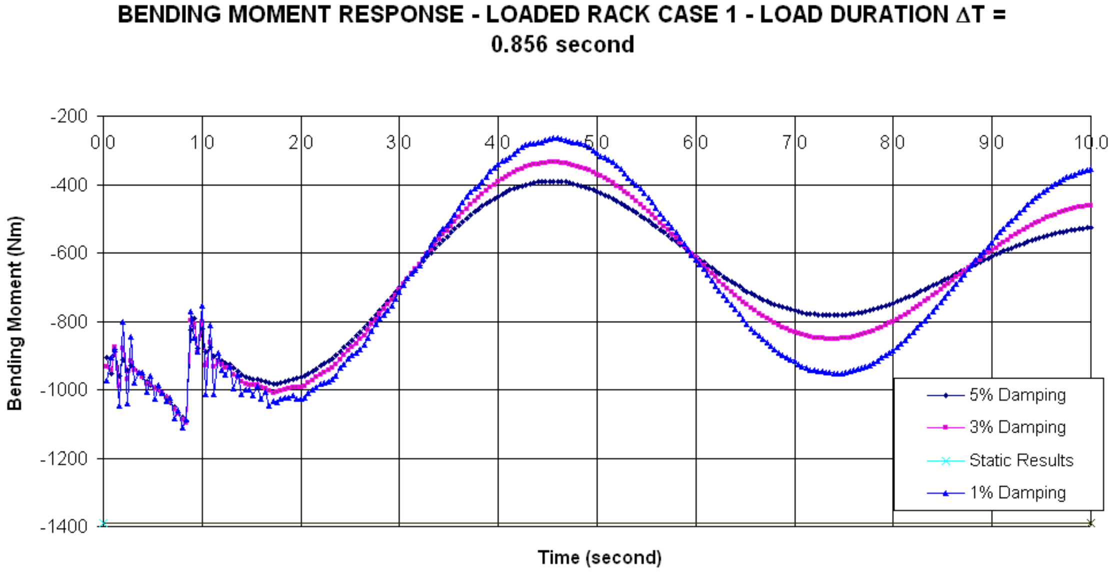

Figure 9q. Bending Moment Response at the base of impacted upright – Loaded Rack Case 1 – Load Duration ΔT = 0.856 second

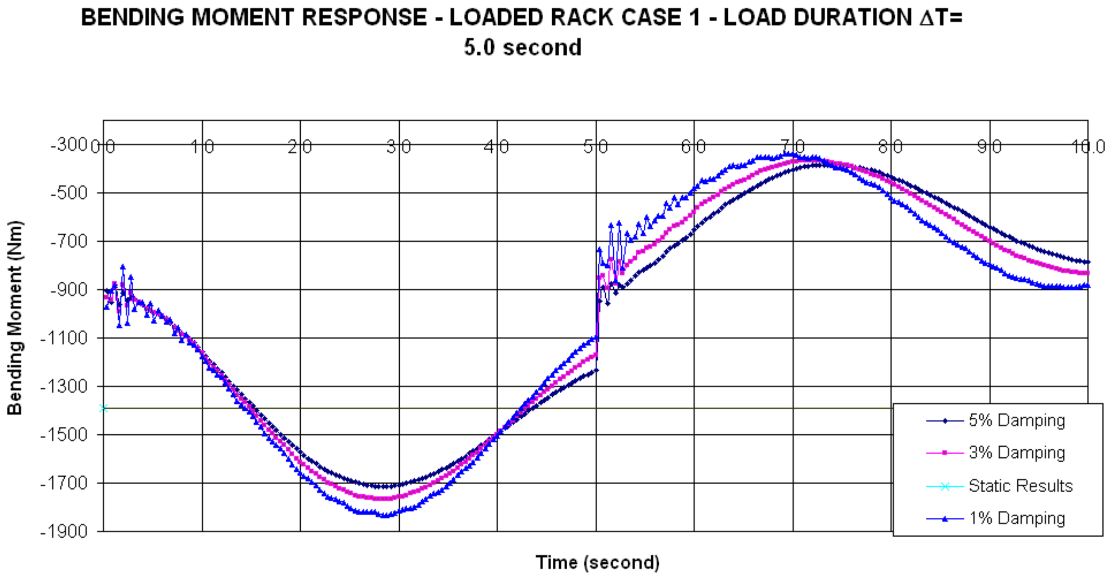

Figure 9r. Bending Moment Response at the base of impacted upright – Loaded Rack Case 1 – Load Duration ΔT = 5.0 second

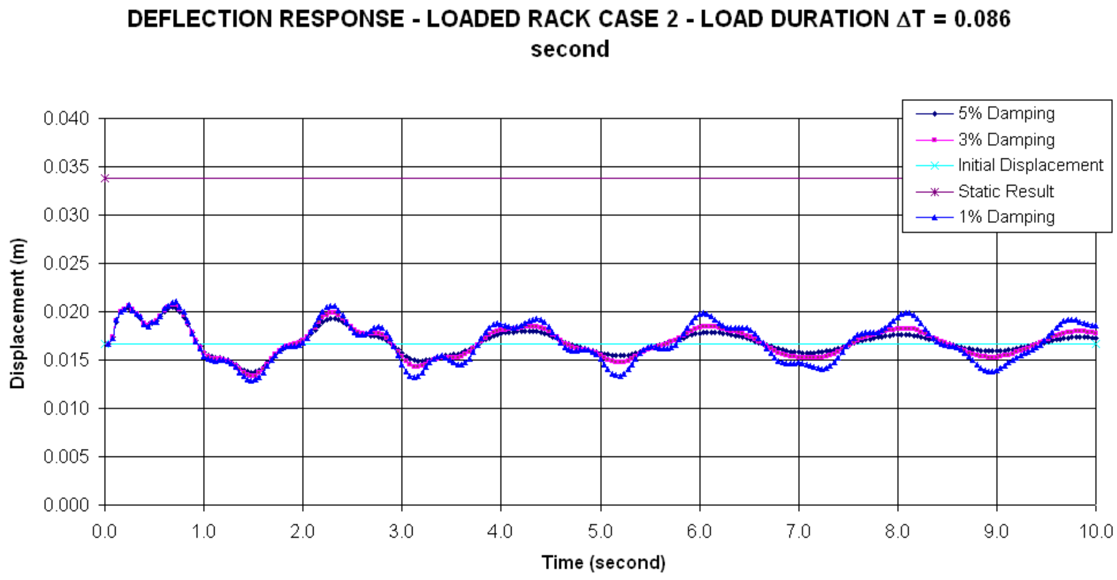

Figure 10a. Deflection Response at the front face of the rack – Loaded Rack Case 2 – Load Duration ΔT = 0.086 second

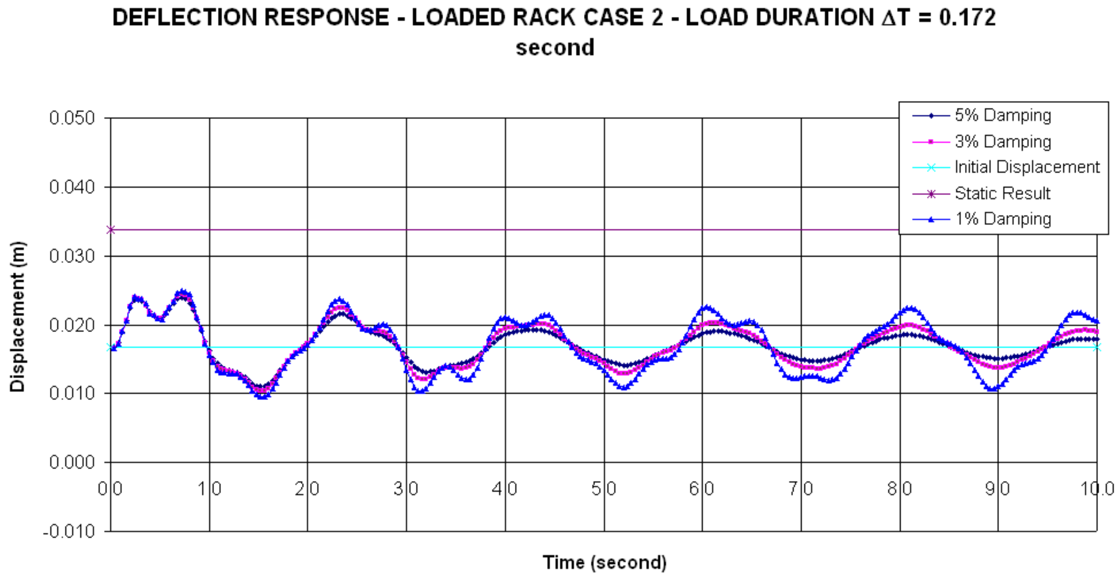

Figure 10b. Deflection Response at the front face of the rack – Loaded Rack Case 2 – Load Duration ΔT = 0.172 second

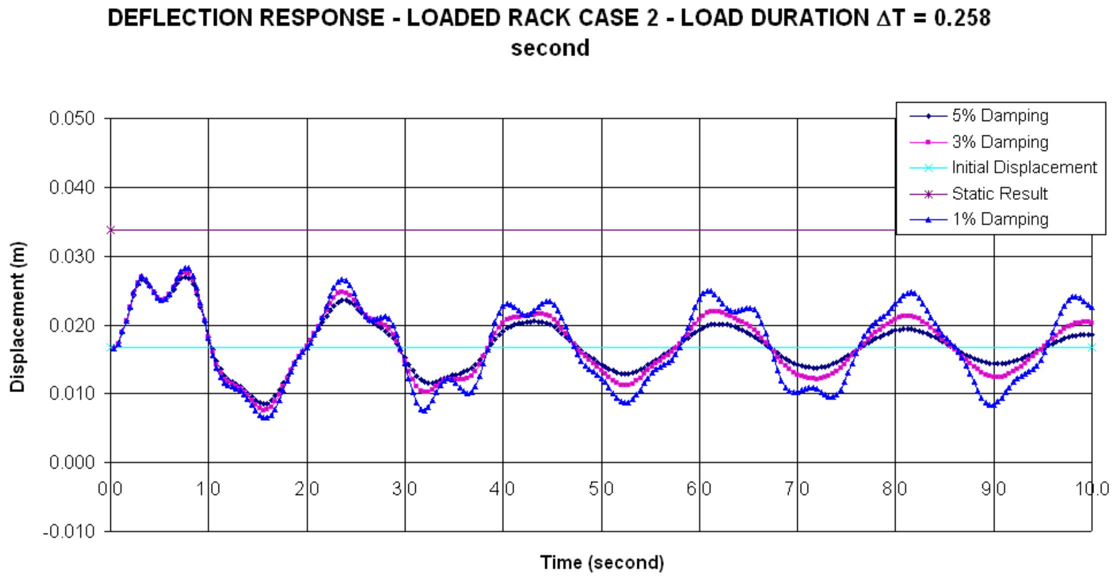

Figure 10c. Deflection Response at the front face of the rack – Loaded Rack Case 2 – Load Duration ΔT/T = 0.258 second

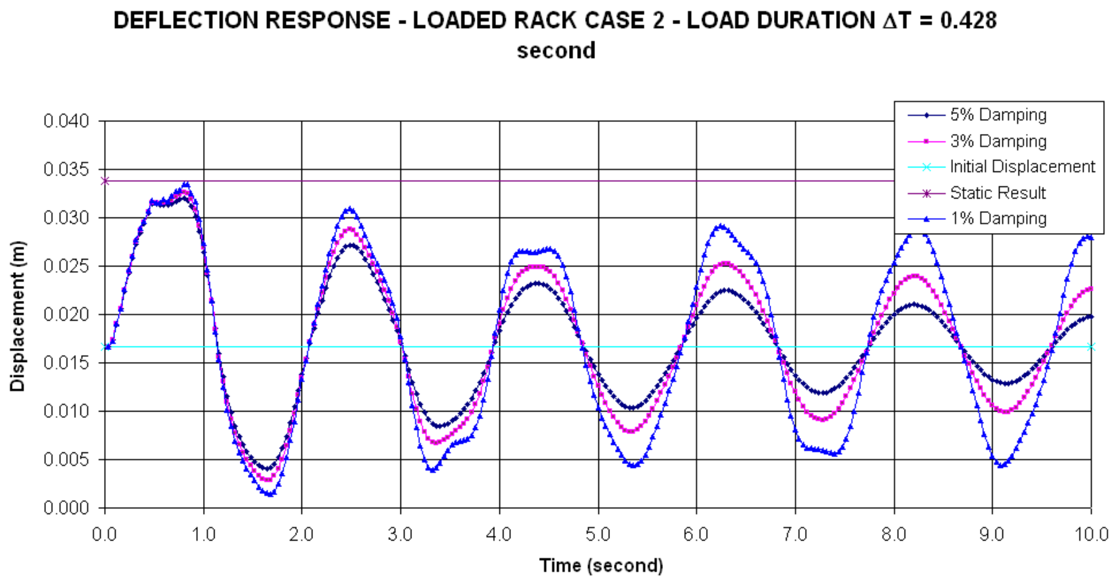

Figure 10d. Deflection Response at the front face of the rack – Loaded Rack Case 2 – Load Duration ΔT = 0.428 second

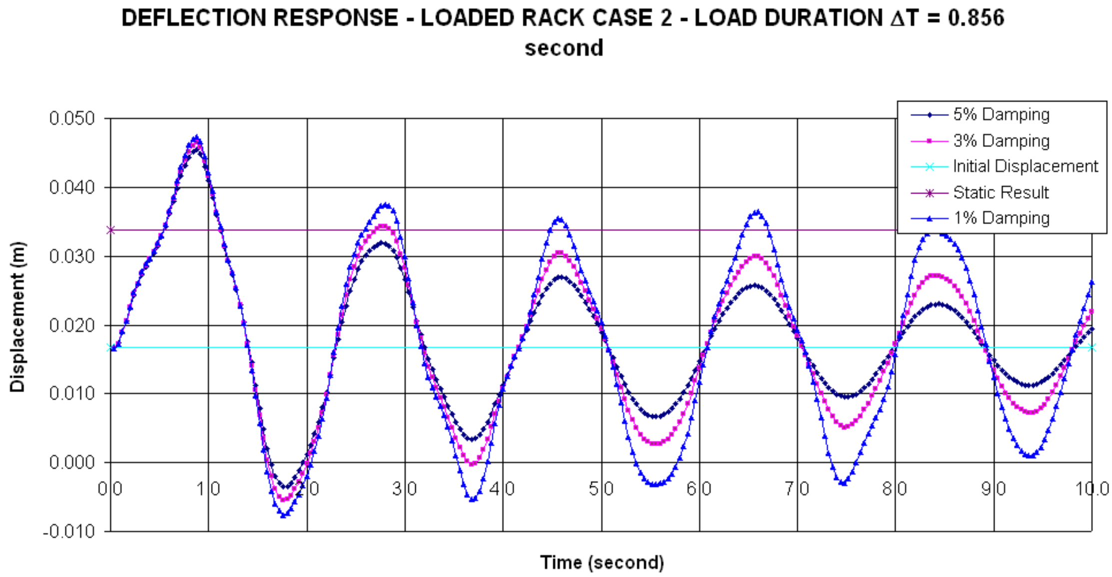

Figure 10e. Deflection Response at the front face of the rack – Loaded Rack Case 2 – Load Duration ΔT = 0.856 second

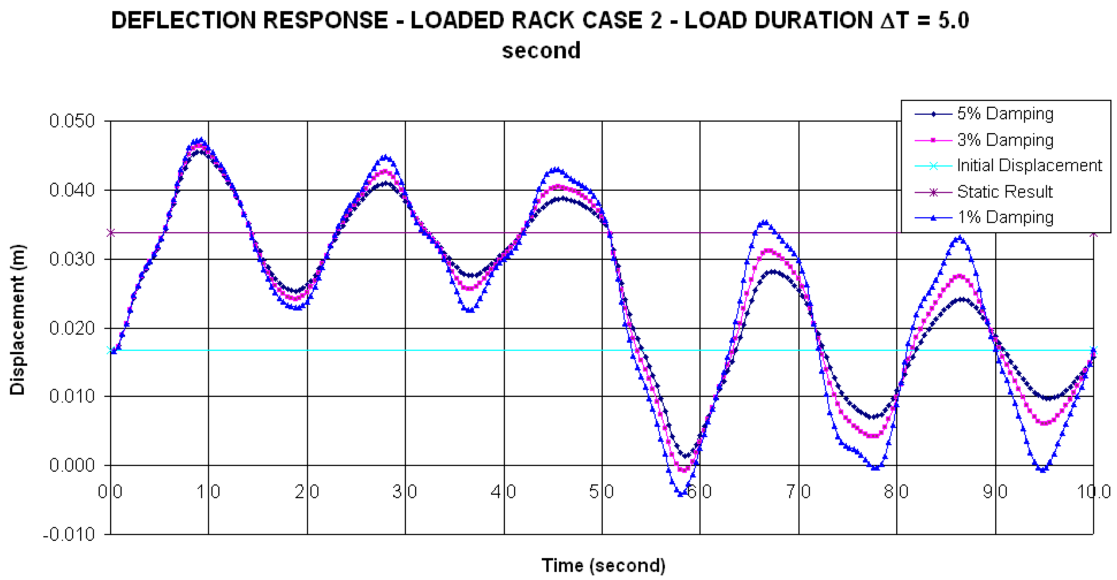

Figure 10f. Deflection Response at the front face of the rack – Loaded Rack Case 2 – Load Duration ΔT = 5.0 second

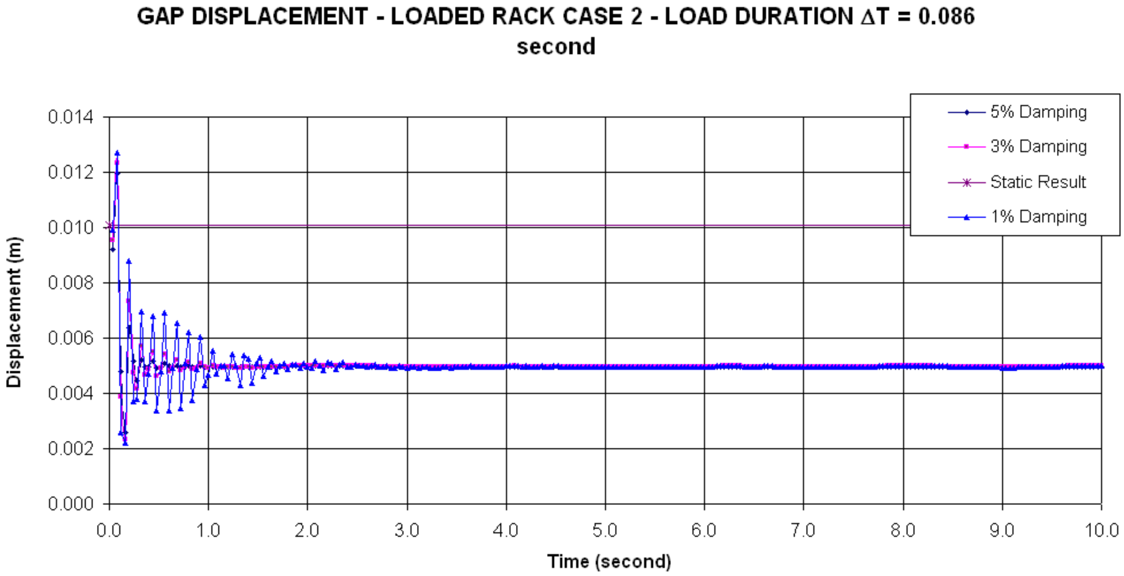

Figure 10g. Displacement Gap Response at the front face of top pallet level – Loaded Rack Case 2 – Load Duration ΔT = 0.086 second

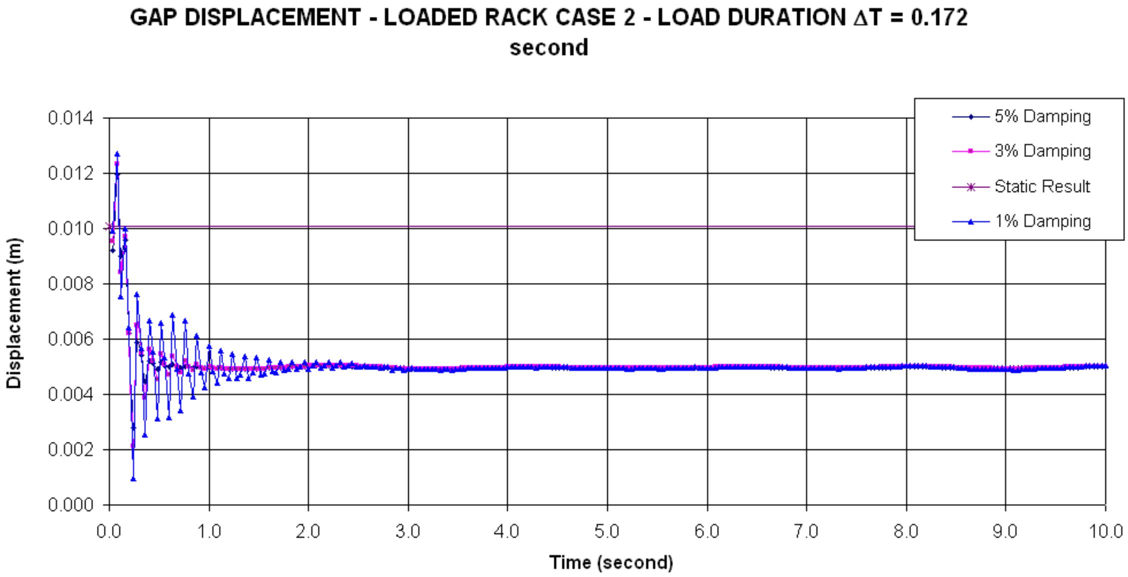

Figure 10h. Displacement Gap Response at the front face of top pallet level – Loaded Rack Case 2 – Load Duration ΔT = 0.172 second

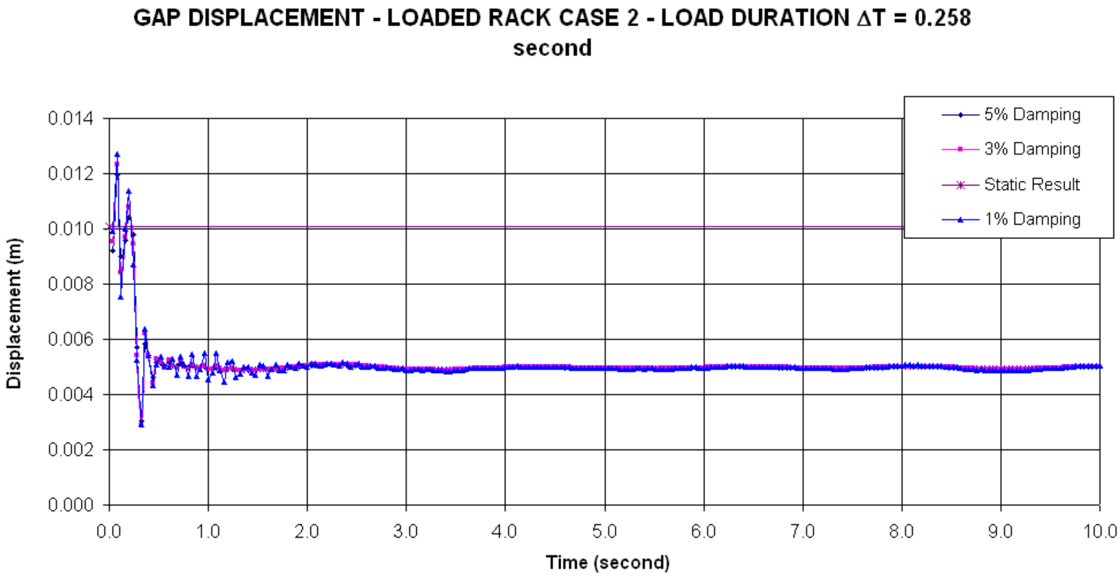

Figure 10i. Displacement Gap Response at the front face of top pallet level – Loaded Rack Case 2 – Load Duration ΔT = 0.258 second

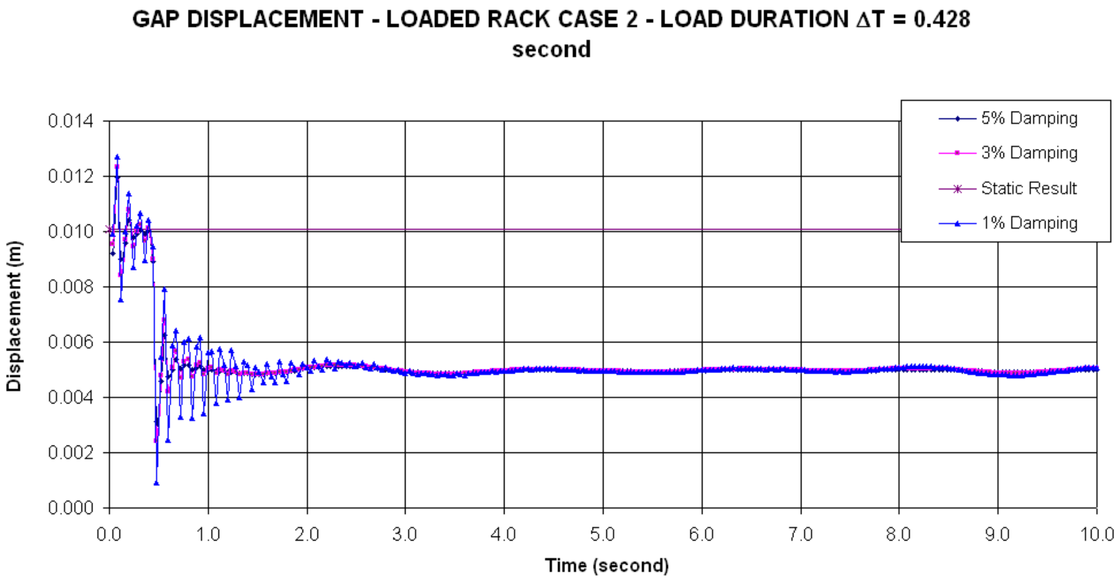

Figure 10j. Displacement Gap Response at the front face of top pallet level – Loaded Rack Case 2 – Load Duration ΔT = 0.428 second

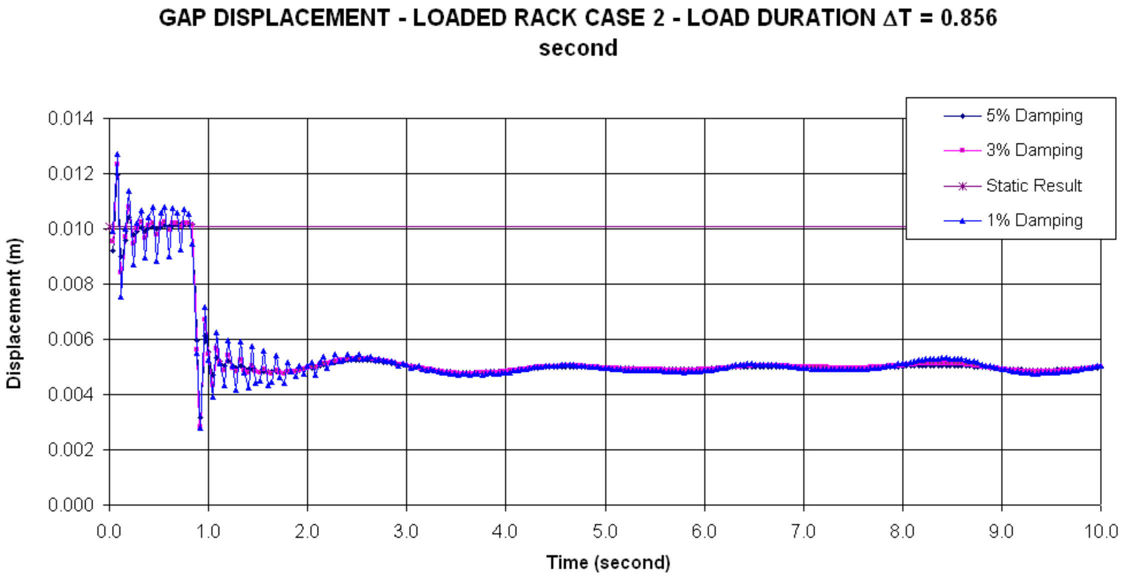

Figure 10k. Displacement Gap Response at the front face of top pallet level – Loaded Rack Case 2 – Load Duration ΔT = 0.856 second

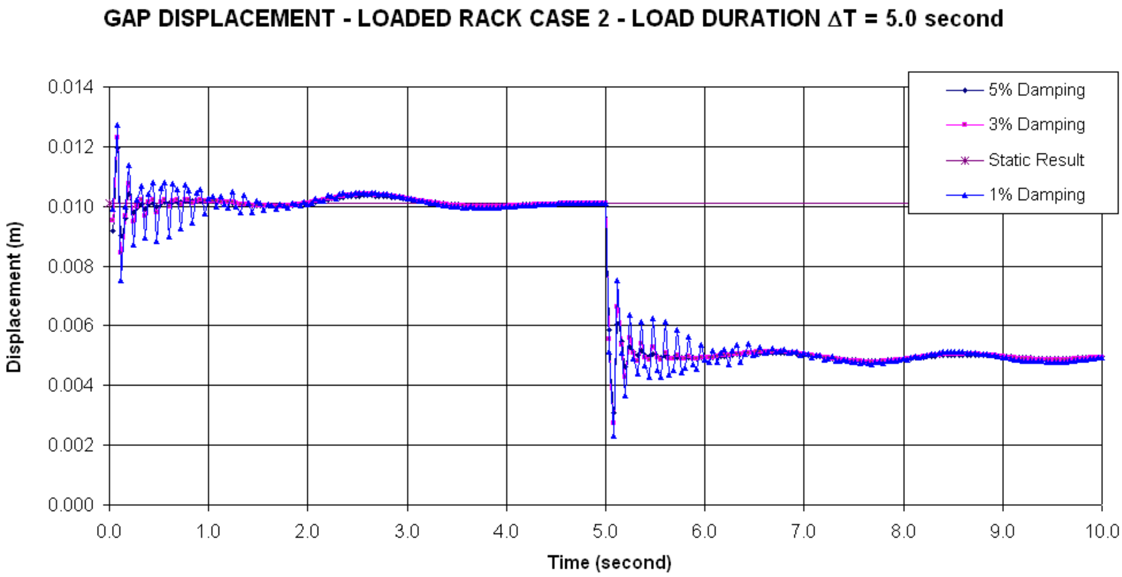

Figure 10l. Displacement Gap Response at the front face of top pallet level – Loaded Rack Case 2 – Load Duration ΔT = 5.0 second

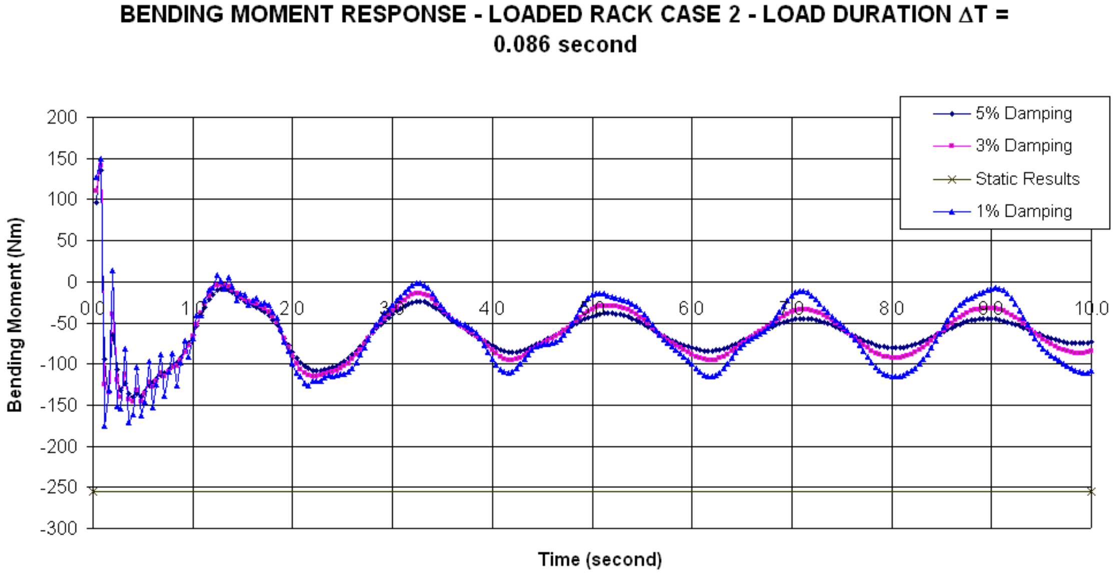

Figure 10m. Bending Moment Response at the base of impacted upright – Loaded Rack Case 2 – Load Duration ΔT = 0.086 second

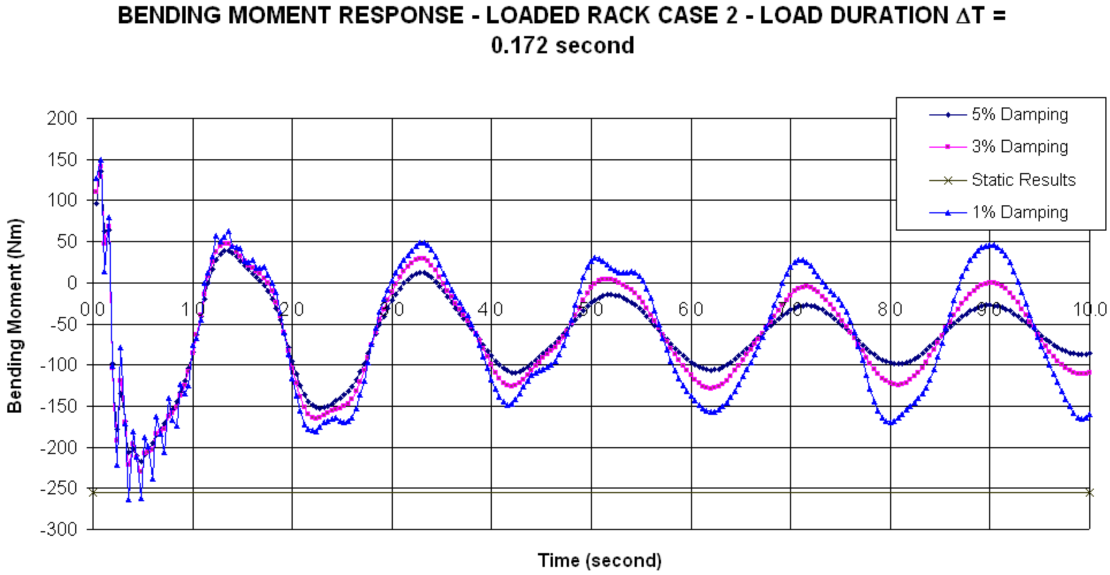

Figure 10n. Bending Moment Response at the base of impacted upright – Loaded Rack Case 2 – Load Duration ΔT = 0.172 second

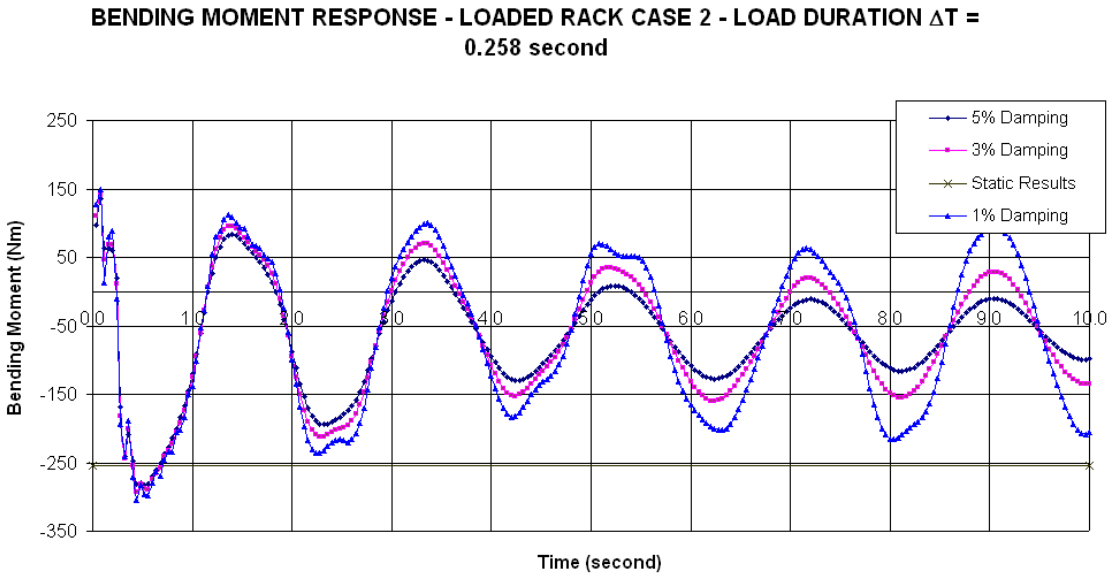

Figure 10o. Bending Moment Response at the base of impacted upright – Loaded Rack Case 2 – Load Duration ΔT/T = 0.258 second

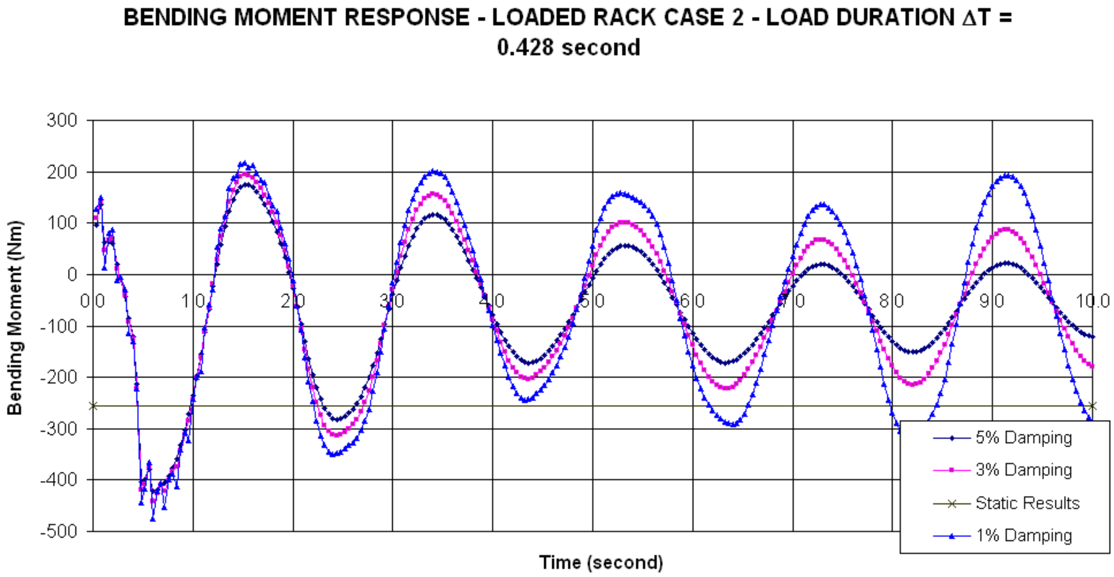

Figure 10p. Bending Moment Response at the base of impacted upright – Loaded Rack Case 2 – Load Duration ΔT = 0.428 second

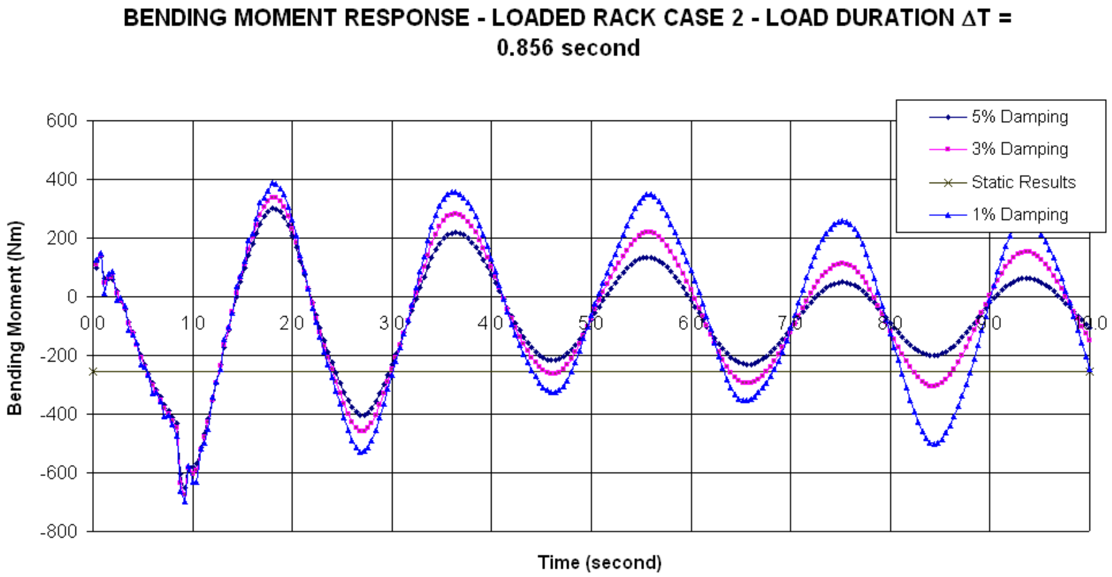

Figure 10q. Bending Moment Response at the base of impacted upright – Loaded Rack Case 2 – Load Duration ΔT = 0.856 second

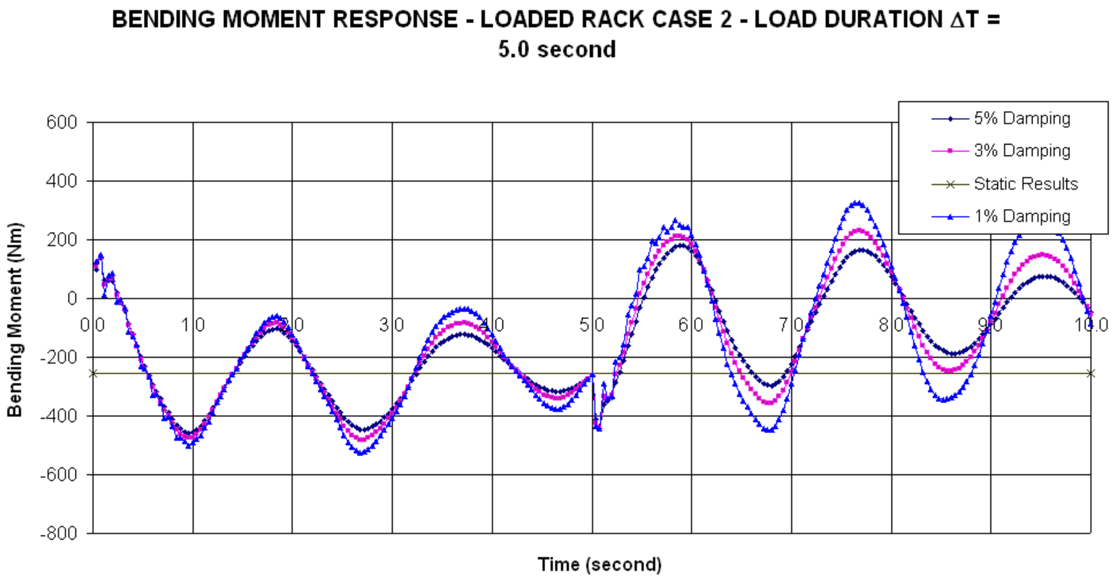

Figure 10r. Bending Moment Response at the base of impacted upright – Loaded Rack Case 2 – Load Duration ΔT = 5.0 second

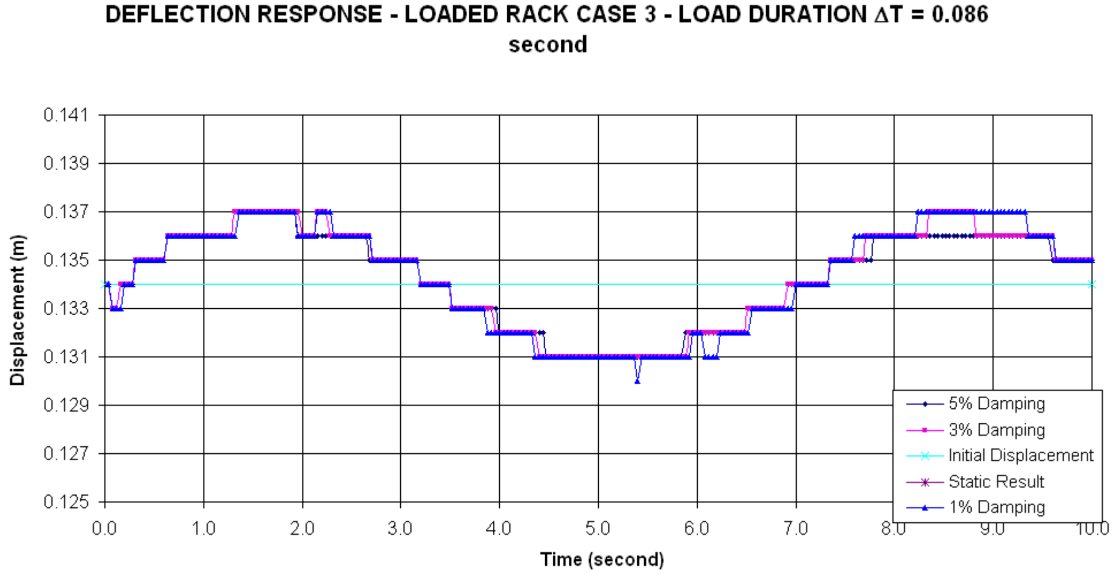

Figure 11a. Deflection Response at the front face of the rack – Loaded Rack Case 3 – Load Duration ΔT = 0.086 second

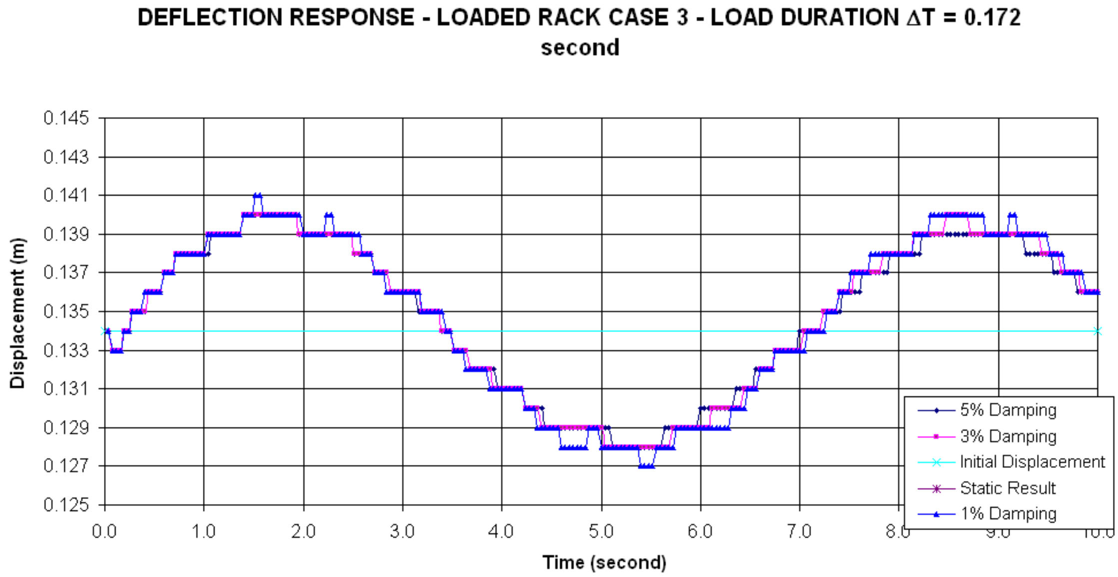

Figure 11b. Deflection Response at the front face of the rack – Loaded Rack Case 3 – Load Duration ΔT = 0.172 second

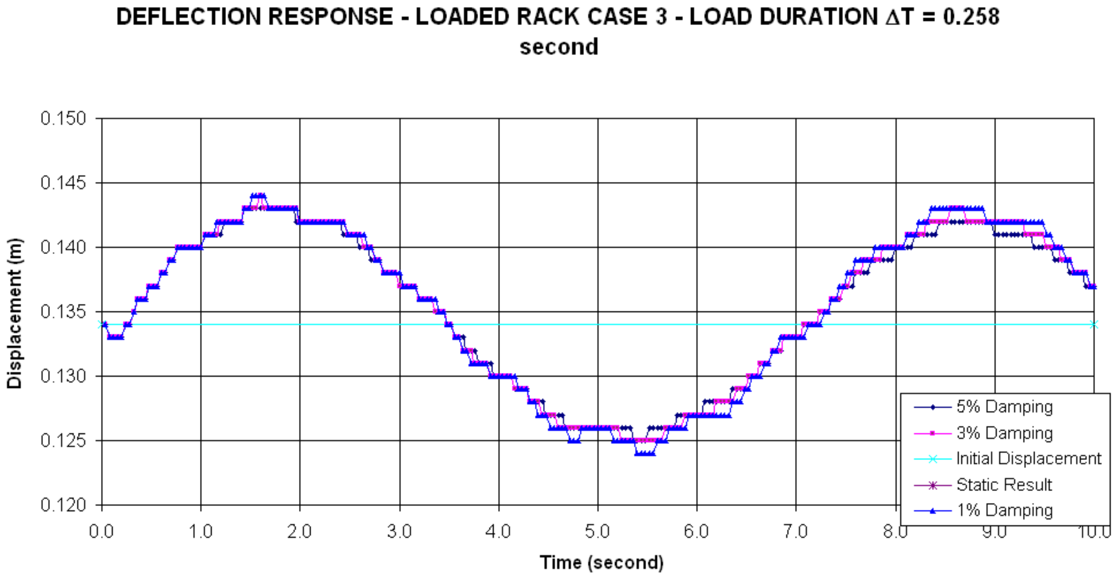

Figure 11c. Deflection Response at the front face of the rack – Loaded Rack Case 3 – Load Duration ΔT = 0.258 second

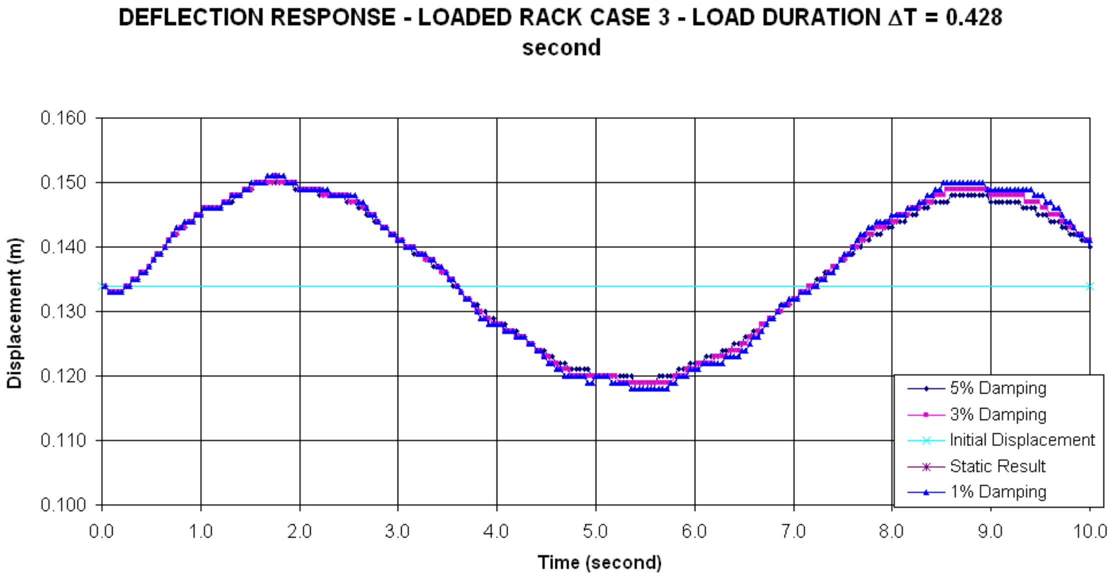

Figure 11d. Deflection Response at the front face of the rack – Loaded Rack Case 3 – Load Duration ΔT = 0.428 second

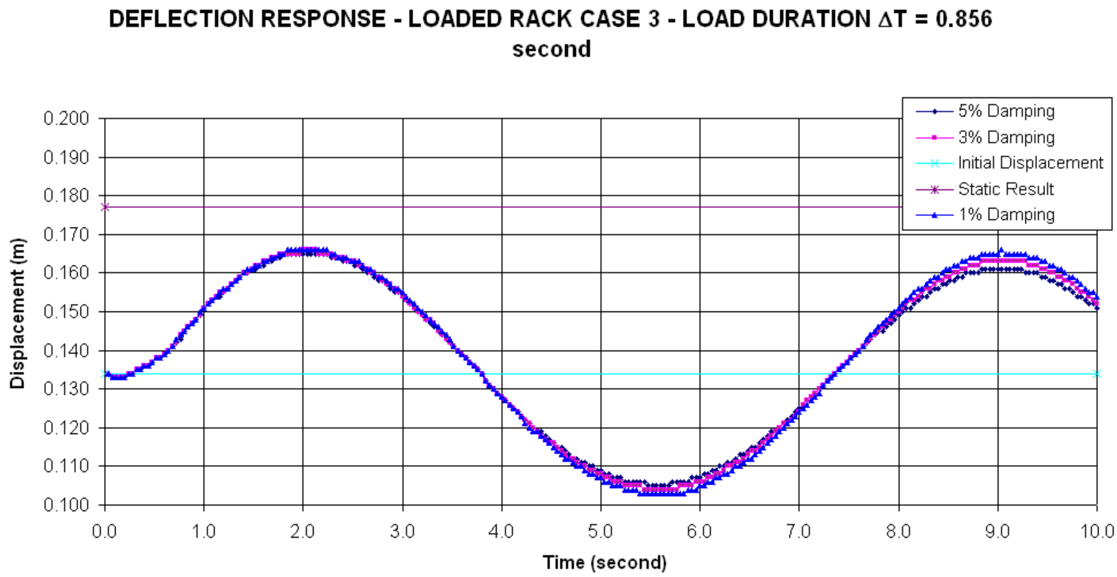

Figure 11e. Deflection Response at the front face of the rack – Loaded Rack Case 3 – Load Duration ΔT = 0.856 second

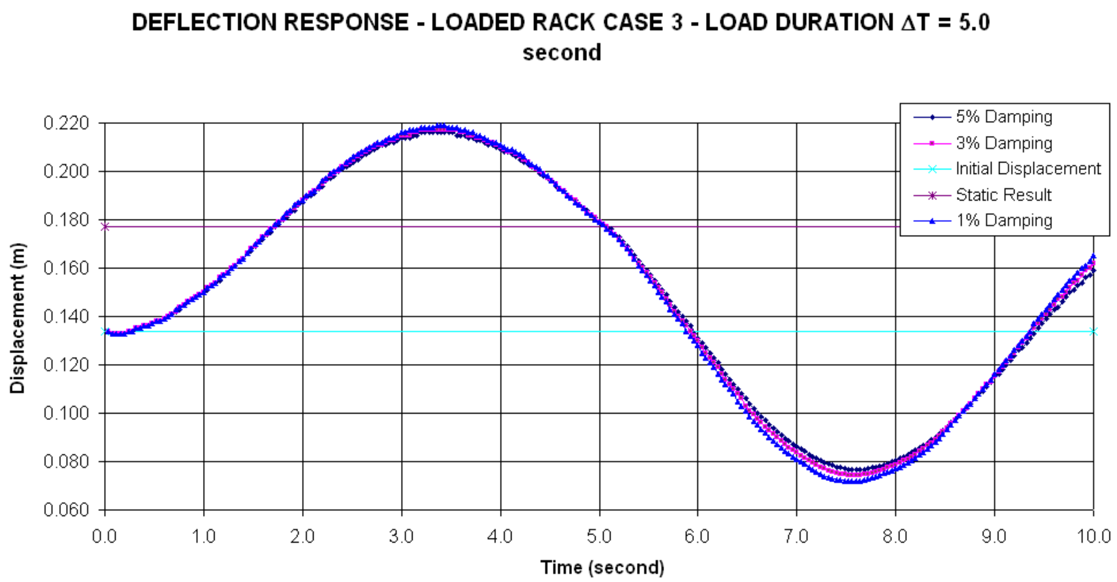

Figure 11f. Deflection Response at the front face of the rack – Loaded Rack Case 3 – Load Duration ΔT = 5.0 second

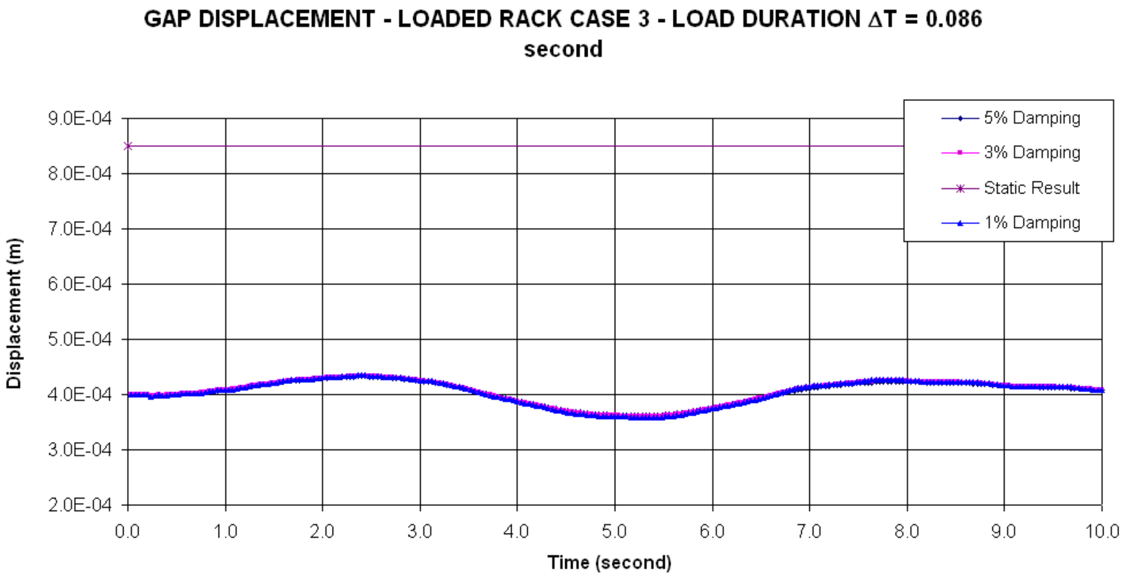

Figure 11g. Displacement Gap Response at the front face of top pallet level – Loaded Rack Case 3 – Load Duration ΔT = 0.086 second

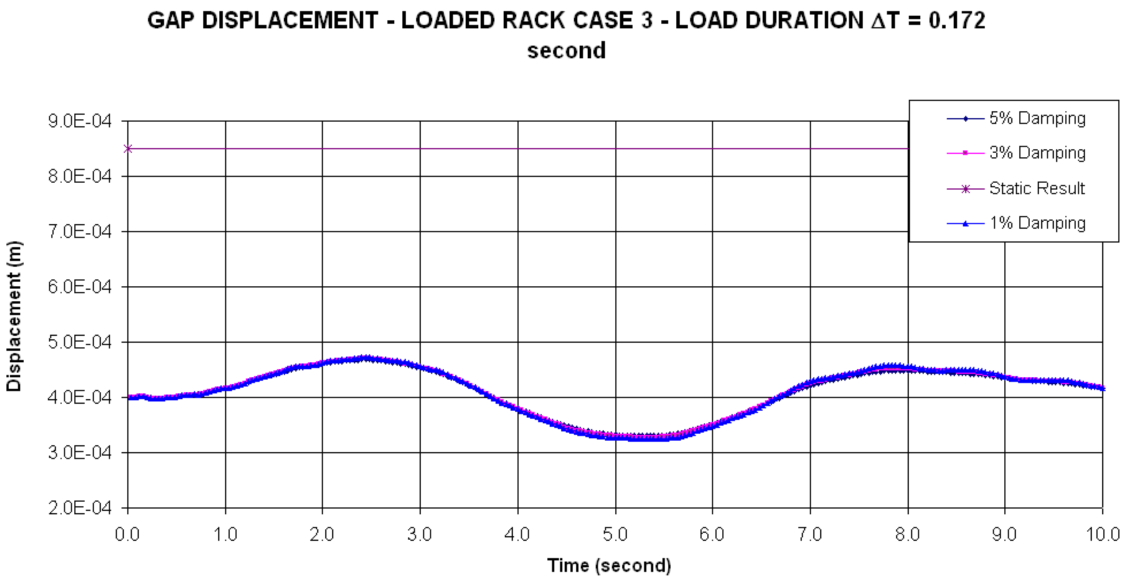

Figure 11h. Displacement Gap Response at the front face of top pallet level – Loaded Rack Case 3 – Load Duration ΔT = 0.172 second

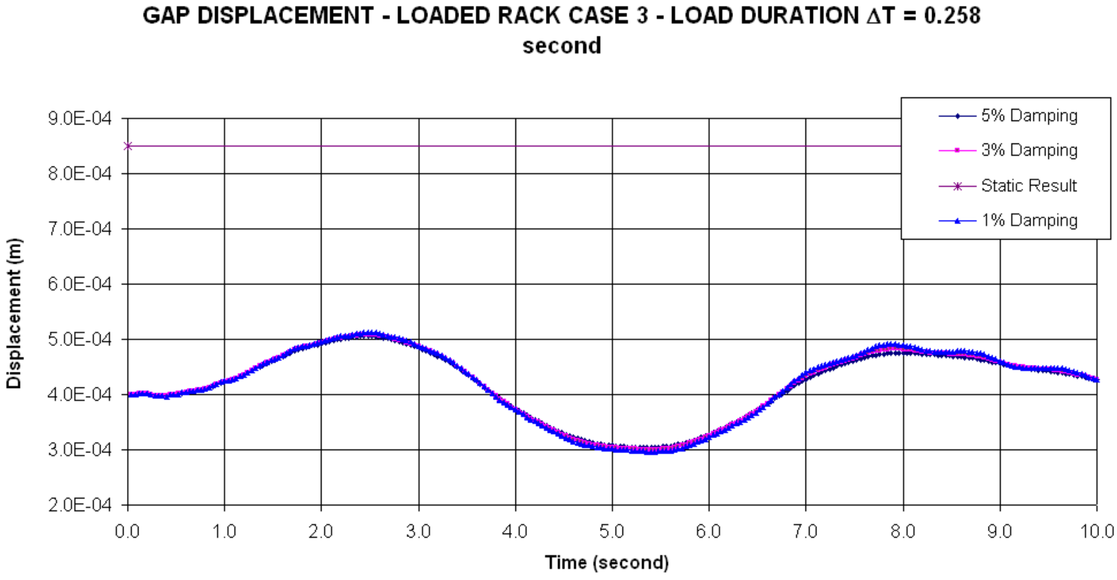

Figure 11i. Displacement Gap Response at the front face of top pallet level – Loaded Rack Case 3 – Load Duration ΔT = 0.258 second

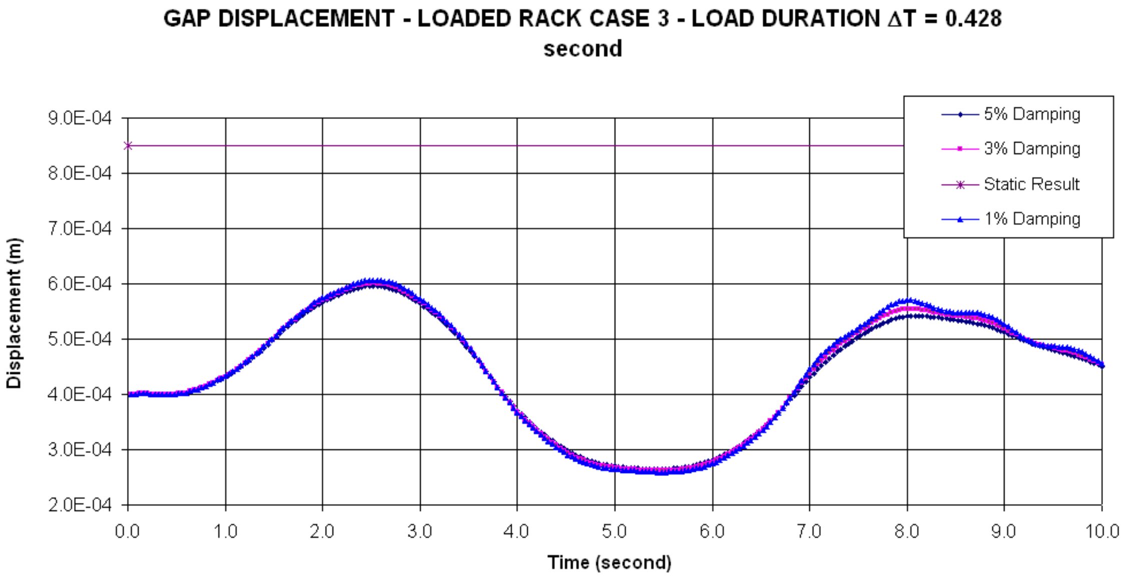

Figure 11j. Displacement Gap Response at the front face of top pallet level – Loaded Rack Case 3 – Load Duration ΔT = 0.428 second

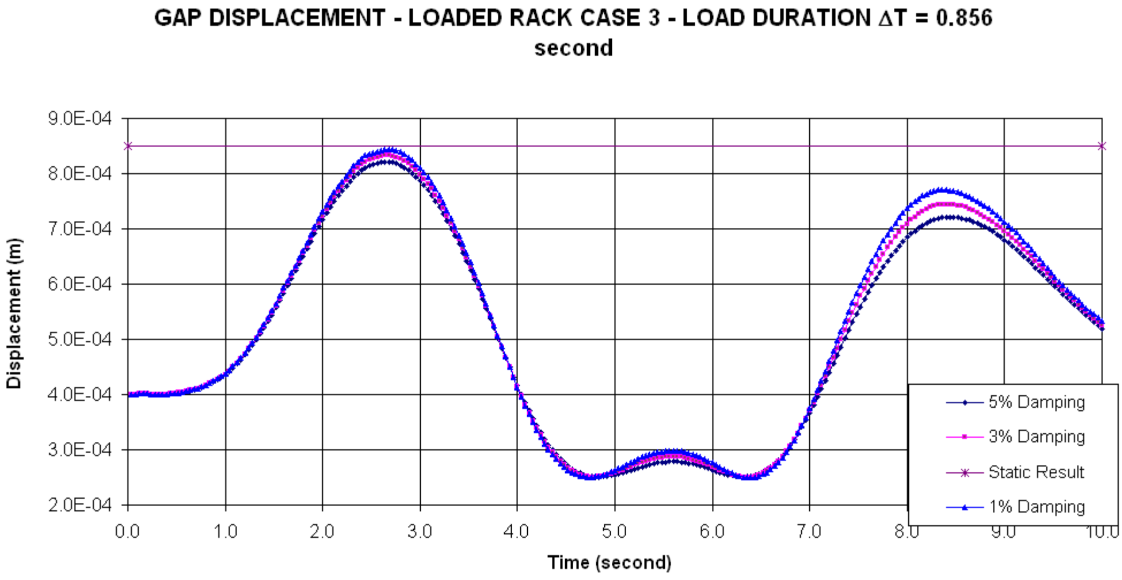

Figure 11k. Displacement Gap Response at the front face of top pallet level – Loaded Rack Case 3 – Load Duration ΔT = 0.856 second

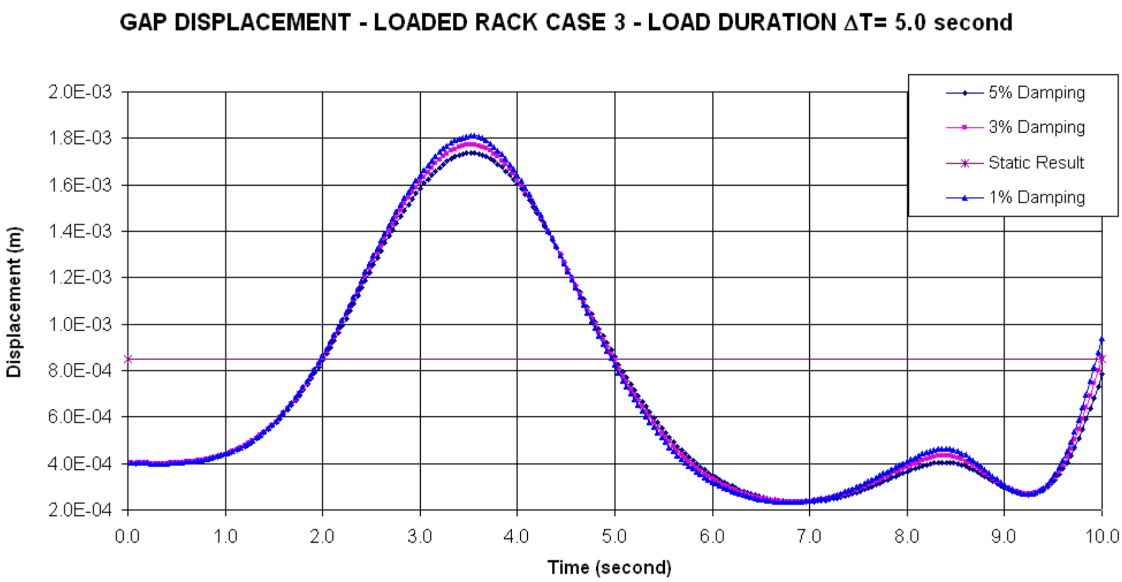

Figure 11l. Displacement Gap Response at the front face of top pallet level – Loaded Rack Case 3 – Load Duration ΔT = 5.0 second

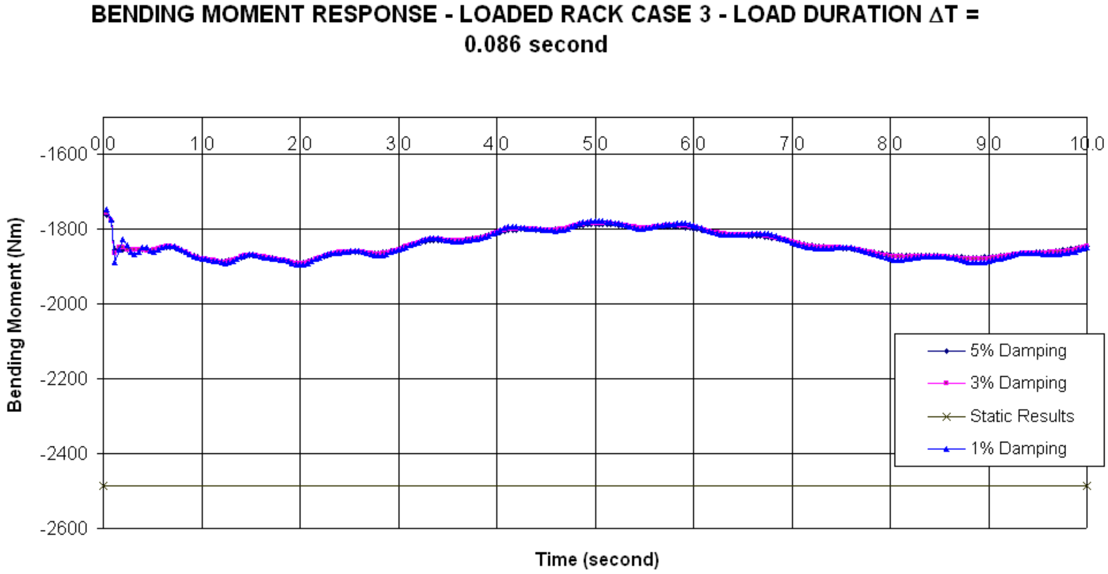

Figure 11m. Bending Moment Response at the base of impacted upright – Loaded Rack Case 3 – Load Duration ΔT = 0.086 second

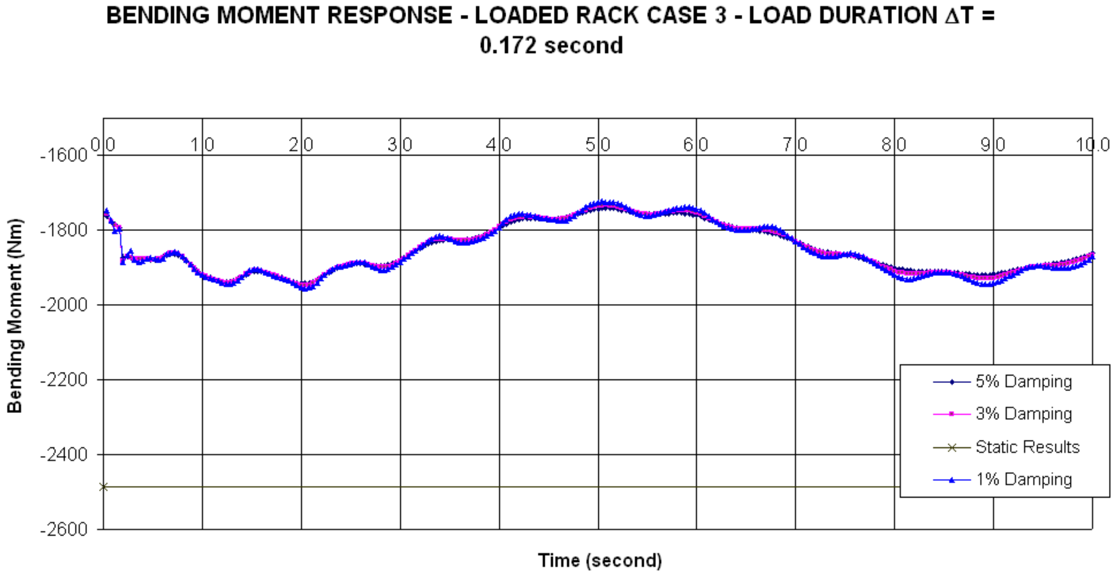

Figure 11n. Bending Moment Response at the base of impacted upright – Loaded Rack Case 3 – Load Duration ΔT = 0. 172 second

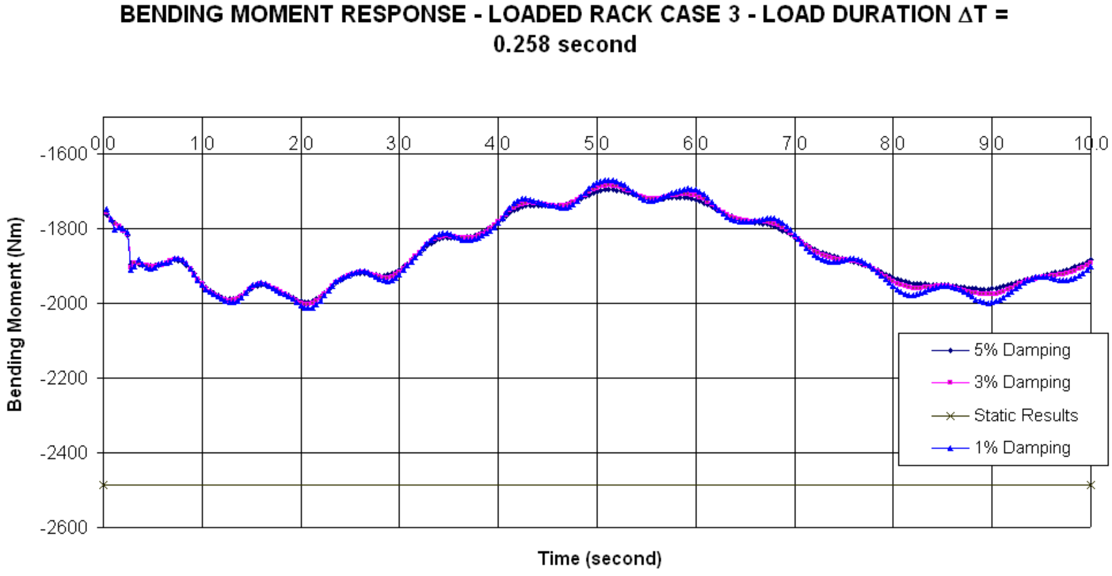

Figure 11o. Bending Moment Response at the base of impacted upright – Loaded Rack Case 3 – Load Duration ΔT = 0.258 second

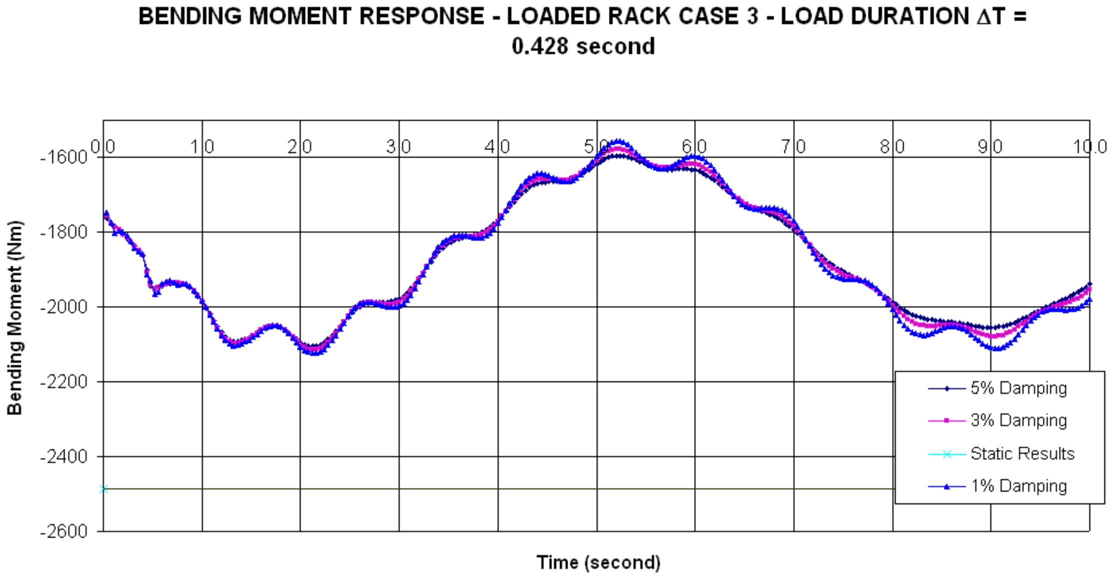

Figure 11p. Bending Moment Response at the base of impacted upright – Loaded Rack Case 3 – Load Duration ΔT = 0.428 second

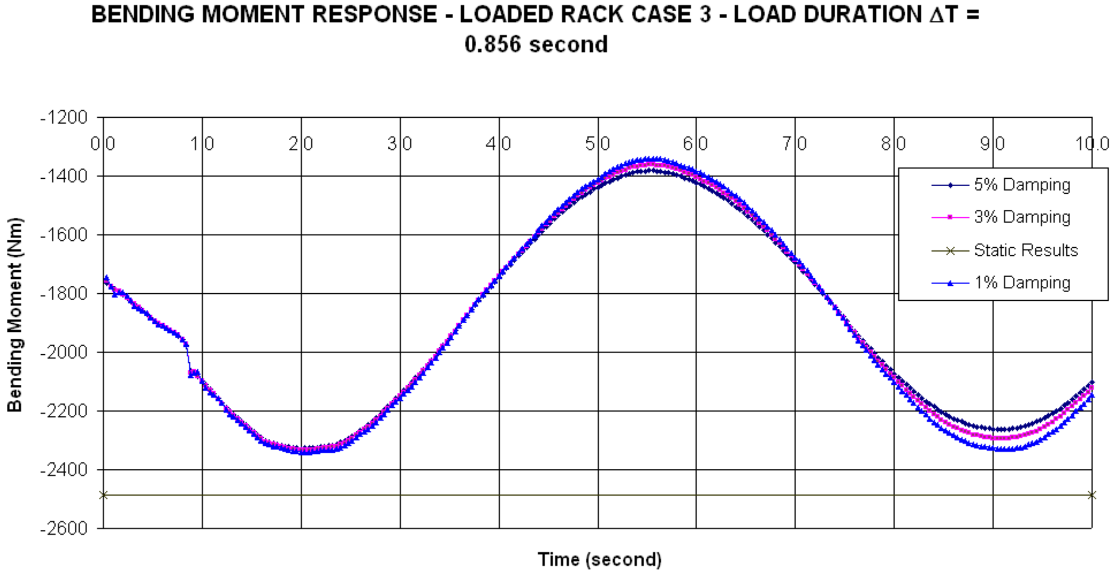

Figure 11q. Bending Moment Response at the base of impacted upright – Loaded Rack Case 3 – Load Duration ΔT = 0.856 second

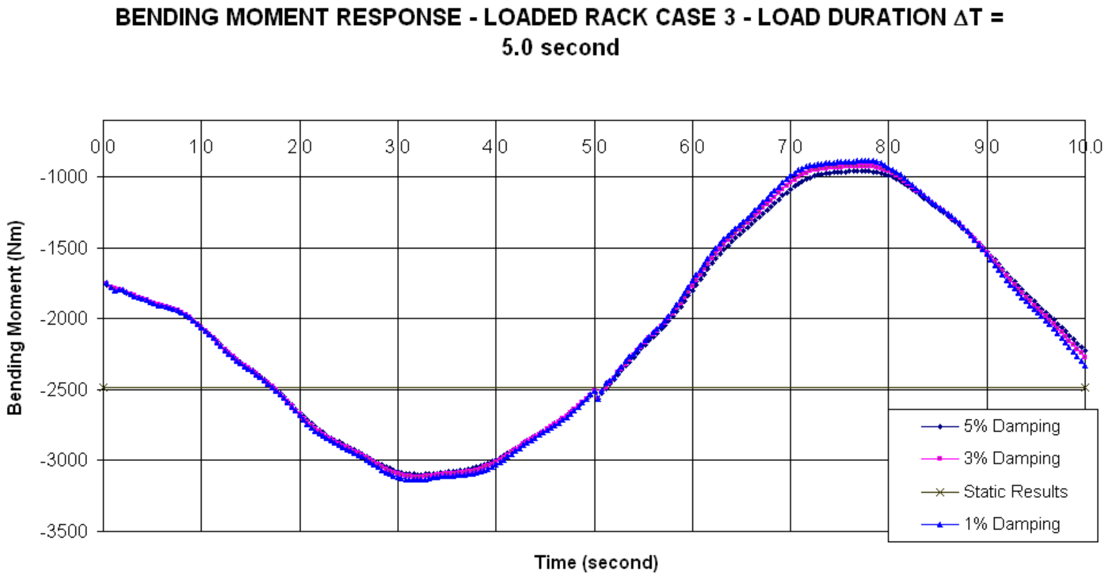

Figure 11r. Bending Moment Response at the base of impacted upright – Loaded Rack Case 3 – Load Duration ΔT = 5.0 second

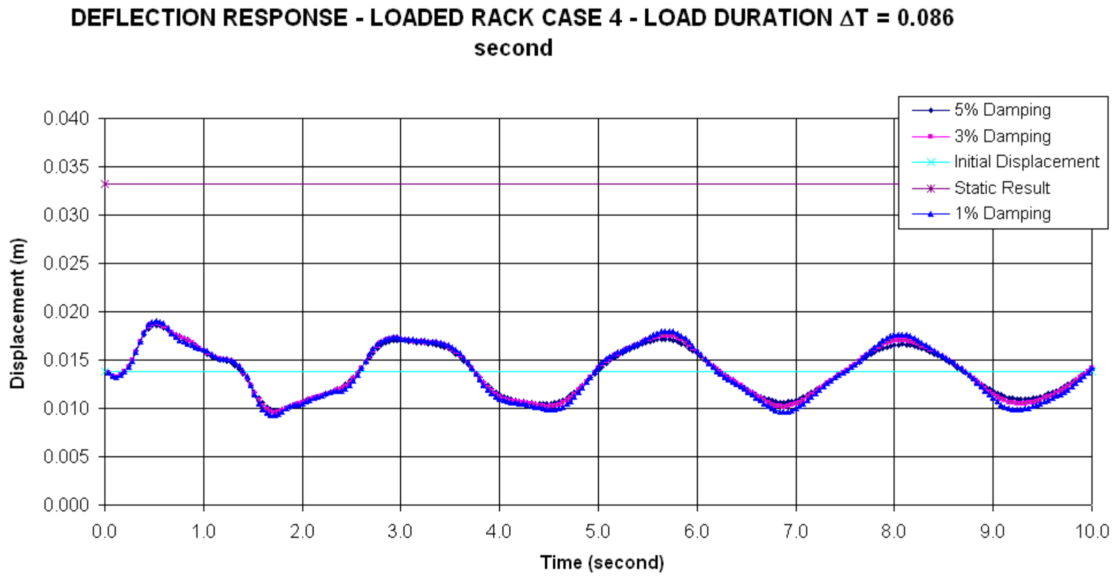

Figure 12a. Deflection Response at the front face of the rack – Loaded Rack Case 4 – Load Duration ΔT = 0.086 second

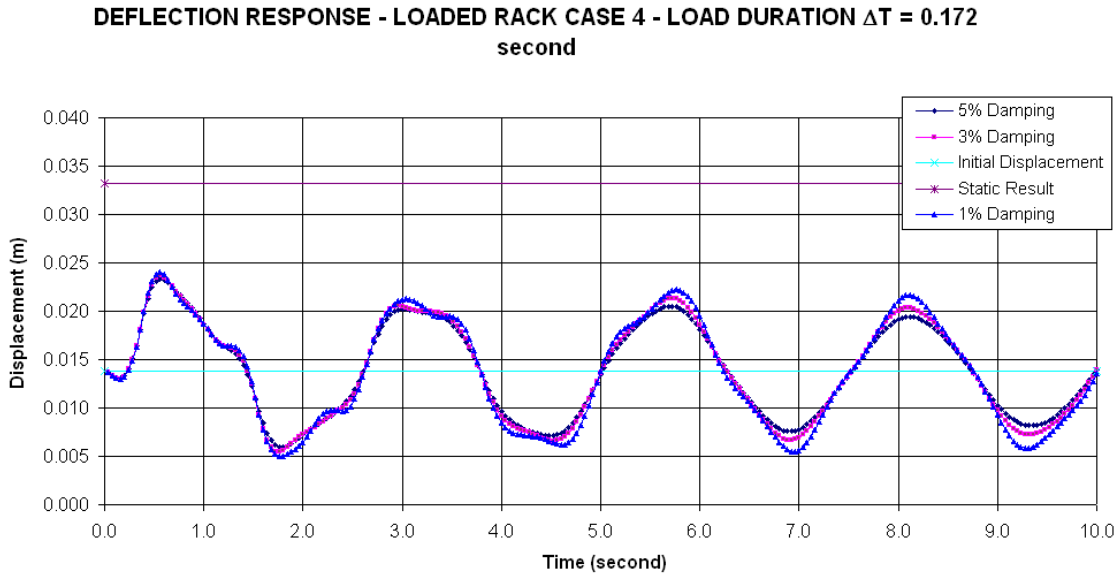

Figure 12b. Deflection Response at the front face of the rack – Loaded Rack Case 4 – Load Duration ΔT = 0.172 second

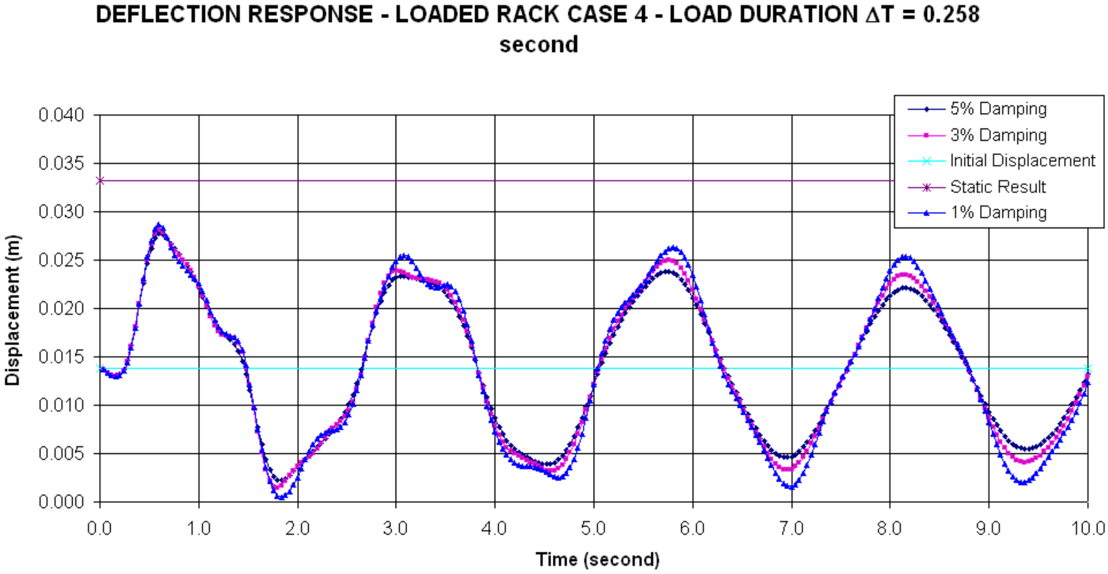

Figure 12c. Deflection Response at the front face of the rack – Loaded Rack Case 4 – Load Duration ΔT = 0.258 second

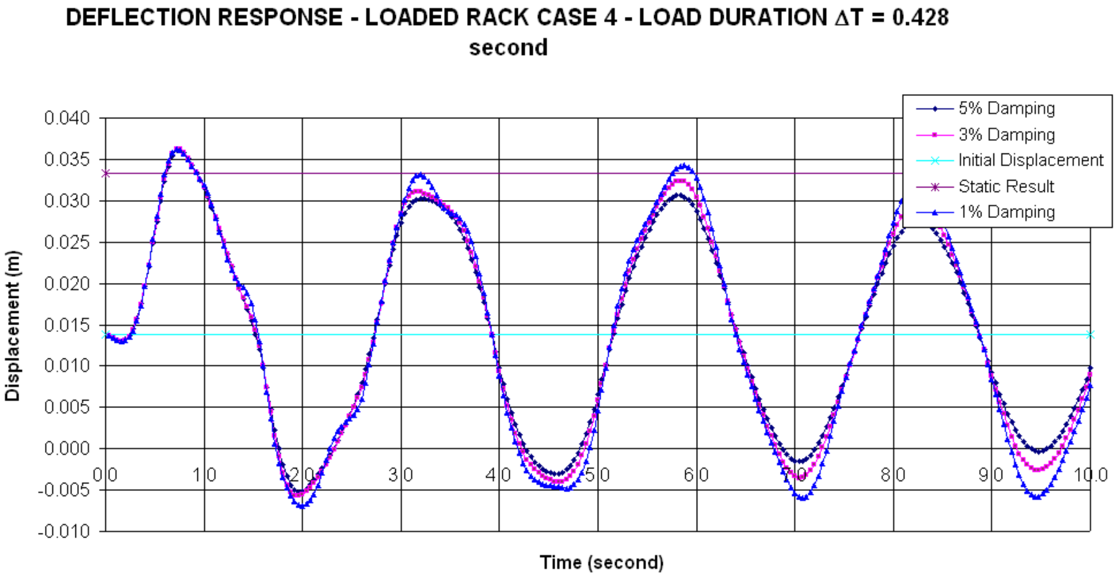

Figure 12d. Deflection Response at the front face of the rack – Loaded Rack Case 4 – Load Duration ΔT = 0.428 second

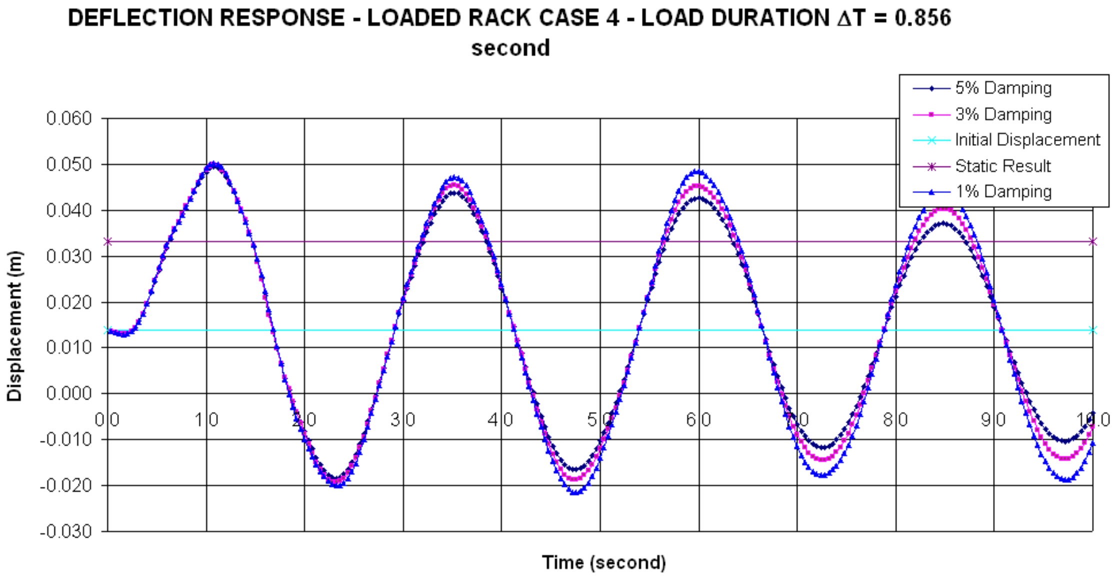

Figure 12e. Deflection Response at the front face of the rack – Loaded Rack Case 4 – Load Duration ΔT = 0.856 second

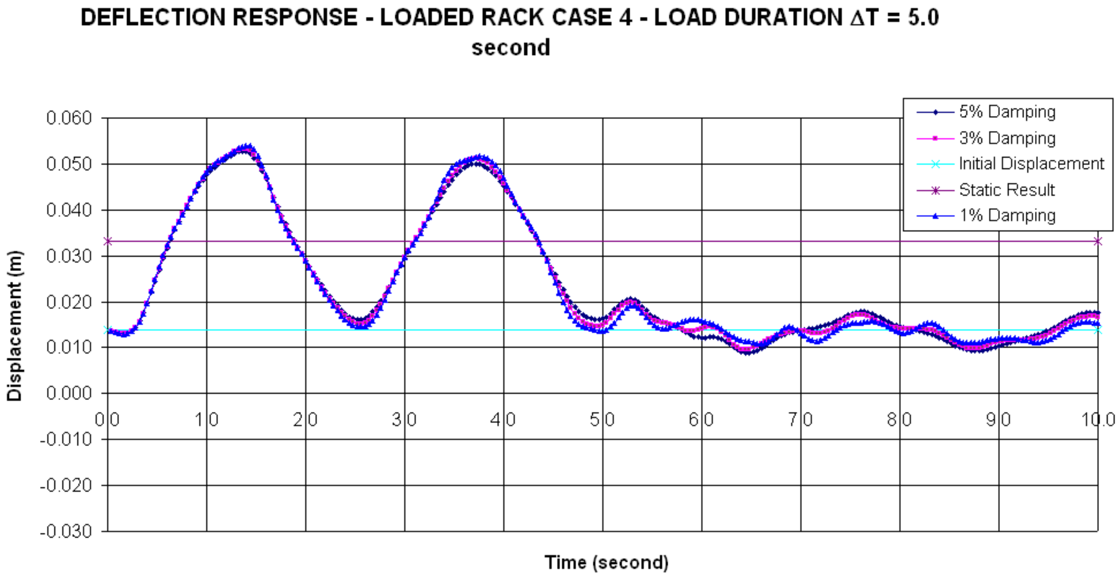

Figure 12f. Deflection Response at the front face of the rack – Loaded Rack Case 4 – Load Duration ΔT = 5.0 second

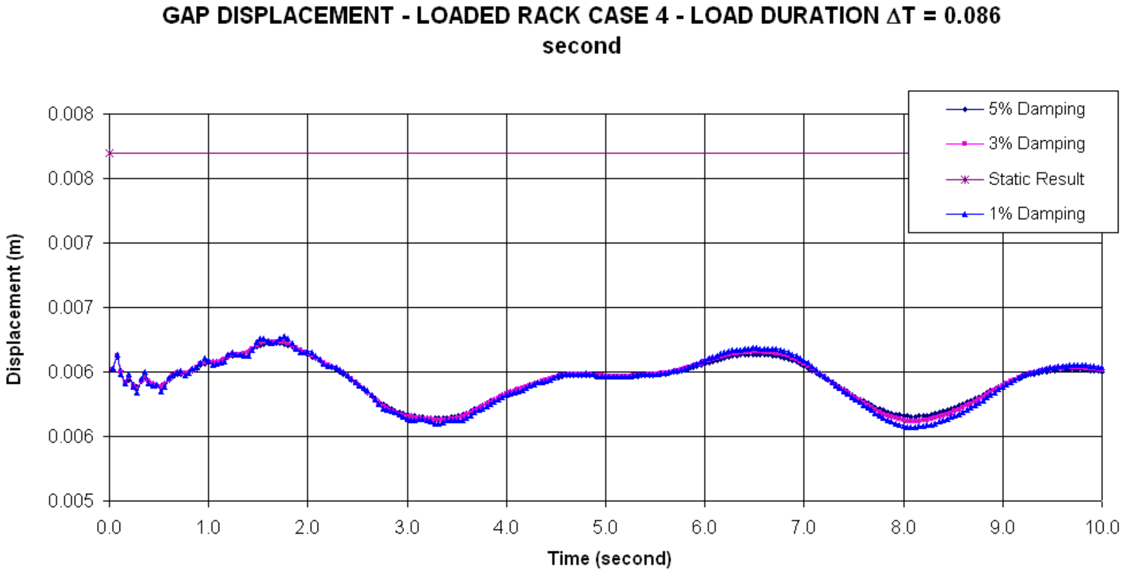

Figure 12g. Displacement Gap Response at the front face of top pallet level – Loaded Rack Case 4 – Load Duration ΔT = 0.086 second

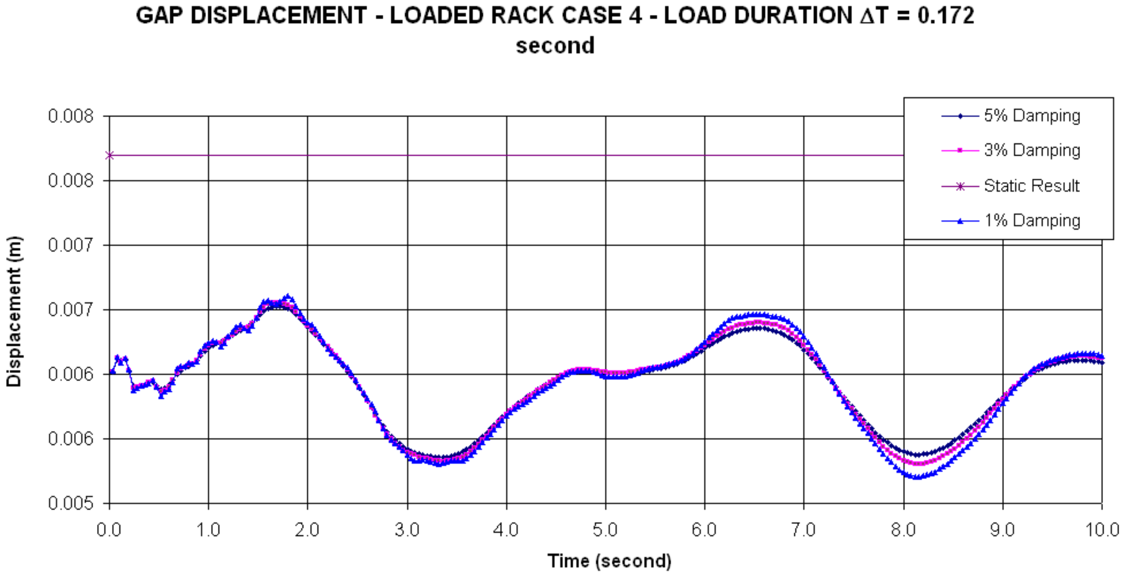

Figure 12h. Displacement Gap Response at the front face of top pallet level – Loaded Rack Case 4 – Load Duration ΔT = 0.172 second

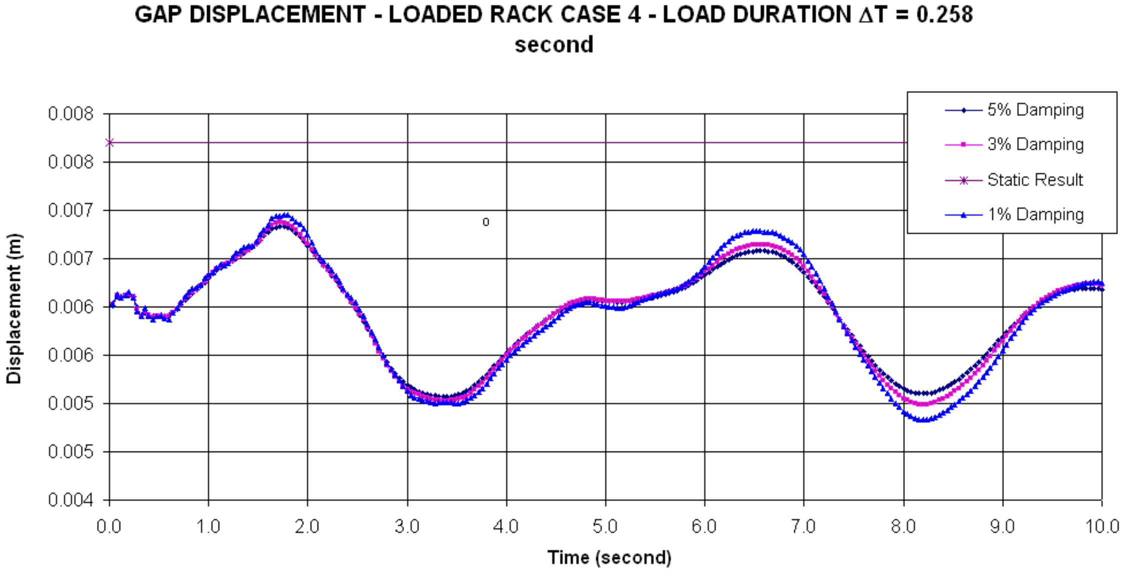

Figure 12i. Displacement Gap Response at the front face of top pallet level – Loaded Rack Case 4 – Load Duration ΔT = 0.258 second

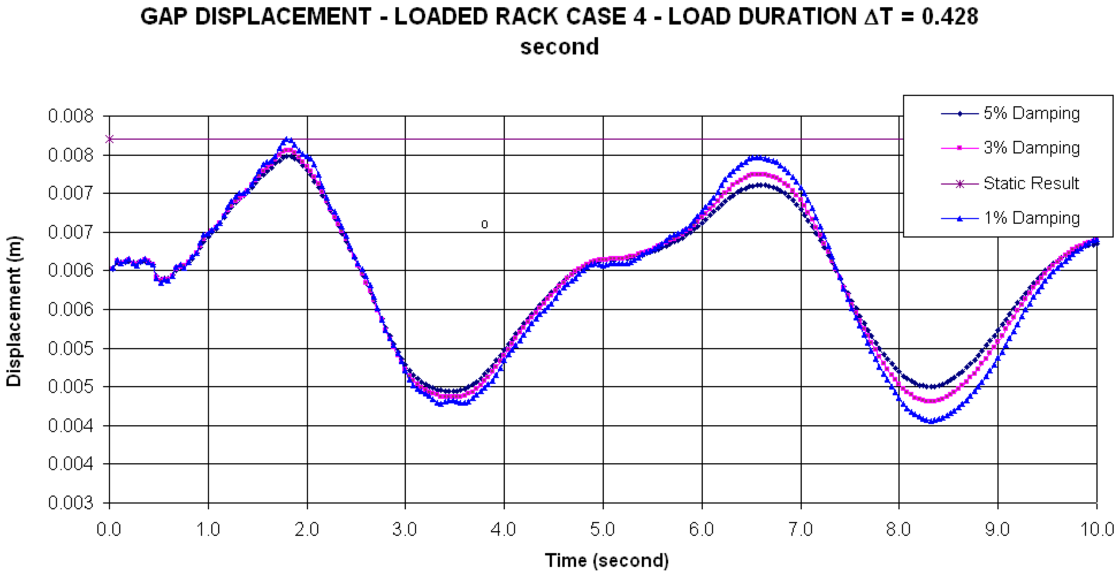

Figure 12j. Displacement Gap Response at the front face of top pallet level – Loaded Rack Case 4 – Load Duration ΔT = 0.428 second

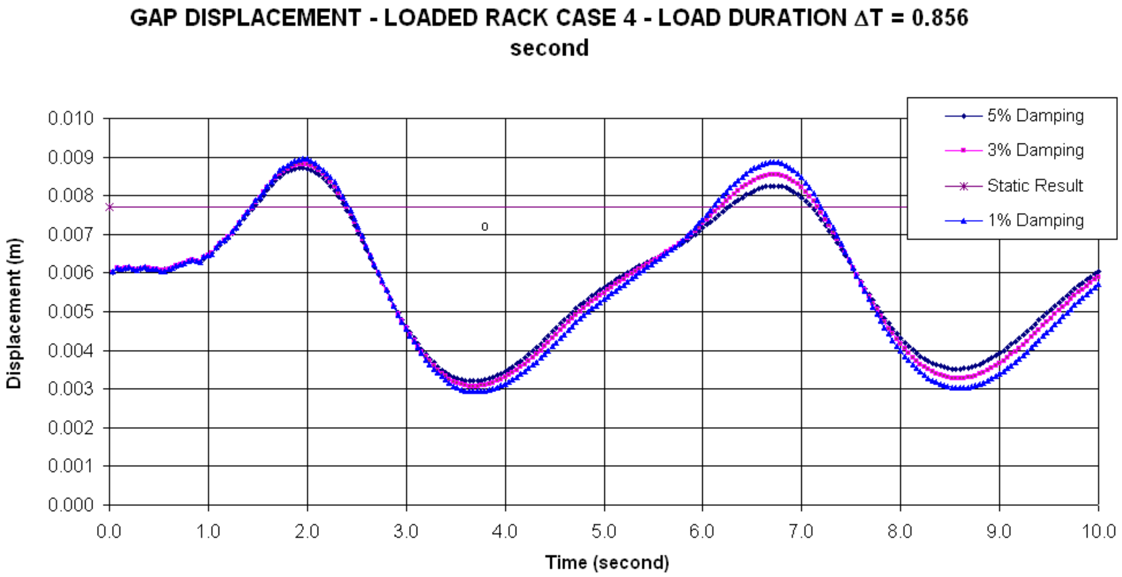

Figure 12k. Displacement Gap Response at the front face of top pallet level – Loaded Rack Case 4 – Load Duration ΔT = 0.856 second

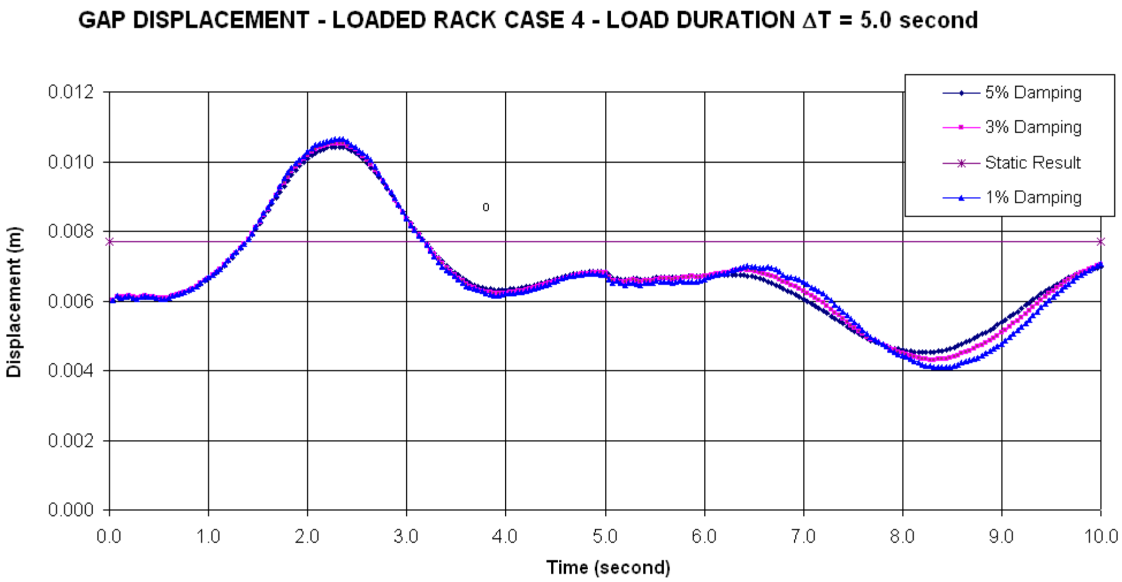

Figure 12l. Displacement Gap Response at the front face of top pallet level – Loaded Rack Case 4 – Load Duration ΔT = 5.0 second

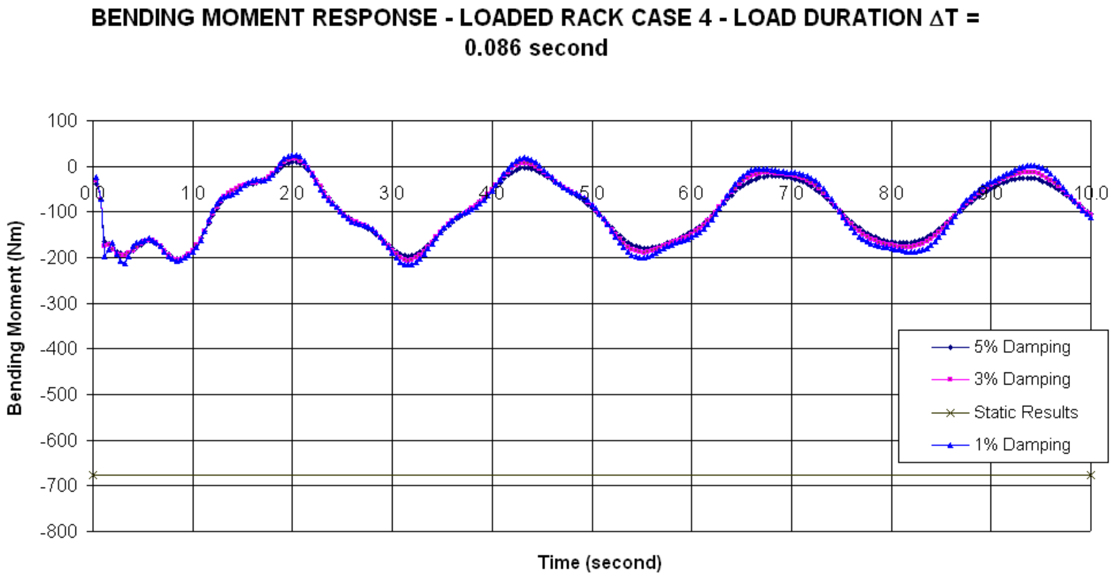

Figure 12m. Bending Moment Response at the base of impacted upright – Loaded Rack Case 4 – Load Duration ΔT = 0.086 second

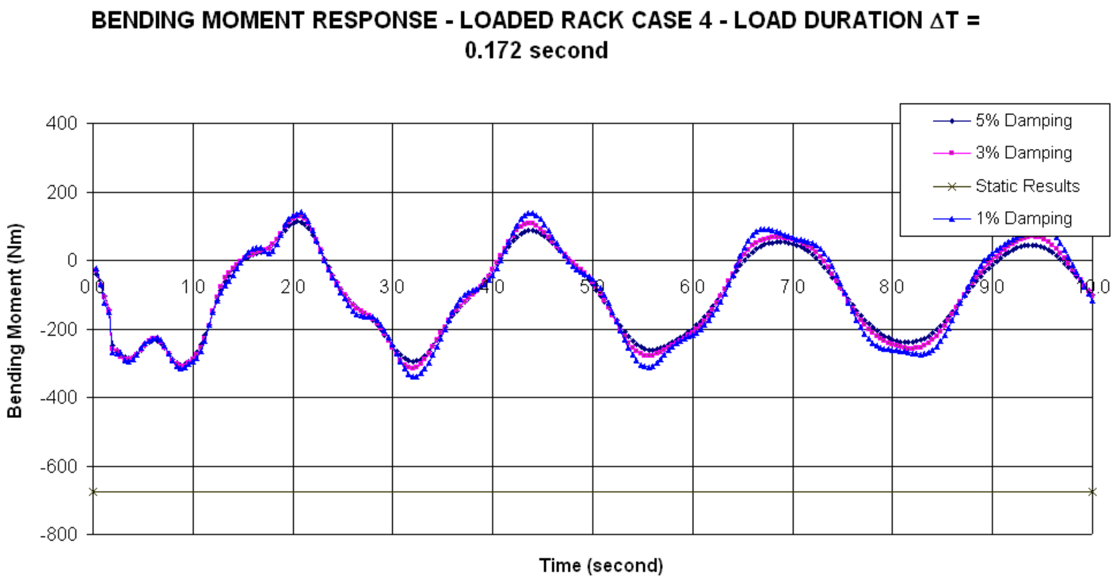

Figure 12n. Bending Moment Response at the base of impacted upright – Loaded Rack Case 4 – Load Duration ΔT = 0.172 second

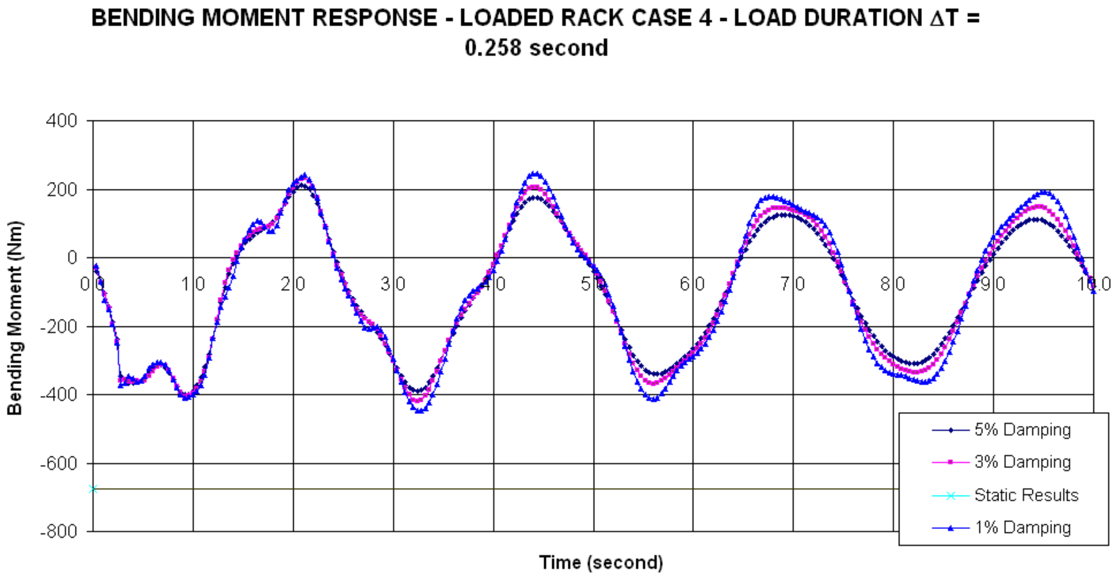

Figure 12o. Bending Moment Response at the base of impacted upright – Loaded Rack Case 4 – Load Duration ΔT = 0.258 second

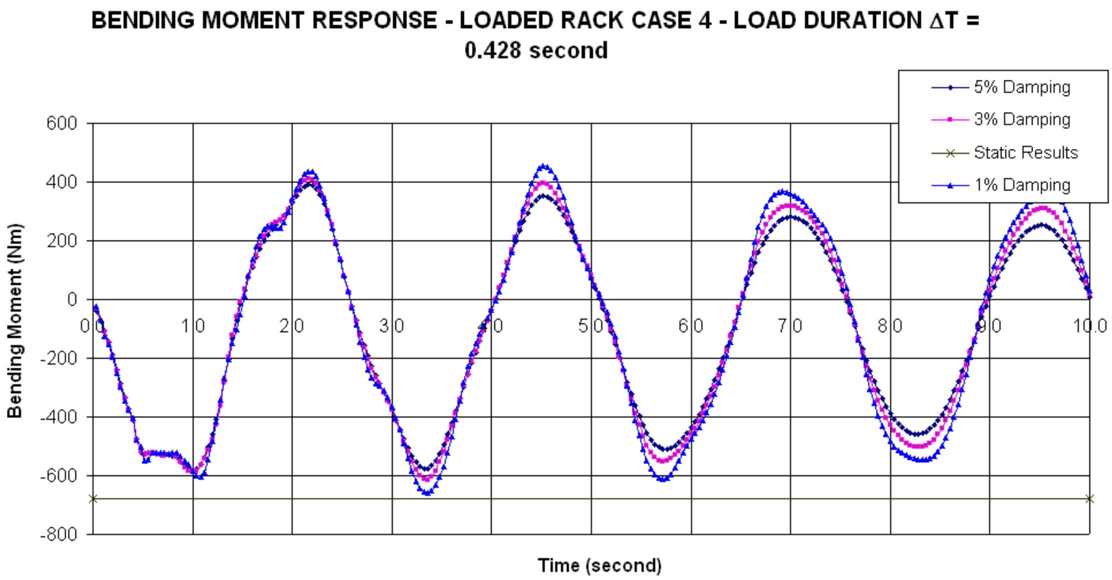

Figure 12p. Bending Moment Response at the base of impacted upright – Loaded Rack Case 4 – Load Duration ΔT = 0.428 second

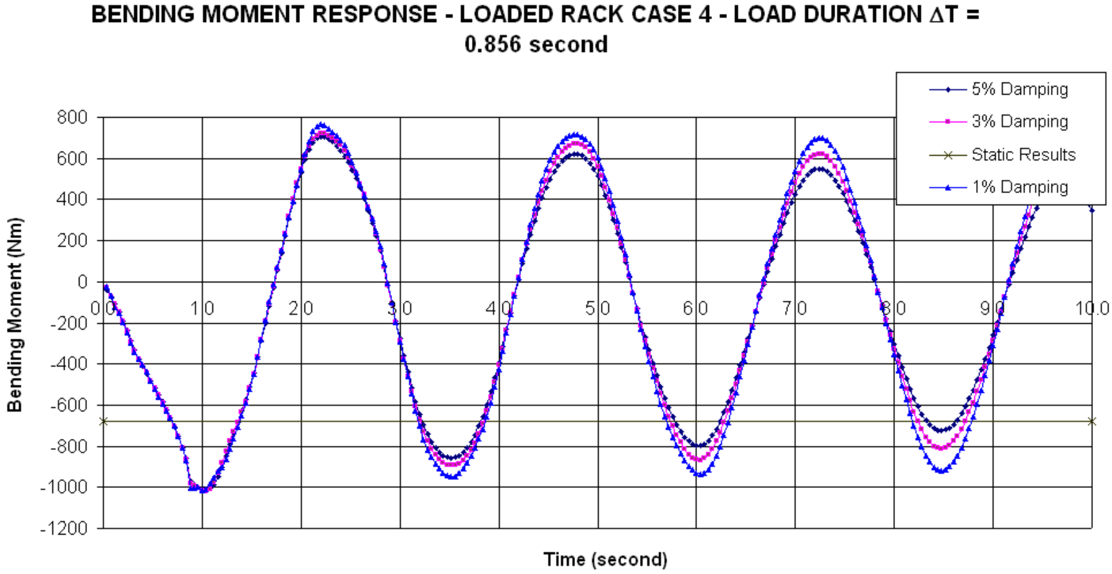

Figure 12q. Bending Moment Response at the base of impacted upright – Loaded Rack Case 4 – Load Duration ΔT = 0.856 second

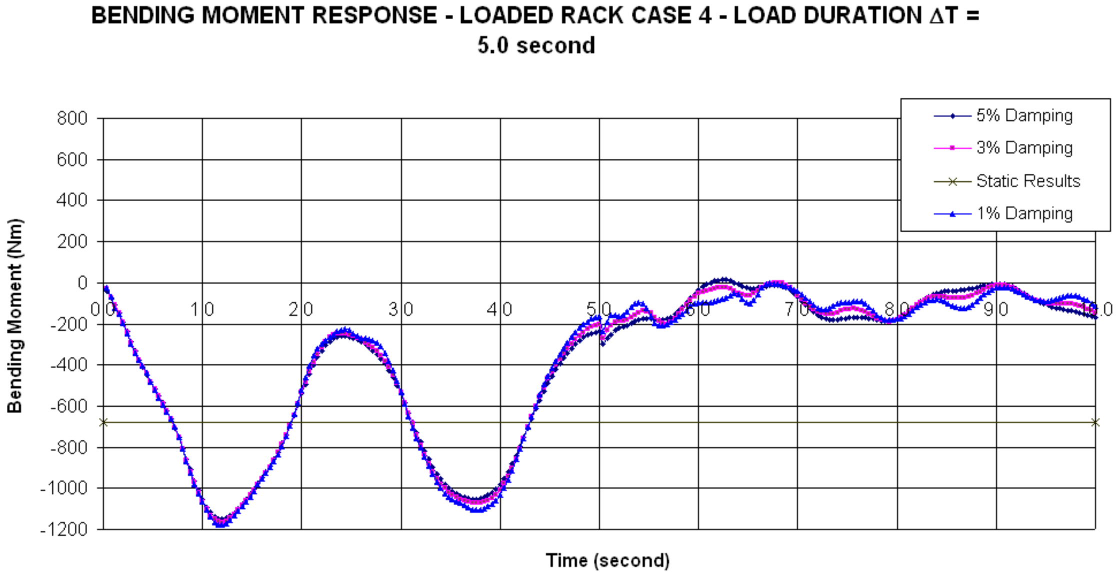

Figure 12r. Bending Moment Response at the base of impacted upright – Loaded Rack Case 4 – Load Duration ΔT = 5.0 second

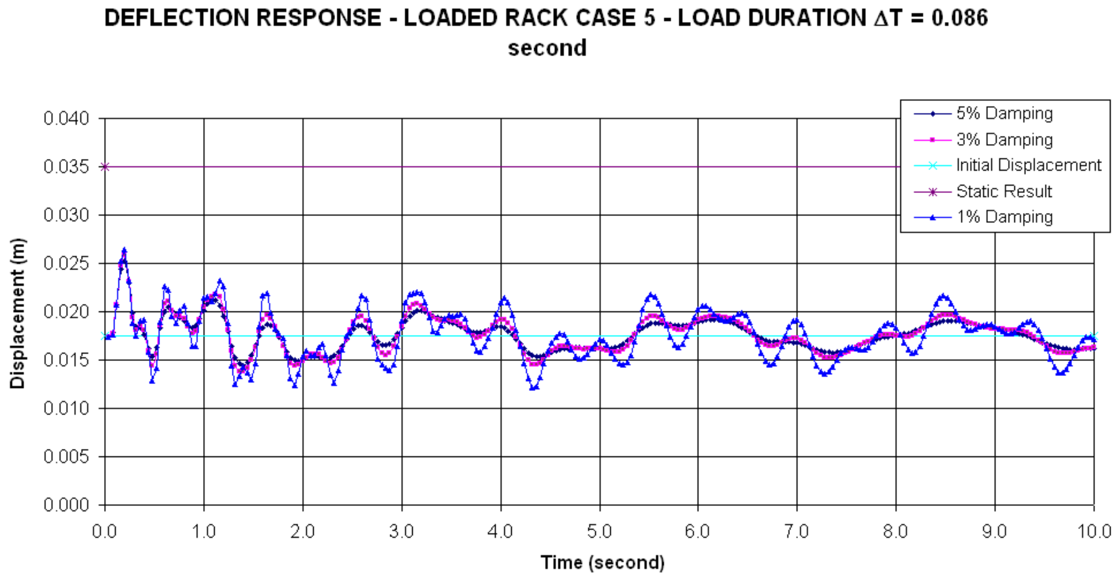

Figure 13a. Deflection Response at the front face of the rack – Loaded Rack Case 5 – Load Duration ΔT = 0.086 second

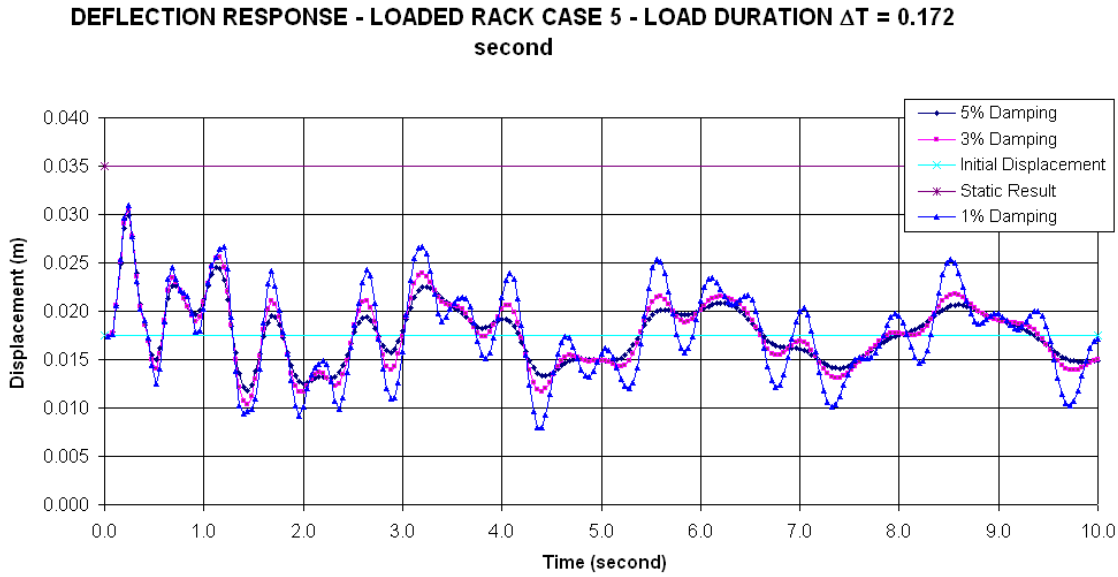

Figure 13b. Deflection Response at the front face of the rack – Loaded Rack Case 5 – Load Duration ΔT = 0.172 second

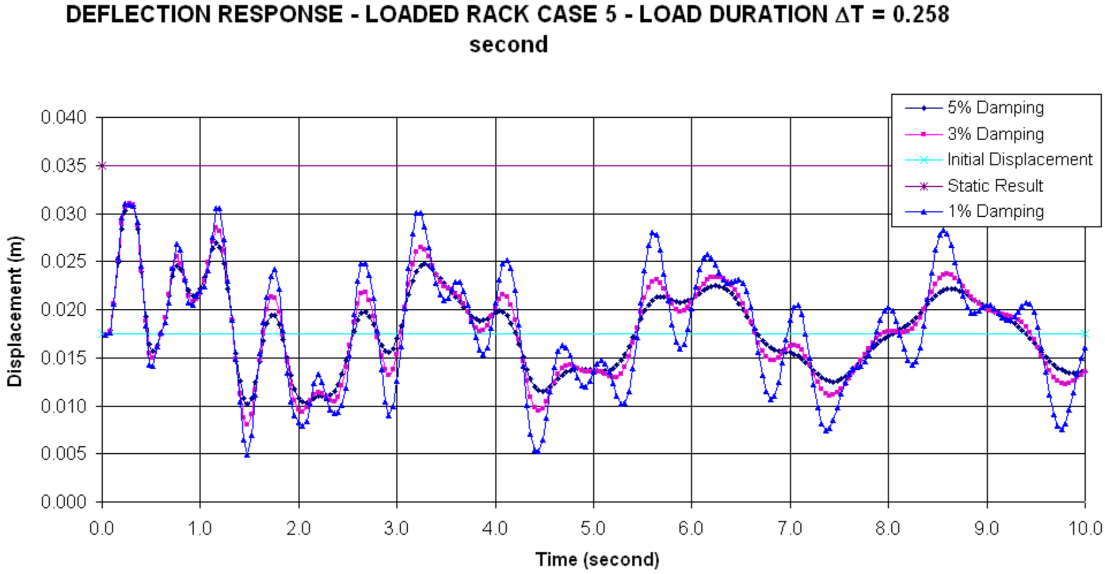

Figure 13c. Deflection Response at the front face of the rack – Loaded Rack Case 5 – Load Duration ΔT/T = 0.258 second

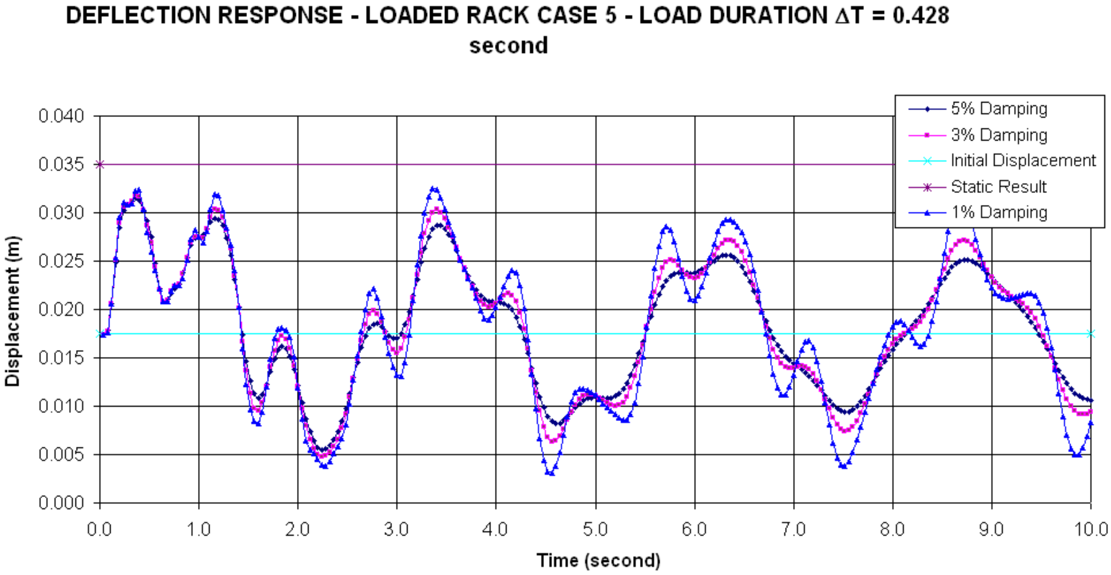

Figure 13d. Deflection Response at the front face of the rack – Loaded Rack Case 5 – Load Duration ΔT = 0.428 second

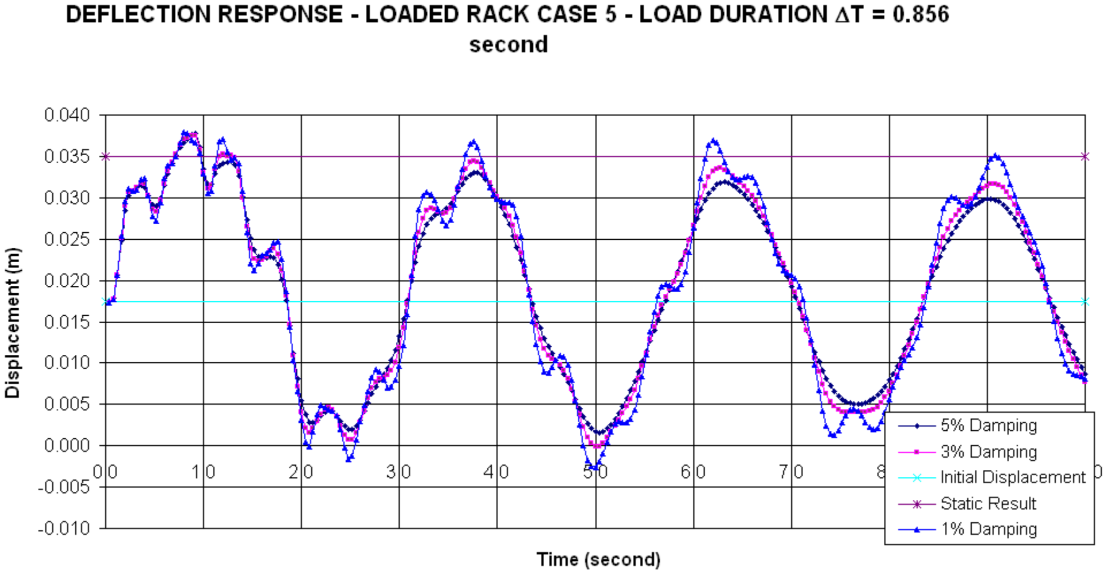

Figure 13e. Deflection Response at the front face of the rack – Loaded Rack Case 5 – Load Duration ΔT = 0.856 second

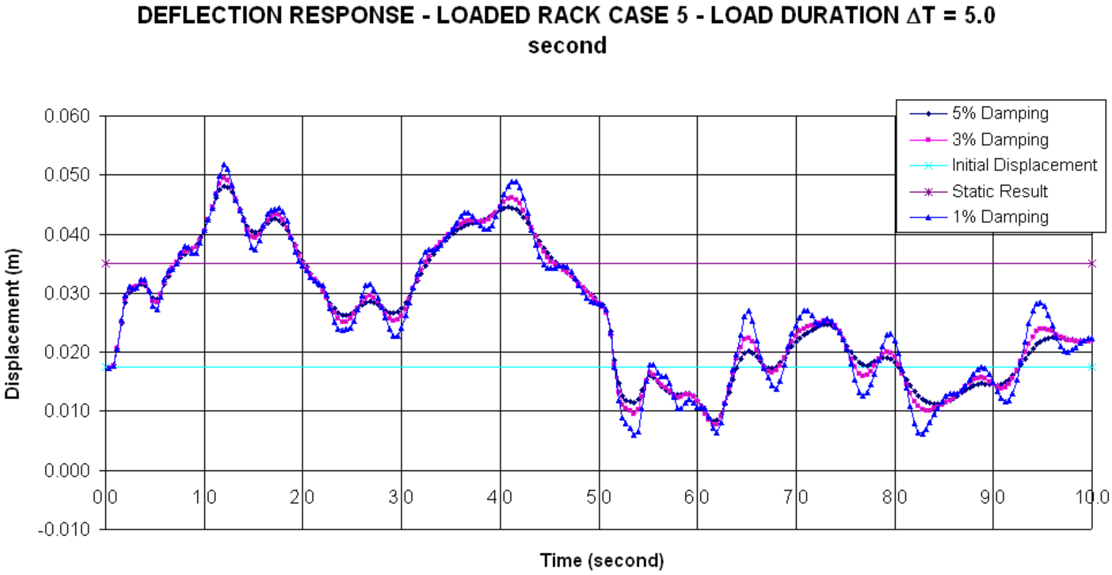

Figure 13f. Deflection Response at the front face of the rack – Loaded Rack Case 5 – Load Duration ΔT = 5.0 second

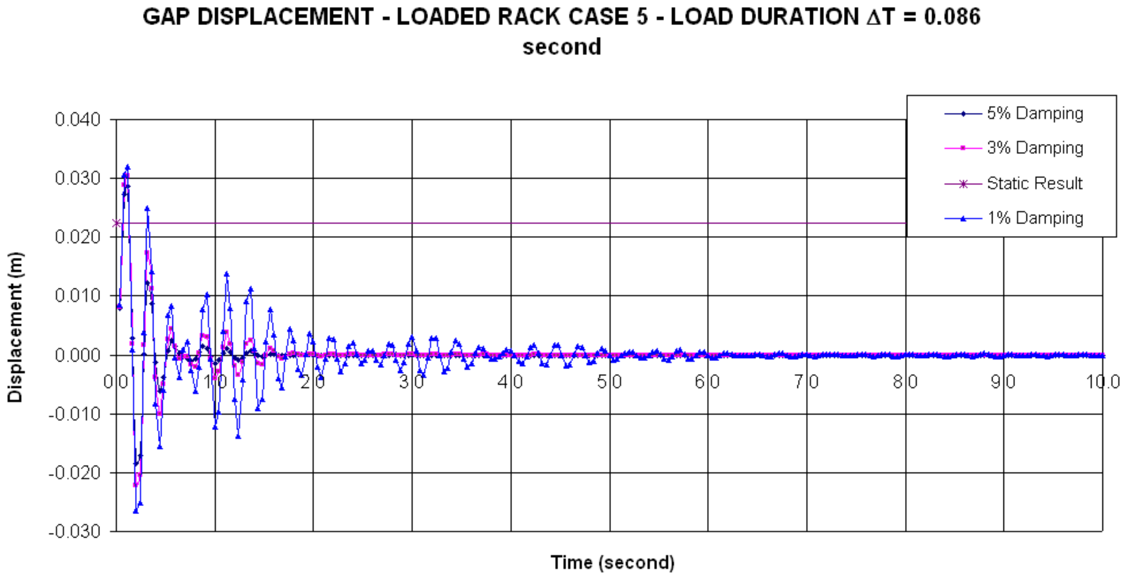

Figure 13g. Displacement Gap Response at the front face of top pallet level – Loaded Rack Case 5 – Load Duration ΔT = 0.086 second

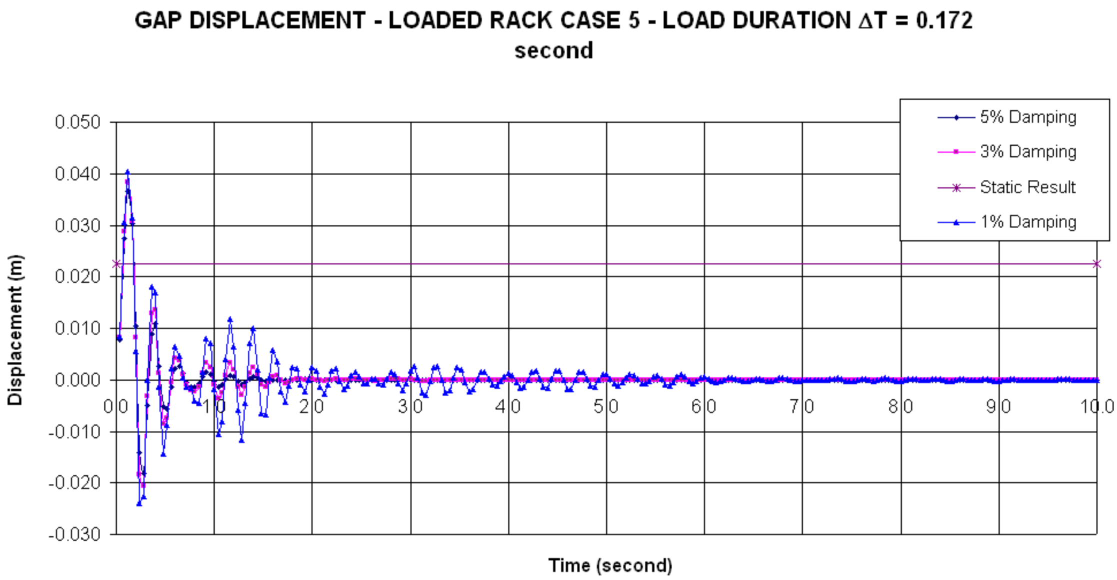

Figure 13h. Displacement Gap Response at the front face of top pallet level – Loaded Rack Case 5 – Load Duration ΔT = 0.172 second

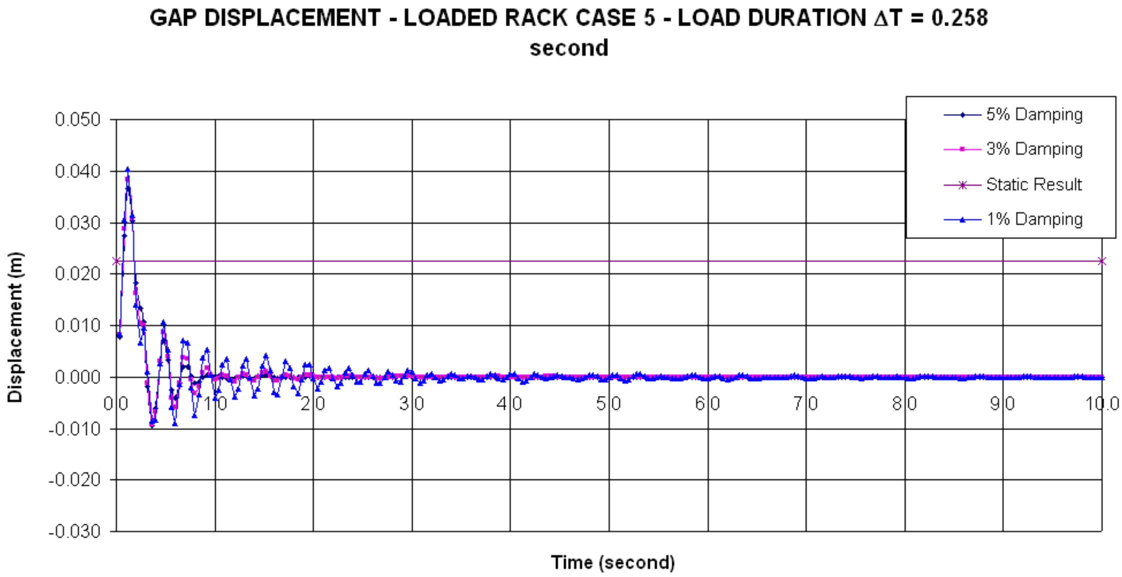

Figure 13i. Displacement Gap Response at the front face of top pallet level – Loaded Rack Case 5 – Load Duration ΔT = 0.258 second

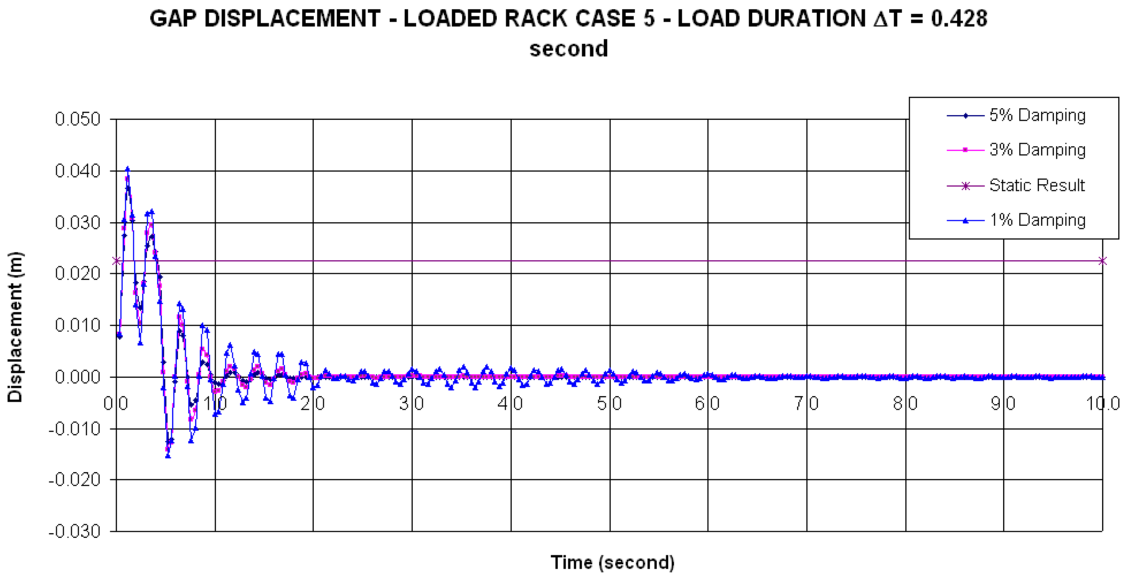

Figure 13j. Displacement Gap Response at the front face of top pallet level – Loaded Rack Case 5 – Load Duration ΔT = 0.428 second

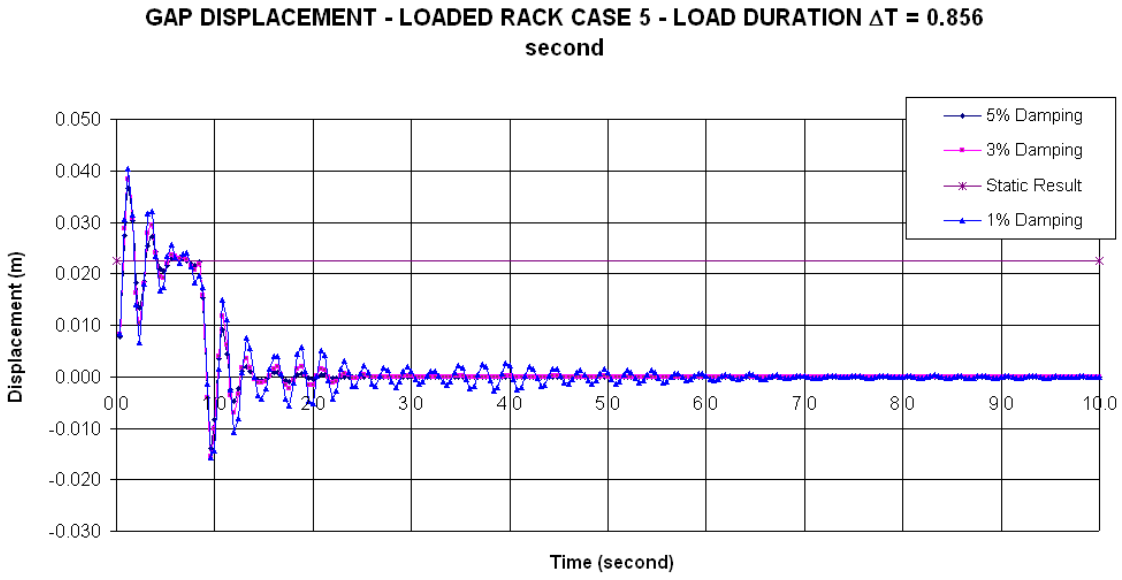

Figure 13k. Displacement Gap Response at the front face of top pallet level – Loaded Rack Case 5 – Load Duration ΔT = 0.856 second

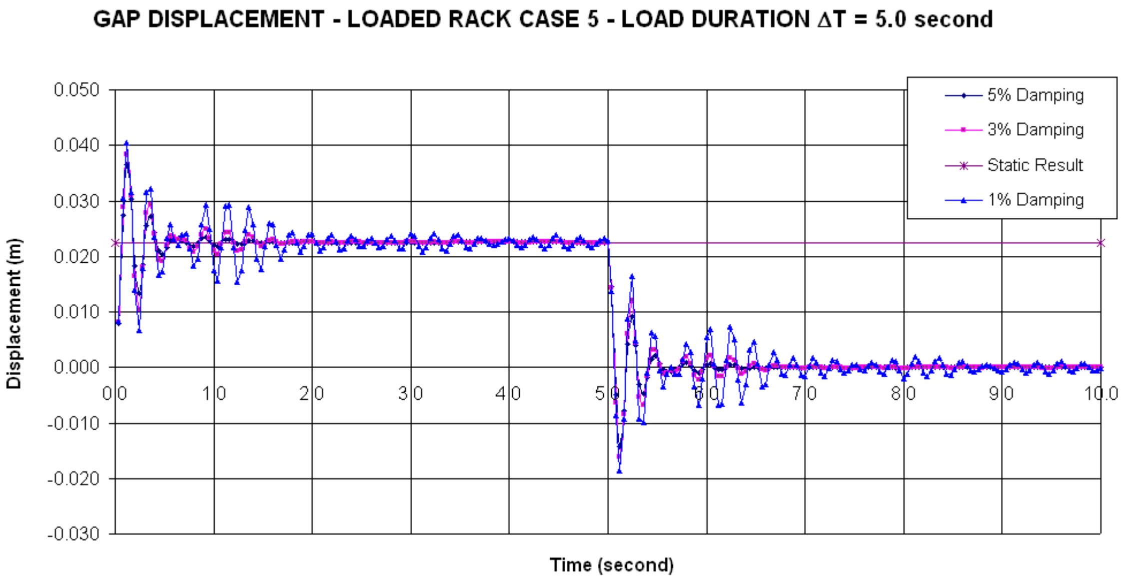

Figure 13l. Displacement Gap Response at the front face of top pallet level – Loaded Rack Case 5 – Load Duration ΔT = 5.0 second

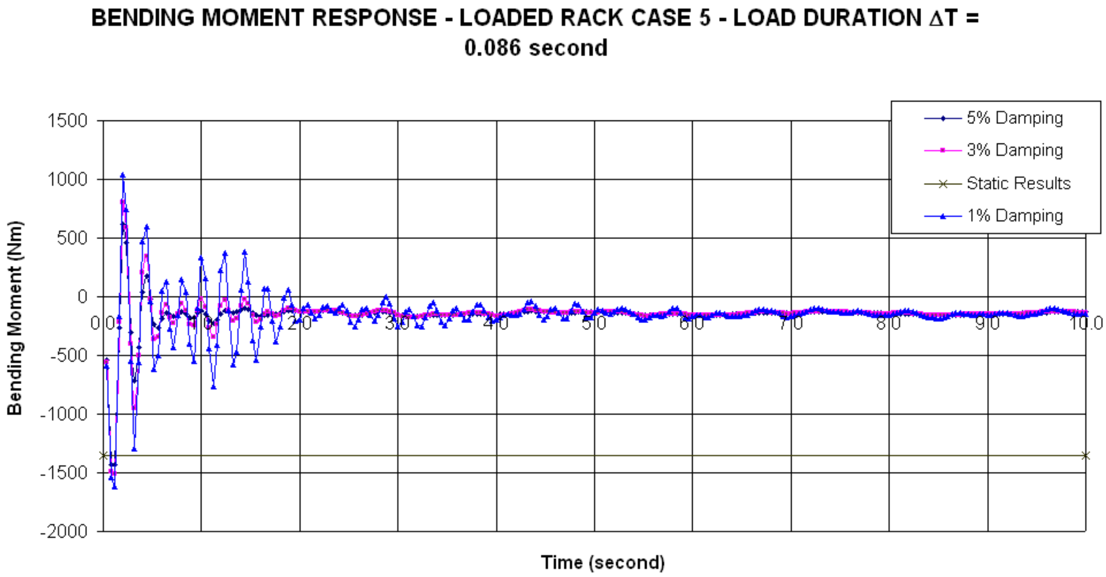

Figure 13m. Bending Moment Response at the base of impacted upright – Loaded Rack Case 5 – Load Duration ΔT = 0.086 second

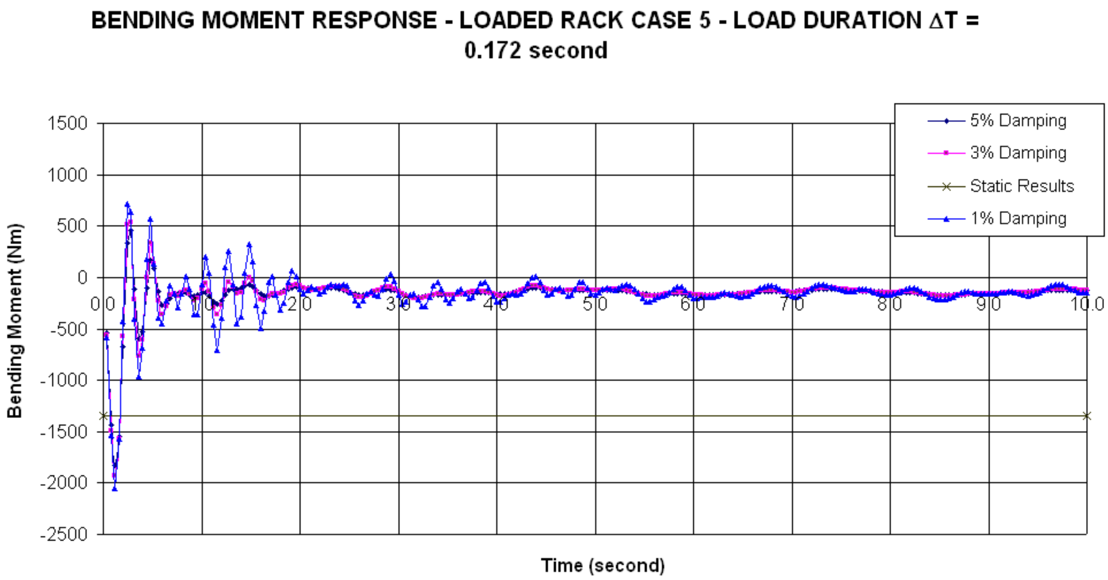

Figure 13n. Bending Moment Response at the base of impacted upright – Loaded Rack Case 5 – Load Duration ΔT = 0.172 second

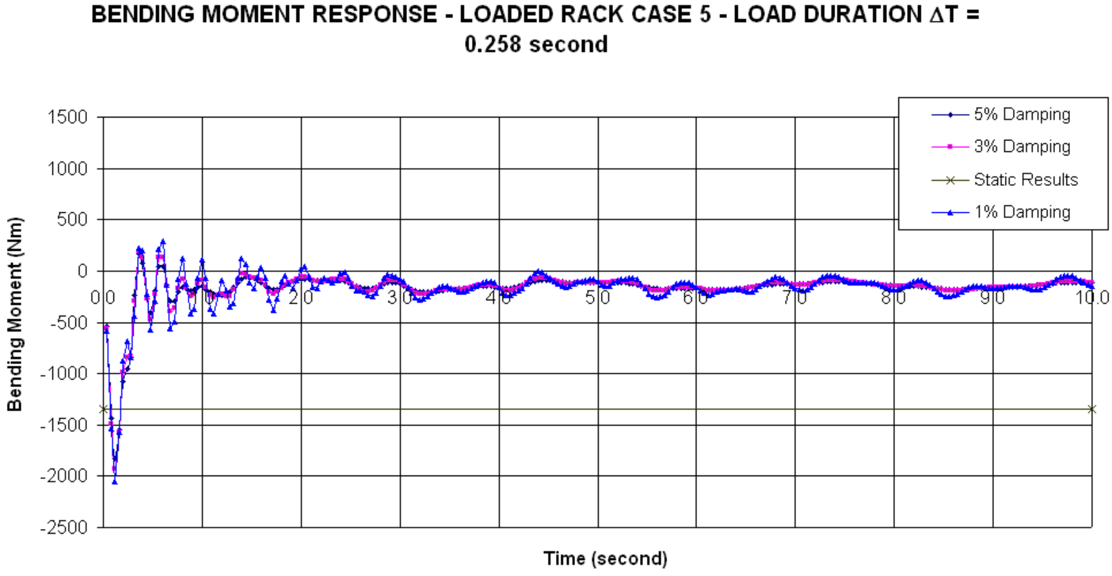

Figure 13o. Bending Moment Response at the base of impacted upright – Loaded Rack Case 5 – Load Duration ΔTT = 0.258 second

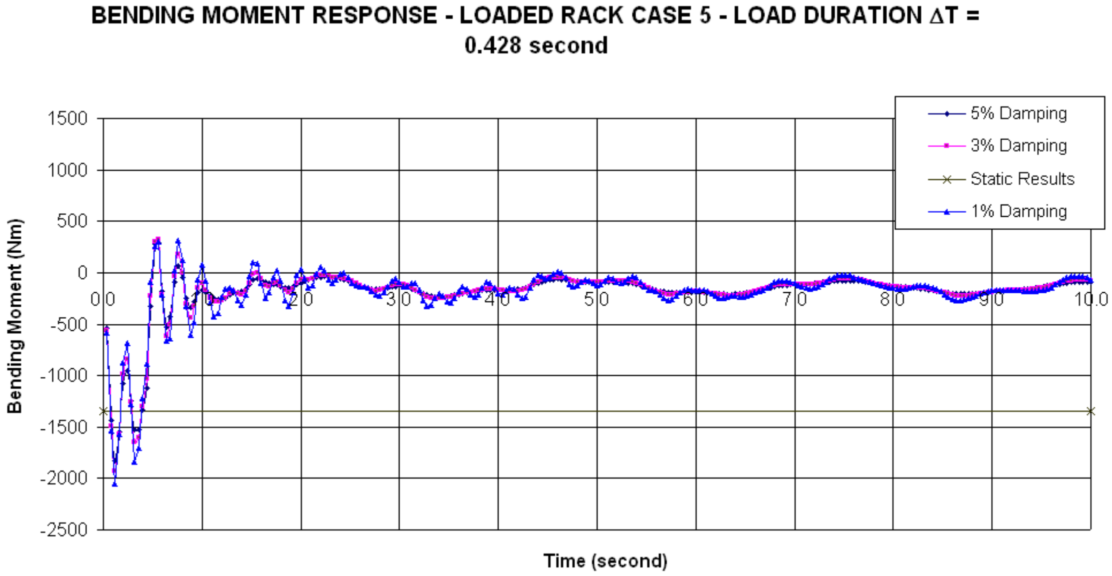

Figure 13p. Bending Moment Response at the base of impacted upright – Loaded Rack Case 5 – Load Duration ΔT = 0.428 second

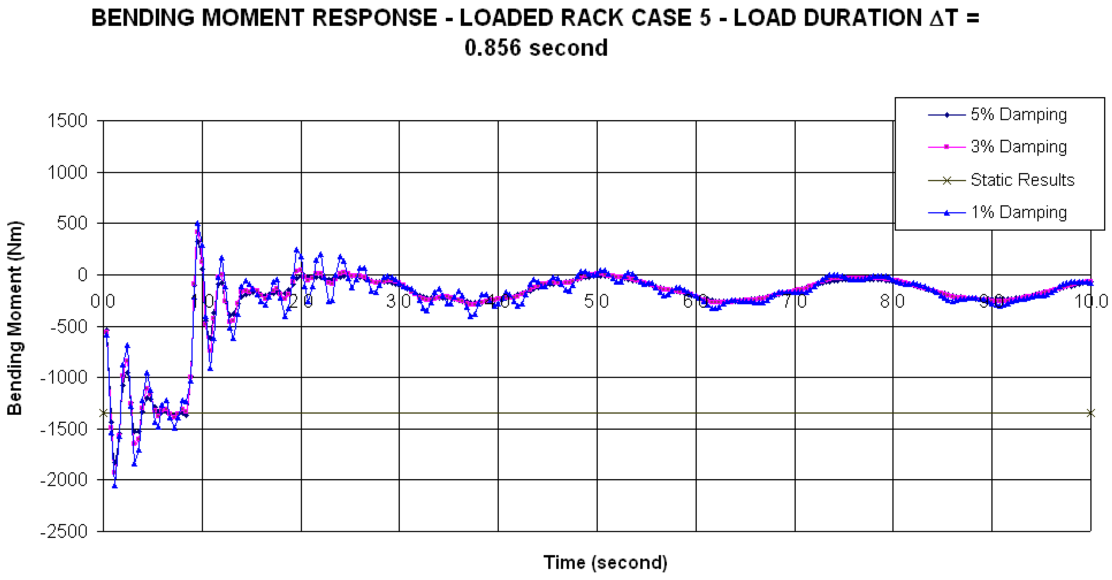

Figure 13q. Bending Moment Response at the base of impacted upright – Loaded Rack Case 5 – Load Duration ΔT = 0.856 second

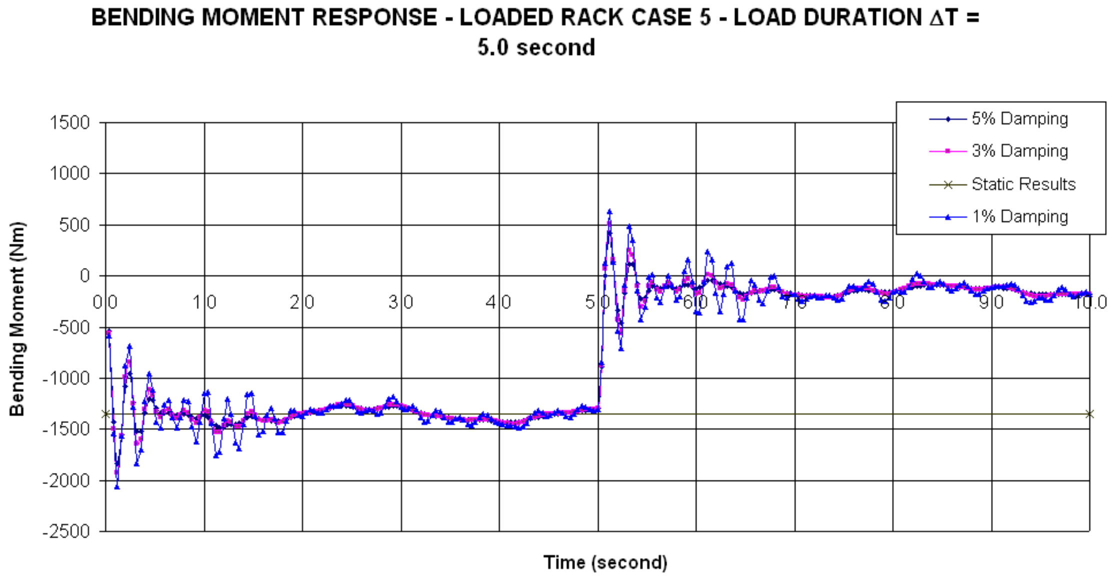

Figure 13r. Bending Moment Response at the base of impacted upright – Loaded Rack Case 5 – Load Duration ΔT = 5.0 second

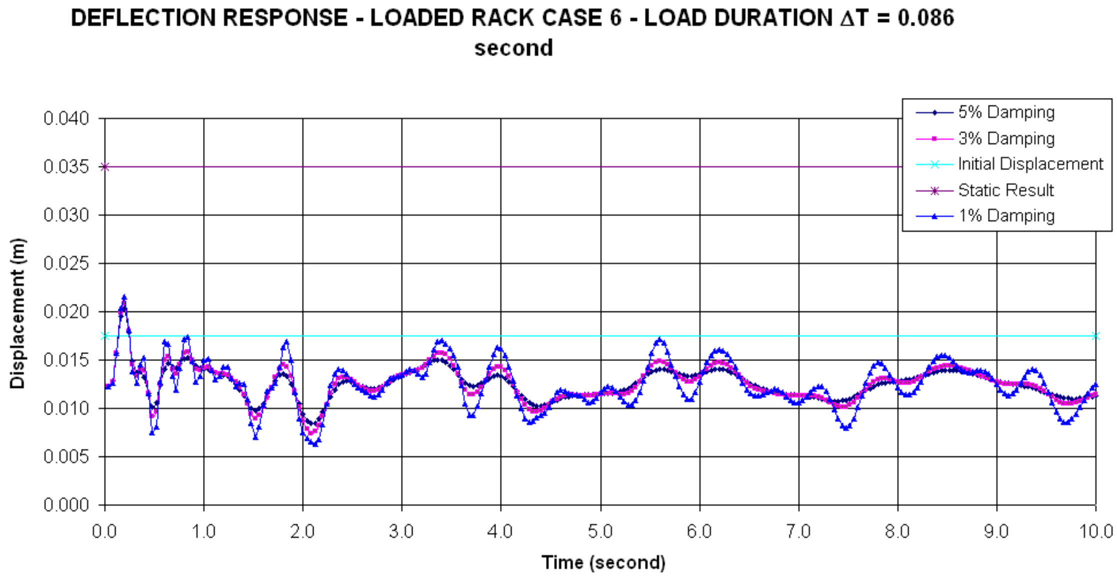

Figure 14a. Deflection Response at the front face of the rack – Loaded Rack Case 6 – Load Duration ΔT = 0.086 second

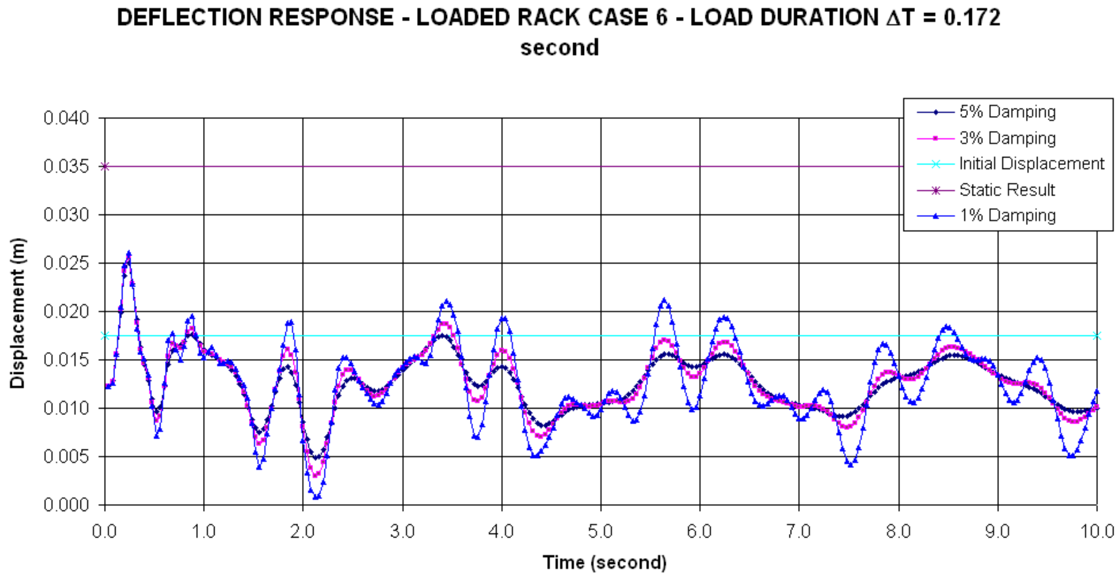

Figure 14b. Deflection Response at the front face of the rack – Loaded Rack Case 6 – Load Duration ΔT = 0.172 second

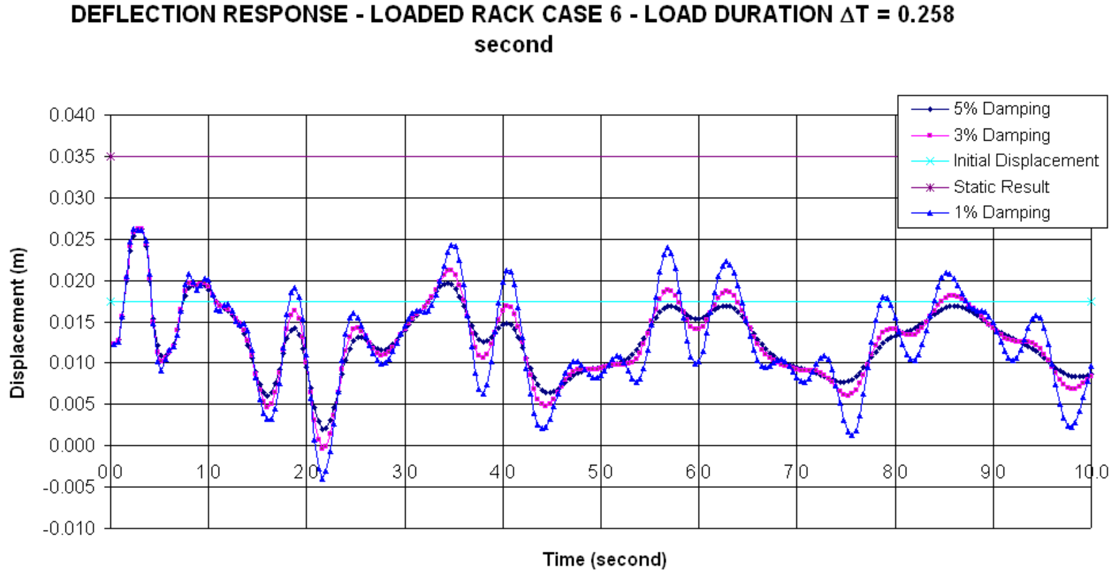

Figure 14c. Deflection Response at the front face of the rack – Loaded Rack Case 6 – Load Duration ΔT = 0.258 second

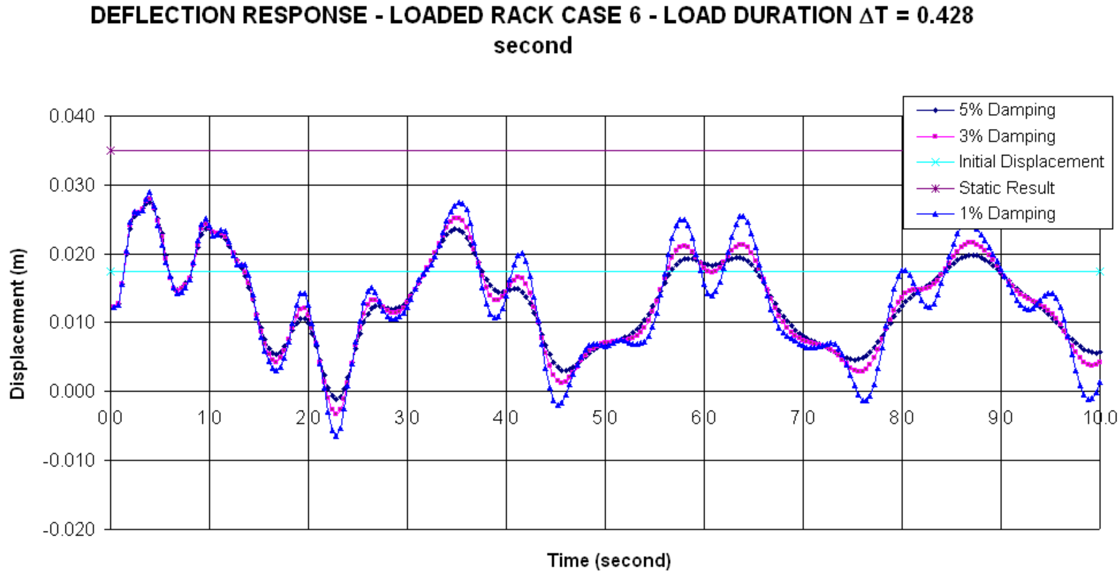

Figure 14d. Deflection Response at the front face of the rack – Loaded Rack Case 6 – Load Duration ΔT = 0.428 second

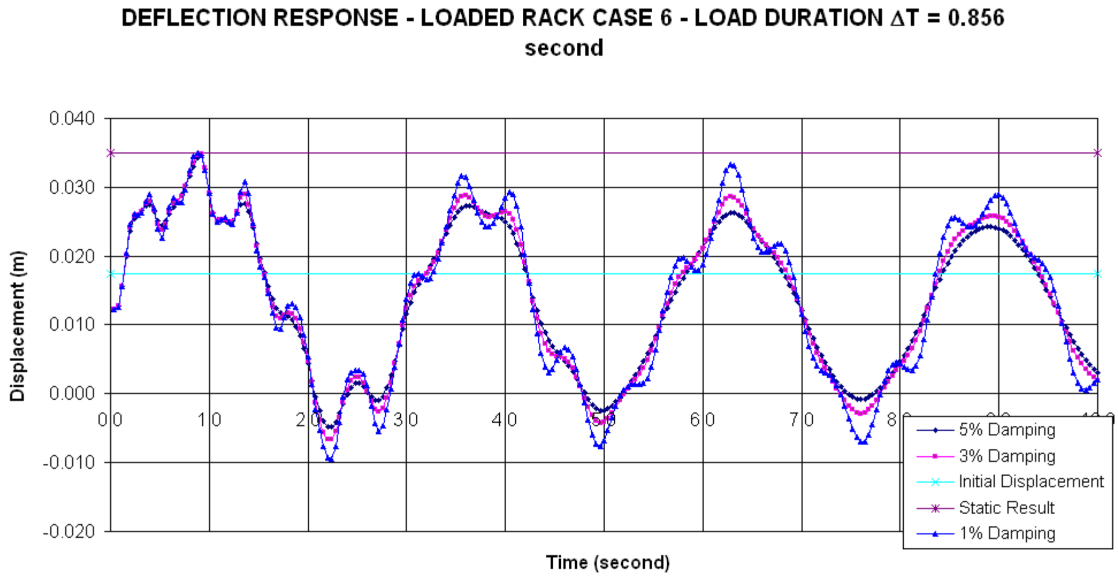

Figure 14e. Deflection Response at the front face of the rack – Loaded Rack Case 6 – Load Duration ΔT = 0.856 second

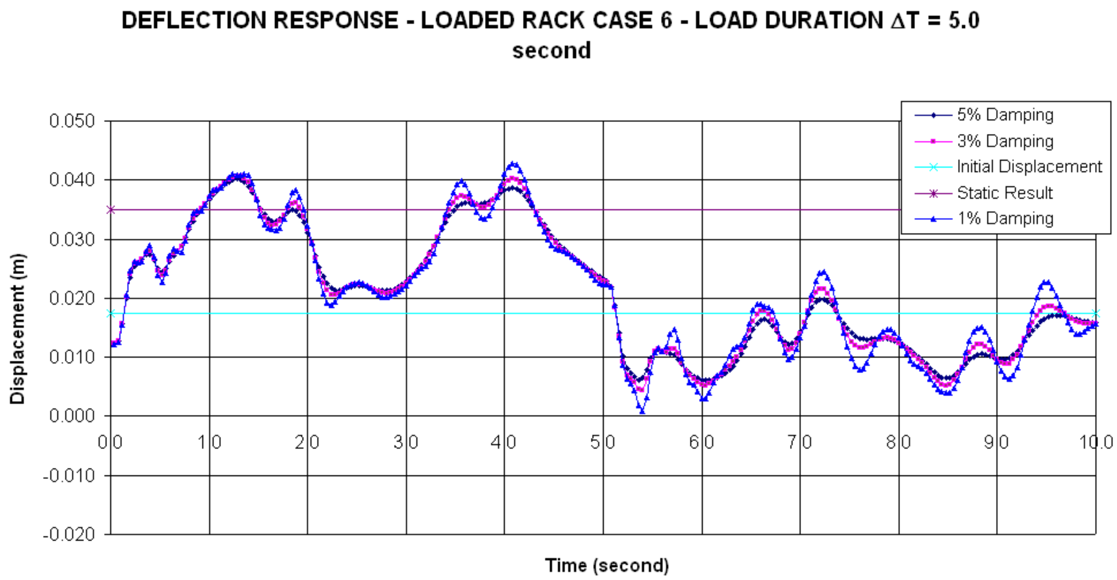

Figure 14f. Deflection Response at the front face of the rack – Loaded Rack Case 6 – Load Duration ΔT = 5.0 second

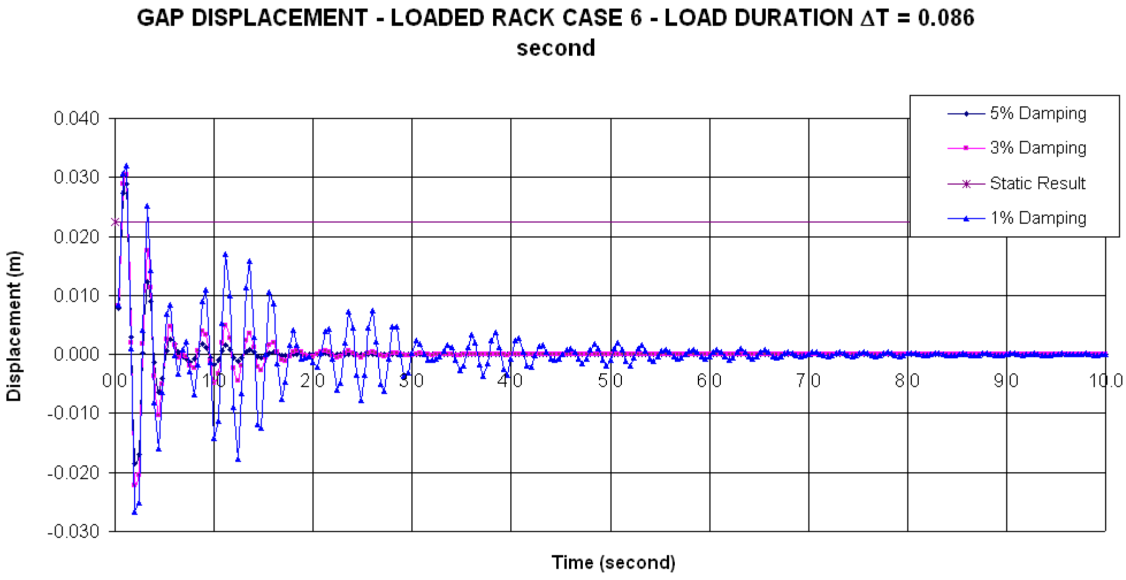

Figure 14g. Displacement Gap Response at the front face of top pallet level – Loaded Rack Case 6 – Load Duration ΔT = 0.086 second

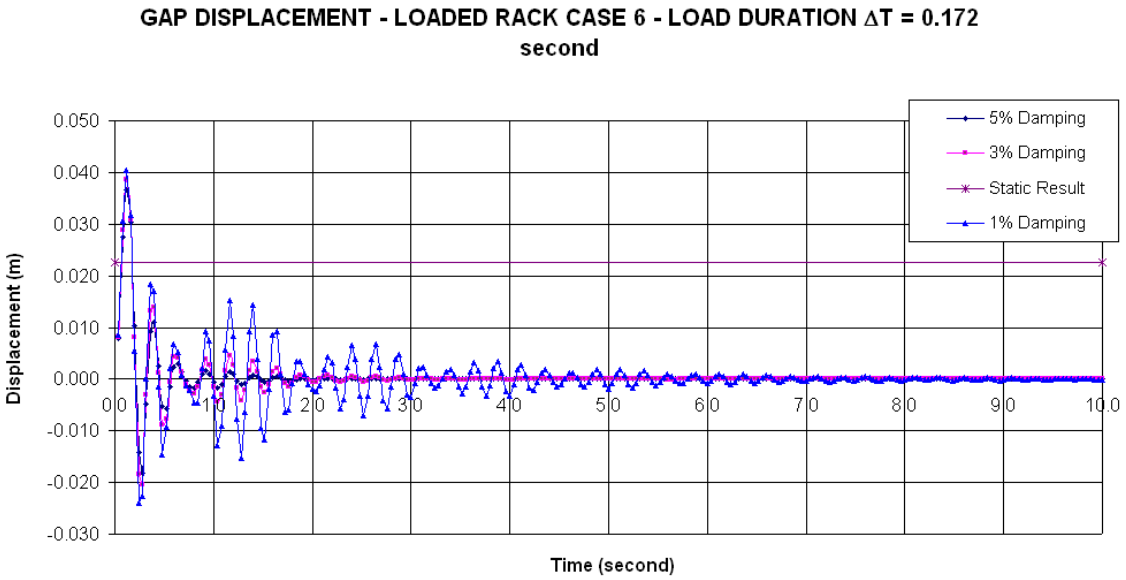

Figure 14h. Displacement Gap Response at the front face of top pallet level – Loaded Rack Case 6 – Load Duration ΔT = 0.172 second

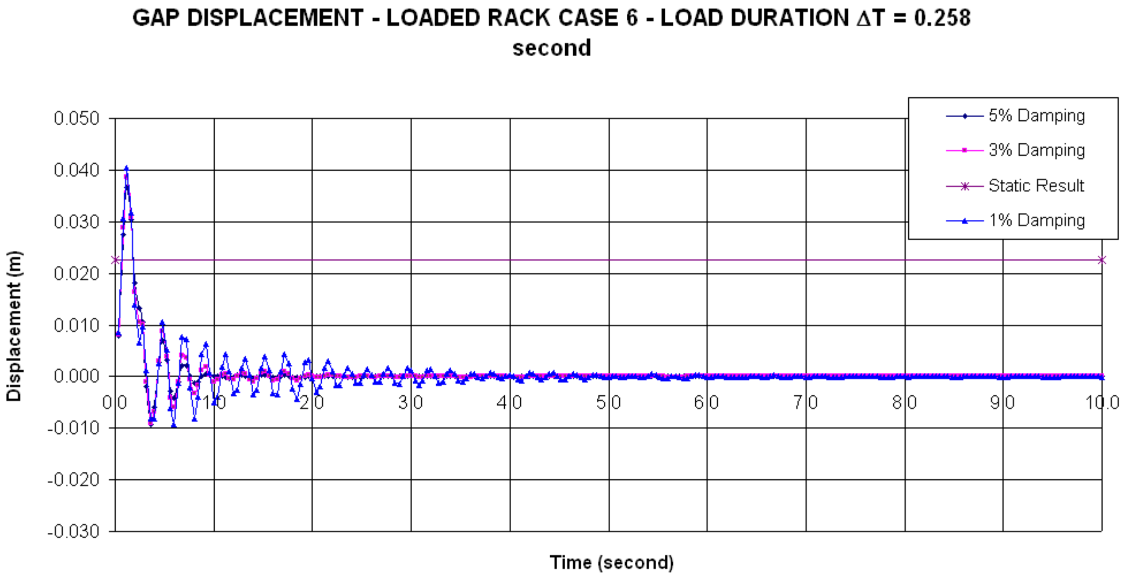

Figure 14i. Displacement Gap Response at the front face of top pallet level – Loaded Rack Case 6 – Load Duration ΔT = 0.258 second

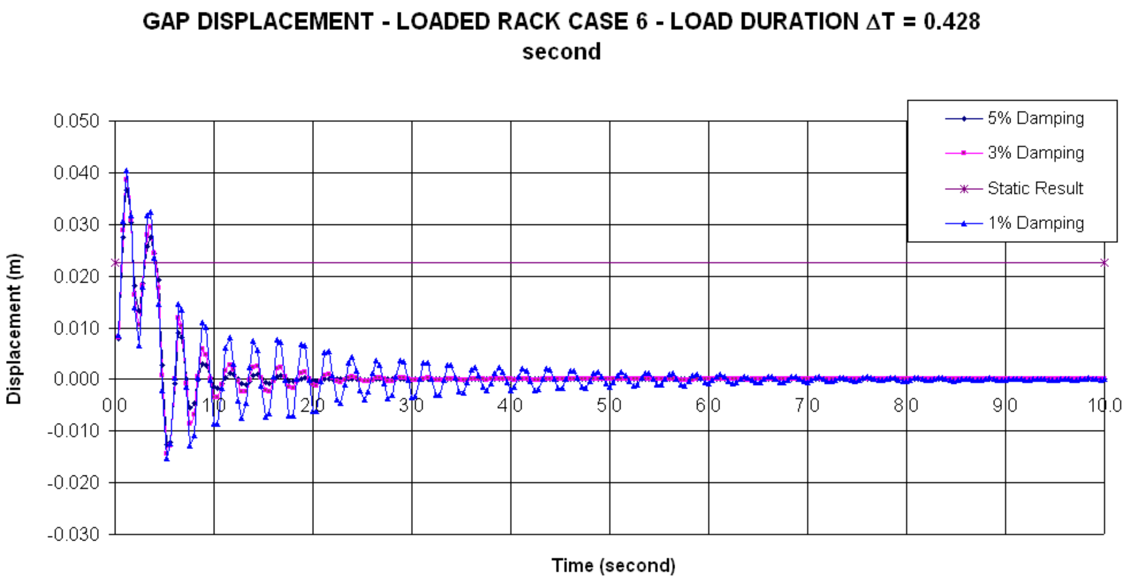

Figure 14j. Displacement Gap Response at the front face of top pallet level – Loaded Rack Case 6 – Load Duration ΔT = 0.428 second

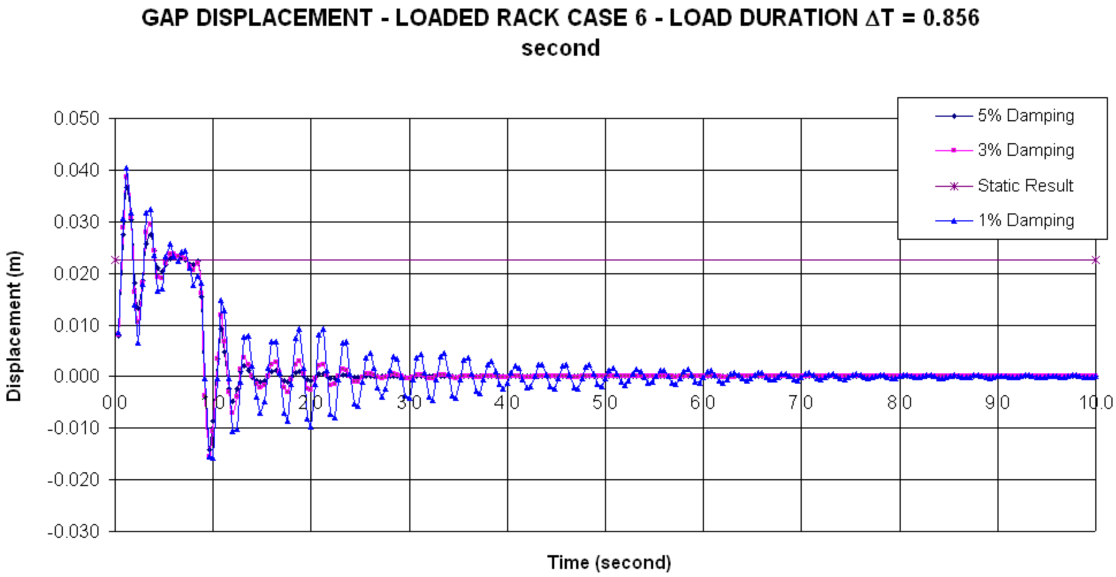

Figure 14k. Displacement Gap Response at the front face of top pallet level – Loaded Rack Case 6 – Load Duration ΔT = 0.856 second

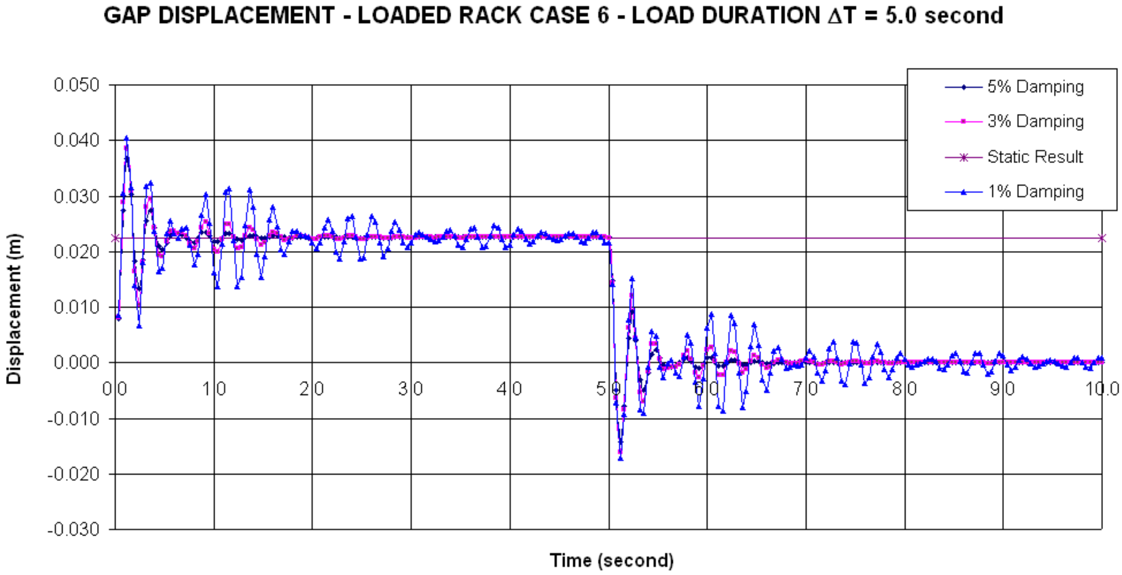

Figure 14l. Displacement Gap Response at the front face of top pallet level – Loaded Rack Case 6 – Load Duration ΔT = 5.0 second

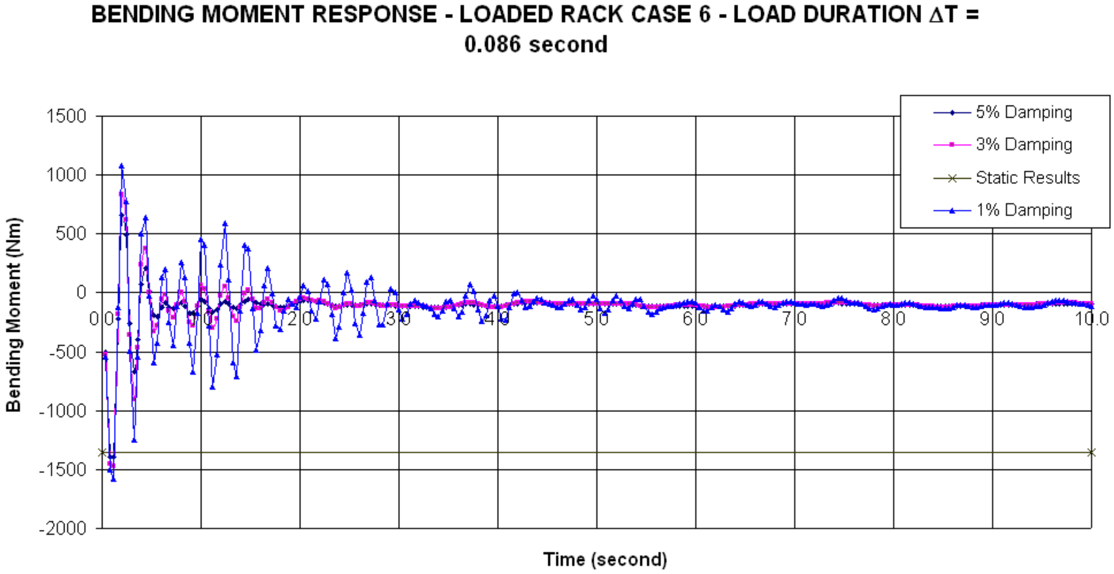

Figure 14m. Bending Moment Response at the base of impacted upright – Loaded Rack Case 6 – Load Duration ΔT = 0.086 second

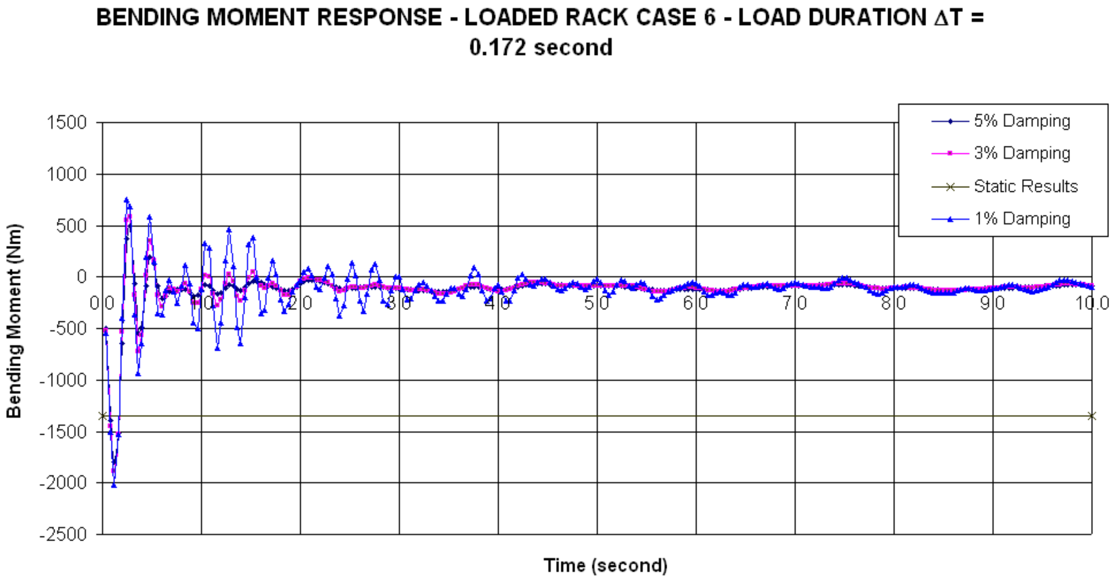

Figure 14n. Bending Moment Response at the base of impacted upright – Loaded Rack Case 6 – Load Duration ΔT = 0.172 second

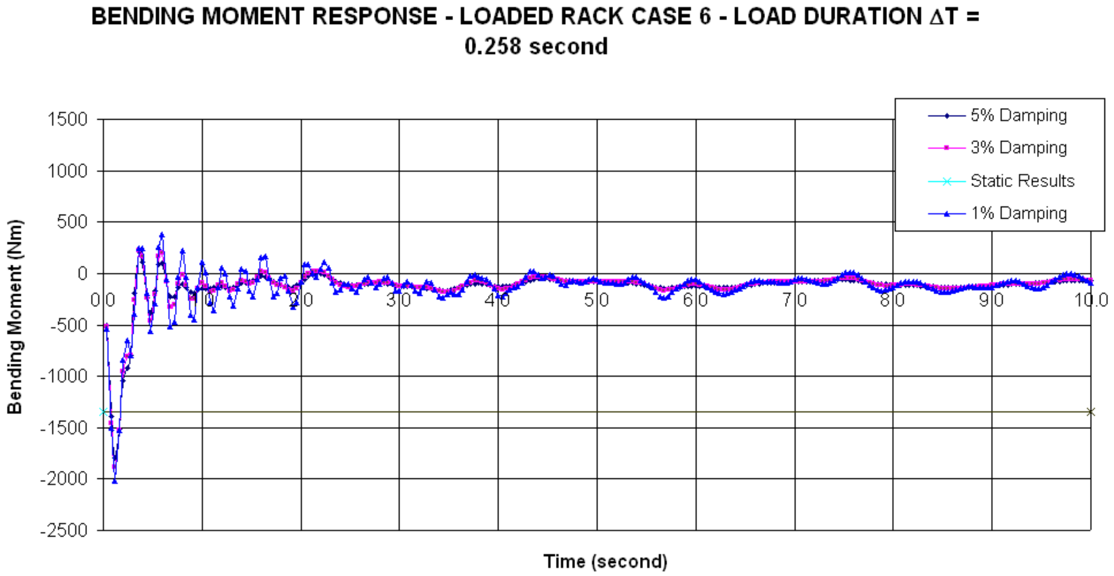

Figure 14o. Bending Moment Response at the base of impacted upright – Loaded Rack Case 6 – Load Duration ΔT = 0.258 second

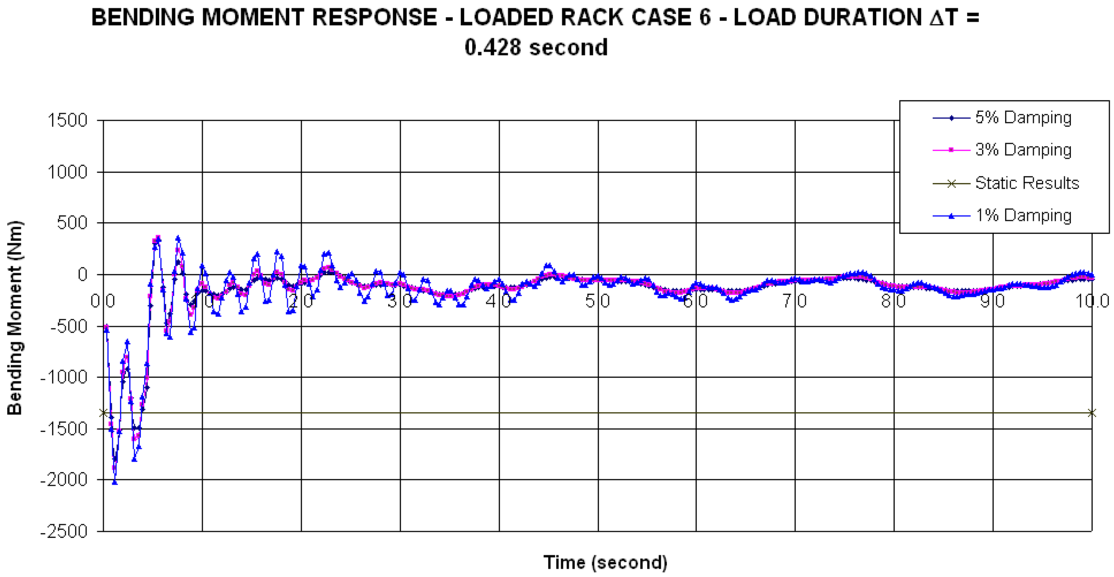

Figure 14p. Bending Moment Response at the base of impacted upright – Loaded Rack Case 6 – Load Duration ΔT = 0.428 second

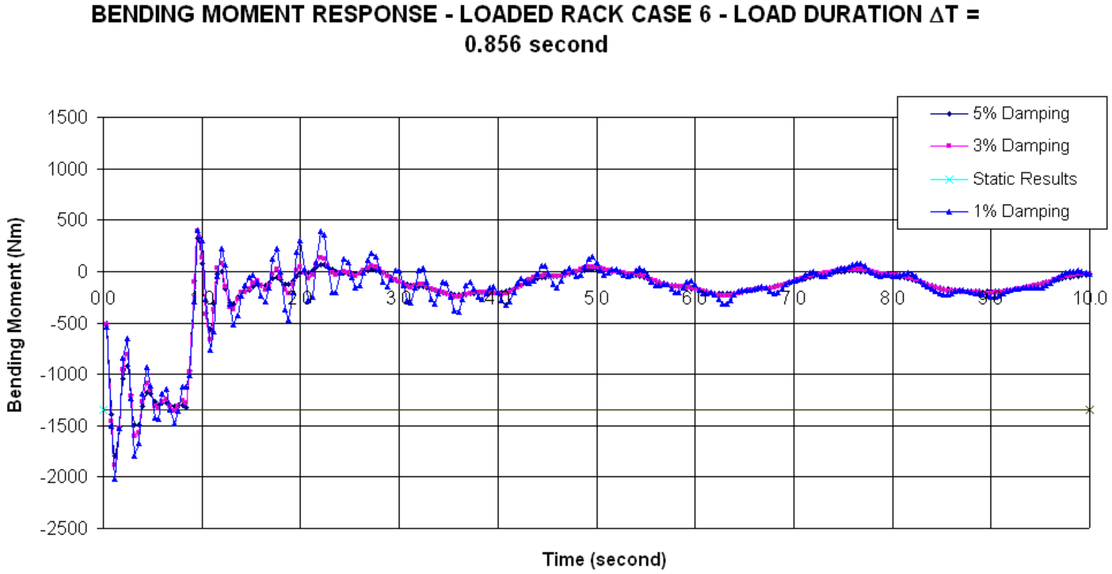

Figure 14q. Bending Moment Response at the base of impacted upright – Loaded Rack Case 6 – Load Duration ΔT = 0.856 second

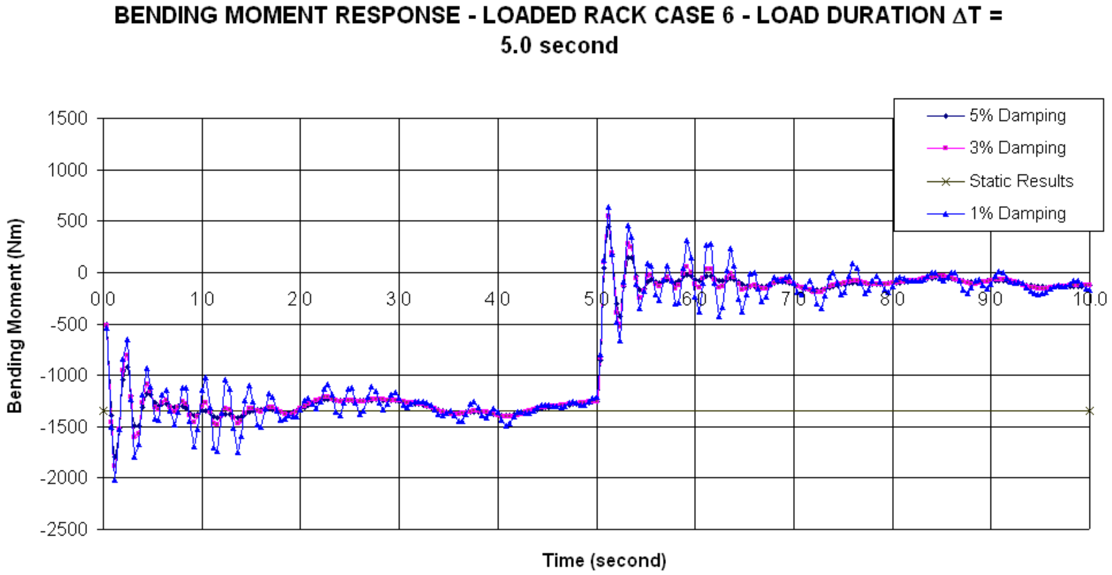

Figure 14r. Bending Moment Response at the base of impacted upright – Loaded Rack Case 6 – Load Duration ΔT = 5.0 second

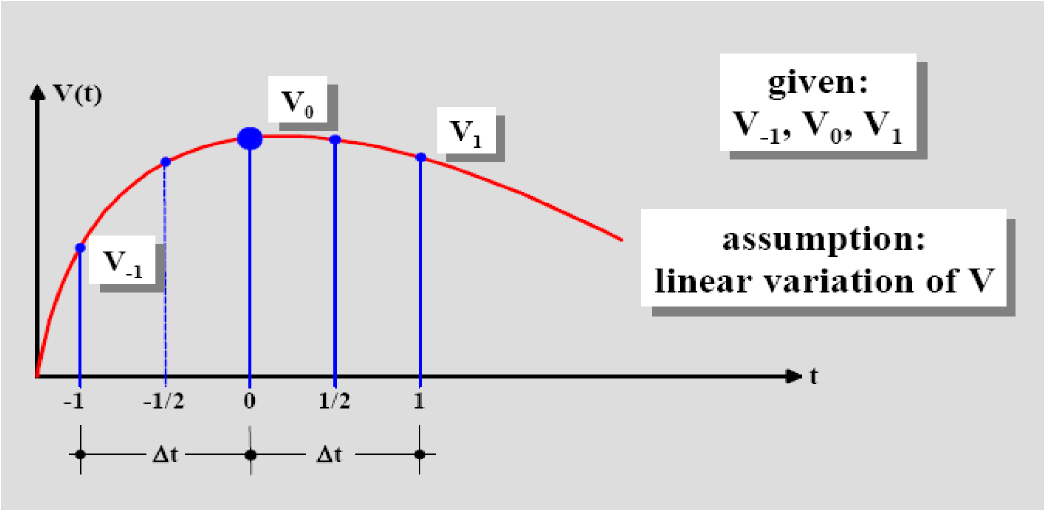

Figure 15. The Central Difference Method

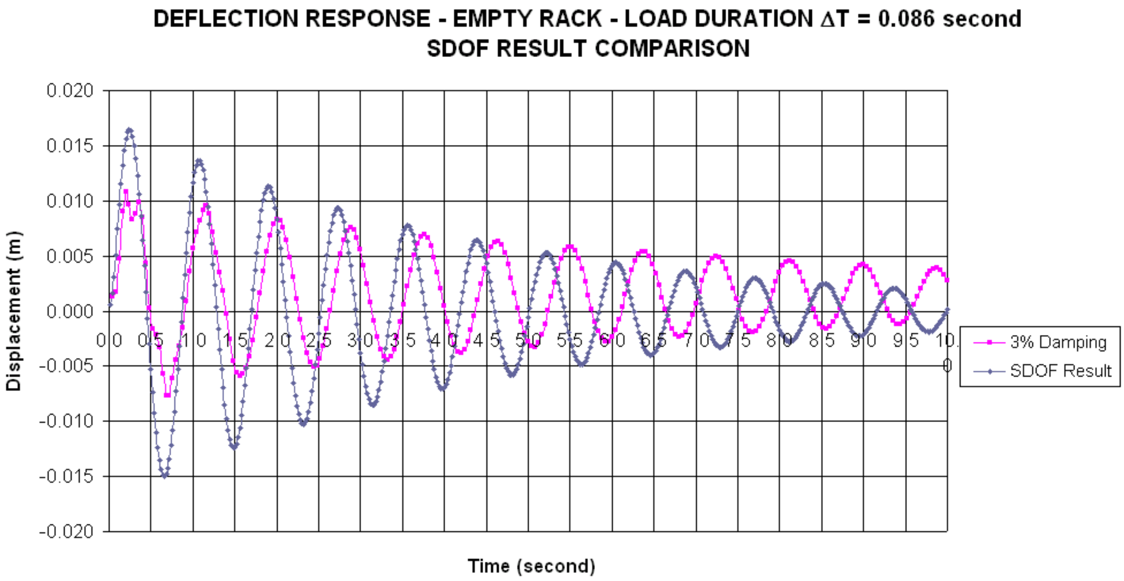

Figure 16a. Deflection Response for Empty Rack Case – Comparison with SDOF Result – Load Duration ΔT = 0.086 second

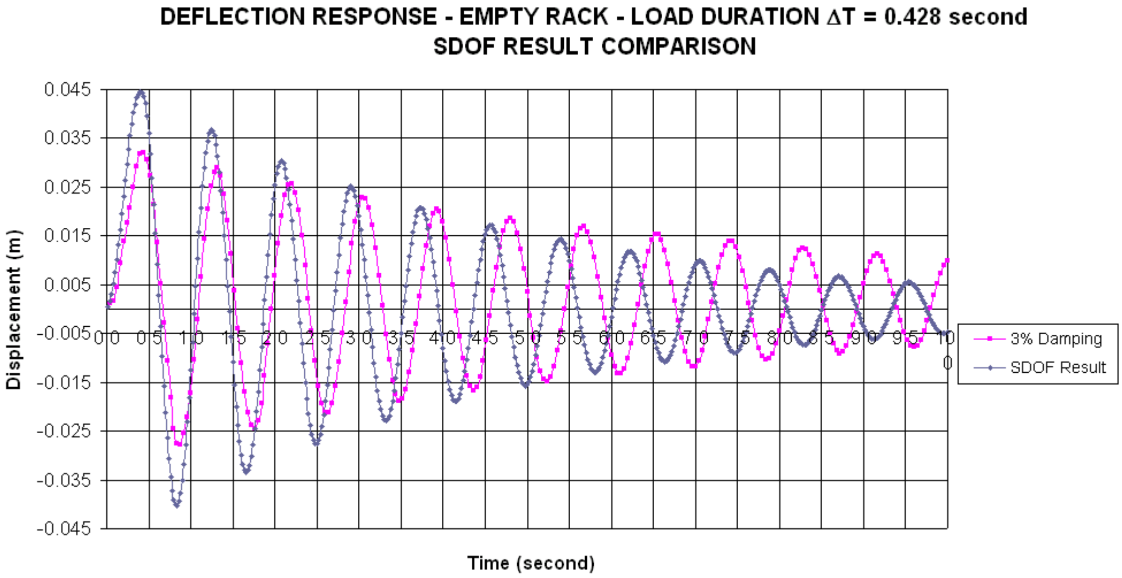

Figure 16b. Deflection Response for Empty Rack Case – Comparison with SDOF Result – Load Duration ΔT = 0.428 second

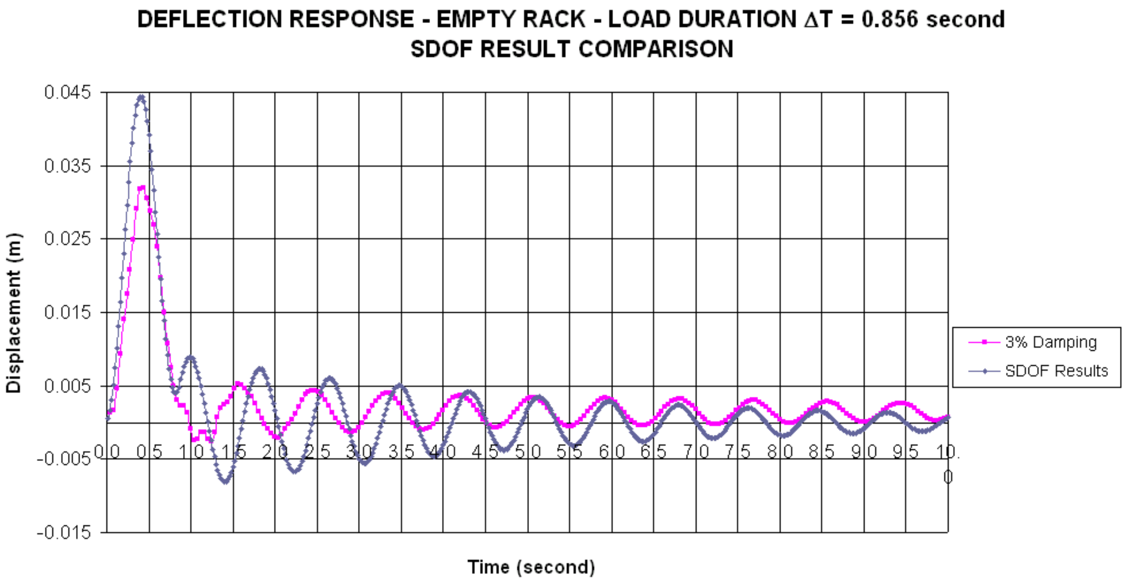

Figure 16c. Deflection Response for Empty Rack Case – Comparison with SDOF Result – Load Duration ΔT = 0.856 second